JPL PUBLICATION 82-33

The Deep Space Network — Noise Temperature Concepts, Measurements, and Performance

C.T. Stelzried

September 15, 1982

National Aeronautics and Space Administration

Jet Propulsion Laboratory
California Institute of Technology
Pasadena, California

JPL PUBLICATION 82-33

The Deep Space Network — Noise Temperature Concepts, Measurements, and Performance

C.T. Stelzried

September 15, 1982

National Aeronautics and
Space Administration

Jet Propulsion Laboratory
California Institute of Technology
Pasadena, California

The research described in this publication was carried out by the Jet Propulsion Laboratory, California Institute of Technology, under contract with the National Aeronautics and Space Administration.

TABLE OF CONTENTS

Tables

Figures

ACKNOWLEDGMENTS

The technical assistance of S. Slobin, R. Clauss, M. Klein, E. Smith and other JPL personnel is gratefully acknowledged. N.A. Renzetti provided help and encouragement. The editorial assistance of D. Maple and typing of M. Tucker and the Word Processing Group of the JPL Documentation Section are appreciated.

-ABSTRACT-

Extremely sensitive receiving systems are required for deep space communications. The NASA Deep Space Network is investigating the use of higher operational frequencies for improved performance. Noise temperature and noise figure concepts are used to describe the noise performance of these receiving systems. The ultimate sensitivity of a linear receiving system is limited by the thermal noise of the source and the quantum noise of the receiver amplifier. The sensitivity of a receiving system consisting of an "ideal" linear receiver with a 2.7 K source temperature (-194.3 dBm/Hz assuming hf<<kT) degrades significantly at frequencies greater than about 50 GHz.

The atmosphere, antenna and receiver amplifier of an earth station receiving system are analyzed separately and as a system. Performance evaluation and error analysis techniques are investigated. System noise temperature and antenna gain parameters are combined to give an overall system figure of merit G/T. This parameter is useful for system sensitivity specifications and is conveniently evaluated using radio "stars".

Radiometers are used to perform radio "star" antenna and system sensitivity calibrations. These are analyzed and the performance of several types compared to an idealized total power radiometer. Thermal noise standards are useful for laboratory and field noise performance evaluations for all aspects of the receiving system. Proper account is taken of the transmission line degradation to realize the full potential of these devices.

The theory of radiative transfer is applicable to the analysis of transmission medium loss, which is useful for the evaluation of both thermal noise standards and the atmosphere. A power series solution in terms of the transmission medium loss is given for the solution of the noise temperature contribution.

1. Introduction

Extremely sensitive receiving systems are required in deep space communications. The NASA Deep Space Network is investigating the use of higher operational frequencies for improved performance. Noise temperature and noise figure concepts are used to describe the noise performance of these receiving systems.

Noise in a receiving system is defined as an undesirable disturbance corrupting the information content. Noise in the context of this report is assumed random with continuous spectral power density. The sources of noise can be separated into external noise and internal noise.

Sources of external noise (Mumford, 68, 3-6; CCIR, 78, 422-427) include: lightning, cosmic, solar, planetary, galactic, radio stars, emission from atmospheric constituents and man-made noise. Cosmic noise is considered to be the residual radiation ($\approx$2.7 K) due to events occurring during the origin of the universe. Solar, planetary and radio "star" noise occur due to radio emission from these sources intercepted by the antenna. Man-made noise includes ignition systems, spark discharges, and transmission of noise and noiselike signals along power lines. Sources of internal noise include thermal, shot, current, Barkhausen, and quantum noise. In this report, thermal noise is treated as the limiting noise source for microwave receiving systems.

Thermal noise is caused by random motion of free electrons in a conductor excited by thermal agitation. The signal-to-noise performance of a receiving system composed of a source and an amplifier is expressed quantitatively most conveniently in terms of noise temperature concepts.

Noise temperature and antenna gain definitions, performance and measurement techniques are presented and analyzed for communications receiving systems. The atmosphere, antenna and receiver are treated individually and as a system.

System noise temperature and antenna gain parameters are combined to give an overall system figure of merit G/T. This parameter is useful for system sensitivity specifications and is conveniently evaluated using radio "stars".

Radio "stars" are used to evaluate both antenna and total receiving system sensitivity performance by measurement of the increased output noise when the antenna is directed to these sources. Measurement error analysis techniques are necessary for proper interpretation of the results. Radiometers are used to perform radio "star" calibrations. These are analyzed and the performance of several types compared to an idealized total power radiometer. Thermal noise standards are useful for laboratory and field noise performance evaluations for all aspects of the receiving system. Proper account is taken of the transmission line degradation to realize the full potential of these devices.

The atmosphere is extremely important to the performance of receiving systems. Not only is there a direct loss due to rain, clouds and other constituents of the atmosphere, but in low noise systems the thermal emission can cause more signal-to-noise degradation than the direct loss. These effects are evaluated.

The theory of radiative transfer is applicable to the analysis of transmission medium loss, which is useful for the evaluation of both thermal noise standards and the atmosphere. A power series solution in terms of the transmission medium loss is given for the solution of the noise temperature contribution. The inverted solution for loss in terms of the measured thermal noise is useful for the determination of atmospheric loss from radiometric noise temperature measurements. These techniques can be used for calibrations of the atmospheric liquid water and water vapor content.

1. References

1968 Mumford, W.W. and Scheibe, E.H., Noise Performance Factors in Communication Systems, Horizon House - Microwave, Inc., (1968).

1978 CCIR, "Worldwide Minimum External Noise Levels, 0.1 Hz to 100 GHz," Report 670, CCIR XIV Plenary Assembly, Kyoto, Japan, Vol I, ITU, Geneva, Switzerland, (1978), pgs. 422-427.

2. Noise Temperature

Thermal noise (Johnson, 28, 97; Nyquist, 28, 110) is caused by random motion of free elections in a conductor excited by thermal agitation. The available thermal noise power P_n (Mumford, 68, 4; Oliver, 65, 441) from a source at the amplifier output is given by (G>>1)

$$P_n = kTBG\left(\frac{hf/kT}{e^{hf/kT} - 1}\right), \text{ W} \qquad (2\text{-}1)$$

where

T = source temperature, K
h = Planck constant = 6.6262×10^{-34} J-s
k = Boltzmann constant = 1.3806×10^{-23} J/K
f = operating frequency, Hz

$$B = \frac{1}{G}\int_0^\infty G(f)\,df = \text{noise bandwidth, Hz}$$

G(f) = available power gain, ratio
G = maximum available power gain, ratio

The amplifier output is approximately (disregarding the contribution of the amplifier; hf<<kT)[1]

$$P_n = kTBG \qquad (2\text{-}2)$$

Eqs. 2-1 and 2-2 are shown plotted in Fig. 2-1 for a large range of hf/kT values. Most microwave applications are restricted to the region near the origin (hf<<kT).

---

[1]Note that (hf/kT) = 0.048 f(GHz)/T(K) = 0.00048 at 1 GHz and 100 K and = 1 at 208 GHz and 10 K indicates that Eq. (2-2) is an extremely good approximation for most microwave applications.

It is computationally convenient to define a temperature T' such that

$$P_n = kT'BG = kTBG \left(\frac{ht/kT}{e^{hf/kT} - 1} \right) \tag{2-3}$$

T' can be conveniently found by subtracting a correction T_c (Viggh, 76, 54) from T, so that

$$(P_n/kBG) = T' = T - T_c \tag{2-4}$$

where

$$T_c = T \left(1 - \frac{hf/kT}{e^{hf/kT} - 1} \right)$$

or conveniently

$$T_c = 0.024f(GHz) - 0.000192 \left[f(GHz) \right]^2/T + \ldots \tag{2-5}$$

These correction terms are shown plotted in Fig. (2-2). At 32 Ghz, the cosmic background temperature (Penzias, 65, 419; Otoshi, 75, 174) of ≈2.7 K, correctly defined for use with Eq. (2-1), is "corrected" to ≈2.0 K for use with Eq. (2-2).

The quantum[2] noise limit (Oliver, 65, 450) of a linear amplifier (where both phase and amplitude information is retained), a manifestation of the quantum mechanics uncertainty principle, is given by

---

[2]Eq. (2-6) is appropriate only for linear amplification. At optical frequencies, using discrete photons, techniques may exist (Pierce, 80, 320) to circumvent this limitation. Equating kTB to quantum noise hfB results in an equivalent quantum noise temperature, $T_q = (hf/k)$. Although T_q is a fictitious temperature, it is useful for computational analysis and can be used with Eq. (2-2) to compute P_n accounting for quantum noise (Stelzried, 82). This is discussed further by others (Siegman, 64, 412; Weber, 57, 540). Gulkis, 82, discusses the intermediate frequency ranges accounting for quantum and thermal noise for both linear and incoherent amplifiers.

$$P_n = hfBG \tag{2-6}$$

Fundamental limits of an ideal receiving system sensitivity are determined by the sum of the source thermal noise and the quantum noise limit of an ideal amplifier (since these noise sources are uncorrelated: Pierce, 80, 320).

$$P_n = kTBG \left(\frac{hf/kT}{e^{hf/kT} - 1} \right) + hfBG \tag{2-7}$$

$$= k(T' + T_q)\, BG$$

or

$$(P_n/kBG) = T' + T_q \tag{2-8}$$

This is plotted in Figs. (2-1, 3 and 4) as functions of (hf/kT), frequency and temperature. The quantum noise limit and thermal noise are equal when (hf/kT) = ln 2 = 0.69 as shown in Fig. 2-1. In Fig. 2-4 the value of P_nkBG for hf>>kT is given by hf/k (or T_q) and for hf<<kT by T + hf/2k (or $T + T_q/2$).

2. References

1928 Johnson J.B., "Thermal Agitation of Electricity in Conductors", Physical Review, Vol. 32, No. 1, (July 1928), pg. 97.

1928 Nyguist, H., "Thermal Agitation of Electric Charge in Conductors", Physical Review, Vol. 32, No. 1, (July 1928), pg. 110.

1957 Weber, J., "Maser Noise Considerations", Physical Review, Vol. 108, No. 3, (Nov. 1957),pgs. 537-541.

1964 Siegman, A.E., Microwave Solid-State Masers, McGraw-Hill, N.Y. (1964), pgs. 1-583.

1965 Oliver, B.M., "Thermal and Quantum Noise", Proceedings of the IEEE, Vol. 53, No. 5 (May 1965), pg. 436.

1965 Penzias, A.A. and Wilson, R.W., "A Measurement of Excess Antenna Temperature at 4080 Mc/s", Astro Phys. J., Vol. 142, No. 1, (July 1965), pg. 419-421.

1968 Mumford, W.W. and Scheibe, E.H., Noise Performance Factors in Communication Systems, Horizon House - Microwave, Inc., (1968).

1975 Otoshi, T.Y. and Stelzried, C.T., "Cosmic Background Noise Temperature at 13-cm Wavelength", IEEE Instrumentation and Measurement, Vol. 24, No. 2, (June 1975), pg. 174.

1976 Viggh, E.V., "How Noisy Is That Load", Microwaves, Vol. 15, No. 1, (Jan. 1976), pg. 54.

1980 Pierce, J.R. and Posner, E.C., Introduction to Communication Science and Systems, Plenum Press, N.Y. (1980).

1982 Gulkis, S., "Thermal Background Noise Limitations," TDA Progress Report, Jet Propulsion Laboratory, Pasadena, CA, (1982).

1982 Stelzried, C.T., "Noise Temperature and Noise Figure Concepts: DC to flight", TDA Progress Report 42-67, Jet Propulsion Laboratory, Pasadena, CA, (Feb. 15, 1982), pgs. 100-111.

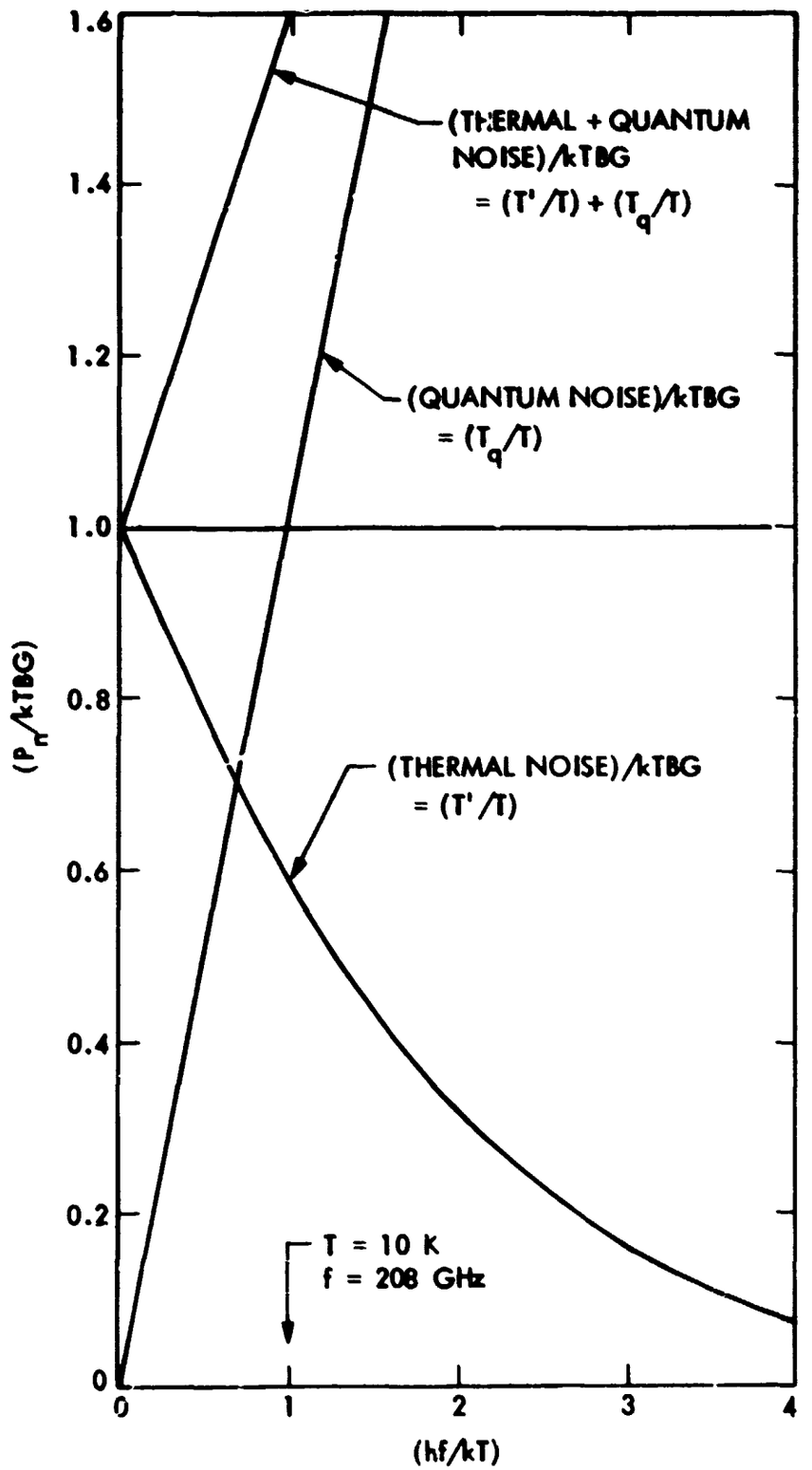

Fig. 2-1. Thermal and quantum noise vs (hf/kT)

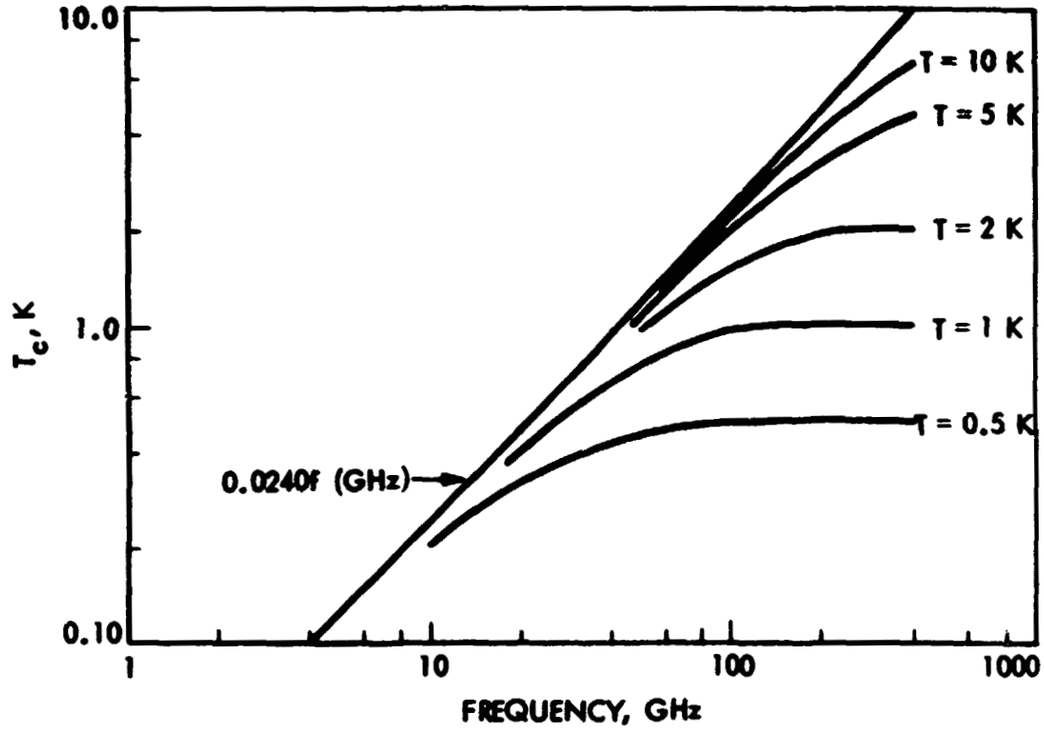

Fig. 2-2. Thermal noise temperature correction T_c vs frequency as a function of temperature

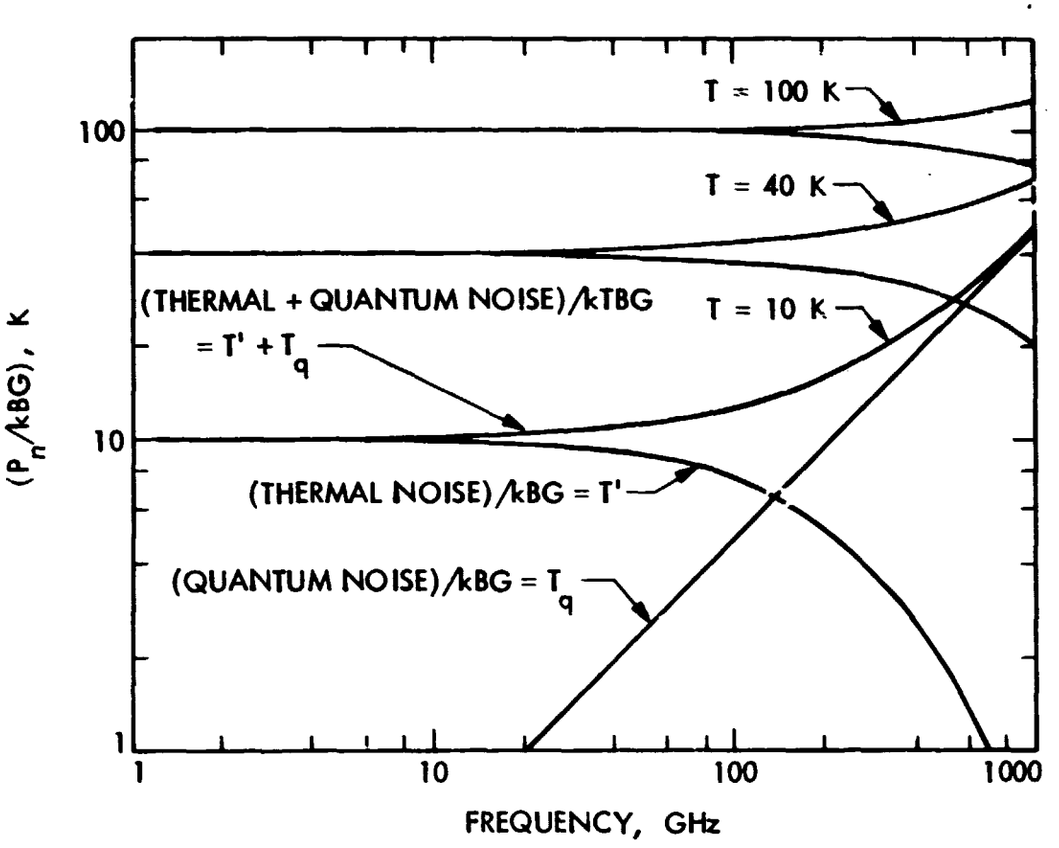

Fig. 2-3. Thermal and quantum noise vs frequency as a function of temperature

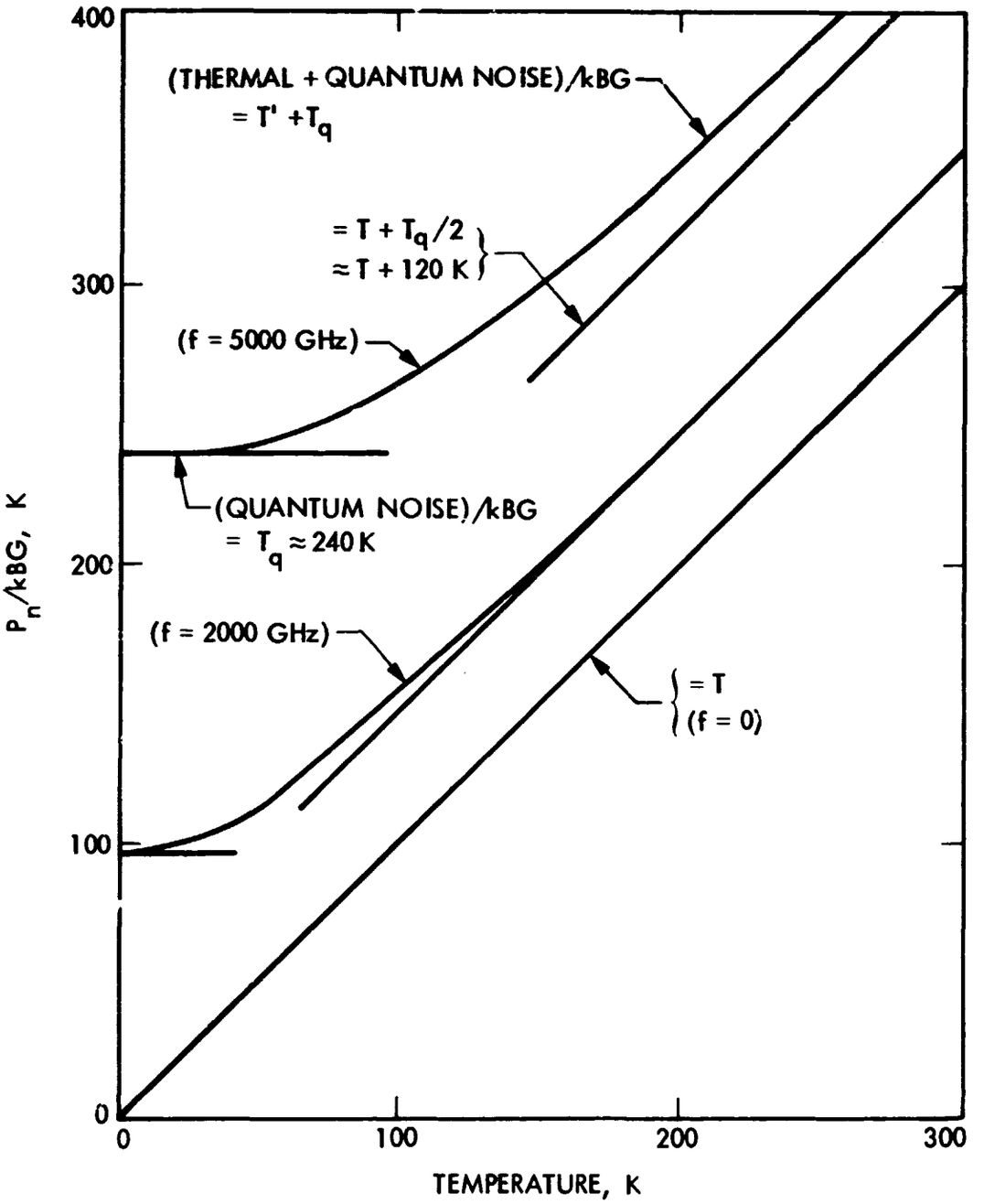

Fig. 2-4. Thermal and quantum noise vs temperature as a function of frequency

3. Antenna Noise Temperature

The noise temperature of an antenna, from Eq. 2-2 (also Rusch, 70,71), is defined, $hf \ll kT$,

$$T_a = P_A/kB, \text{ K} \tag{3-1}$$

where

P_A = noise power delivered by the antenna, over a bandwidth B, into a matched termination, W

Also

$$T_a = \frac{1}{4\pi}\int T(\Omega)\, G(\Omega)\, d\Omega \tag{3-2a}$$

$$= \int_{4\pi} T(\Omega)\, P(\Omega)\, d\Omega \Big/ \int_{4\pi} P(\Omega)\, d\Omega \tag{3-2b}$$

where

$T(\Omega)$ = equivalent blackbody temperature of area $d\Omega$, K

$P(\Omega)$ = normalized antenna pattern gain in direction Ω, ratio
= $G(\Omega)/G_m$

$G(\Omega)$ = antenna gain in direction Ω, ratio

G_m = antenna maximum gain, ratio
= $4\pi A_e/\lambda^2$

A_e = antenna effective area, m^2

D_e = antenna effective diameter, m

Measurement requirements dictate the appropriate method for evaluation of T_a. Absolute antenna calibrations (Sec. 10) require thermal noise standards. The individual contributions to T_a include cosmic noise (Penzias, 65, 419), atmospheric noise (Sec. 4), spillover (Schuster, 62, 286), and ground contributions (Otoshi, 65, 262), all evaluated separately.

Antenna noise temperature calibrations involve the measurement of the increase (Sec. 14) in antenna temperature (antenna gain known) to evaluate an external noise source (such as a planet, radio star, the moon or the sun). Alternately, a known external noise source can be used to evaluate the antenna performance (radio stars: Freiley, 80, 168; Baars, 73, 461; Baars, 77,99; Sun: Kuseski, 76; Linsky, 73).

The increase in antenna temperature due to a "small" ($\Omega_s << \Omega_A$) source in the antenna beam far field ($R >> 2D^2/\lambda$; Silver, 49, 199) is

$$\left.\begin{aligned} \Delta T_a &= T_s\, \Omega_s/\Omega_A \\ &= T_s\, A_e\, A_s/(R\lambda)^2 \end{aligned}\right\} \qquad (3\text{-}3)$$

where

T_s = average temperature of source, K

Ω_s = source solid angle, rad^2

$$= \int_{\text{on-source}} d\Omega$$

$$= A_s/R^2$$

R = range from antenna to source, m

A = antenna physical area, m^2

A_s = projected surface area of source, m^2

Ω_A = antenna beam solid angle, rad^2

$$= \int_{4\pi} P(\Omega)\, d\Omega$$

$$= \lambda^2/A_e$$

Eq. 3-3 provides a convenient form for estimating ΔT_a for a distant radio source such as a planet (Fig. 3-1). For the JPL 64-m antenna at 8.5 GHz (Freiley, 80, 168 14, Fig. 3-2, $D_e \approx 45.6$ m), $\Delta T_a \approx 55$ K for Venus at inferior conjunction. It is frequently convenient to use (assuming an antenna which abstracts half of the incident energy of a randomly polarized source),

$$\Delta T_a = SA_e/2k \qquad (3\text{-}4)$$

where[3]

S = source flux density, $J\text{-}m^2$
(1 Jansky (J_y) $= 10^{-26}$ $J\text{-}m^2$)

$= 2k\, T_s\, A_s/(R\lambda)^2$, $(\Omega_s \ll \Omega_A)$

External contributions to antenna noise temperature as a function of frequency can be estimated from Fig. 3-3 (Smith, 82). At zenith, galactic noise (diurnal variations to $\approx$ 2900 K at 0.1 GHz) dominates at the lower frequencies and atmospheric noise (discussed in Sec. 4) dominates at the higher frequencies. The lowest antenna noise temperatures (for ground-based antennas) occur between these regions from about 1.5 to 15 GHz.

---

[3]For completeness (Kraus, 66, 86),

Planck's law: $S = 2\,hf^3\,\Omega_s/c^2\,(e^{hf/kT_s} - 1)$

Rayleigh-Jean's law ($hf \ll kT$): $S = 2\,kT_s\,\Omega_s/\lambda^2$

Wein's law ($hf \gg kT$): $S = 2\,hf^3\,\Omega_s/c^2(e^{hf/kT_s})$

3. References

1949 Silver, S., Microwave Antenna Theory and Design, McGraw-Hill, N.Y., (1949).

1962 Schuster, D., Stelzried, C.T., and Levy, G.S., "The Determination of Noise Temperatures of Large Paraboloidal Antennas", IRE Inst. on Antennas and Propagation, Vol. AP-10, (May 1962), pg. 286.

1965 Otoshi, T.Y., and Stelzried, C.T., "Antenna Temperature Analysis", SPS No. 37-36, Vol. IV, Jet Propulsion Laboratory, Pasadena, CA, (Dec. 1965), pg. 262.

1965 Penzias, A.A. and Wilson, R.W., "A Measurement of Excess Antenna Temperature at 4080 Mc/s", Astro. Phys. J., Vol. 142, No. 1, (July 1965), pgs. 419-421.

1966 Kraus, J.D., Radio Astronomy, McGraw-Hill, N.Y. (1966).

1970 Rusch, W.V.T. and Potter, P.D., Analysis of Reflector Antennas, Academic Press, N.Y., (1970).

1973 Baars, J.W.M., "The Measurement of Large Antennas with Cosmic Radio Sources", IEEE Trans. on Antennas and Propagation, Vol. AP-21, No. 4, (July 73), pg. 461.

1973 Linsky, J.L., "A Recalibration of the Quiet Sun Millimeter Spectrum Based on the Moon as an Absolute Radiometric Standard", Solar Physics, Vol. 28, (1973), pg. 419.

1976 Kaseski, R.A. and Swanson P.N., "The Solar Brightness Temperature at Millimeter Wavelengths," Solar Physics, Vol. 48, (1976), pg. 41.

1977 Baars, J.W.M. et al., "The Absoluate Spectrum of CasA; An Accurate Flux Density Scale and a Set of Secondary Calibrators", Astron. Astrophysics, Vol. 61, (1977), pgs. 99-106.

1978 CCIR, "Worldwide Minimum External Noise Levels, 0.1 Hz to 100 GHz", Report 670, CCIR XIV Plenary Assembly, Kyoto, Japan, Vol I, ITU, Geneva, Switzerland, (1978), pgs. 422-427.

1980 Freiley, A.J., "Radio Frequency Performance of DSS 14 64-Meter Antenna at X-Band Using an Improved Subreflector", TDA Progress Report 42-60, Jet Propulsion Laboratory, Pasadena, CA, (Dec 15, 1980), pg. 168.

1982 Smith, E., "The Natural Noise Source Environment Existing at Surface and Elevated Locations," IEEE Transactions of Electromagnetic Compatibility Society, (1982).

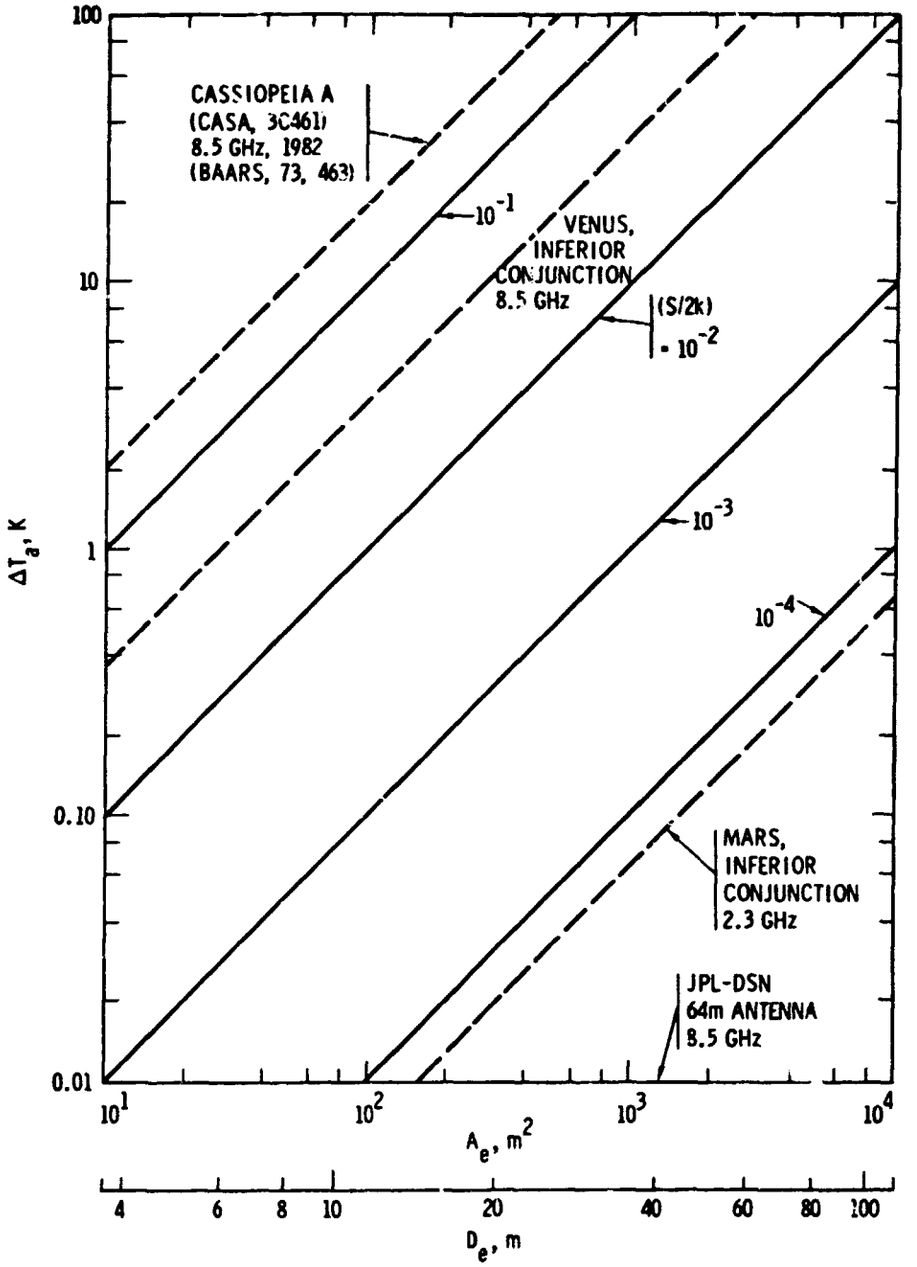

Fig. 3-1. ΔT_a vs D_e (or A_e) for various radio source parameter values

Fig. 3-2. Photograph of JPL 64-m antenna, DSS 14, Goldstone, California

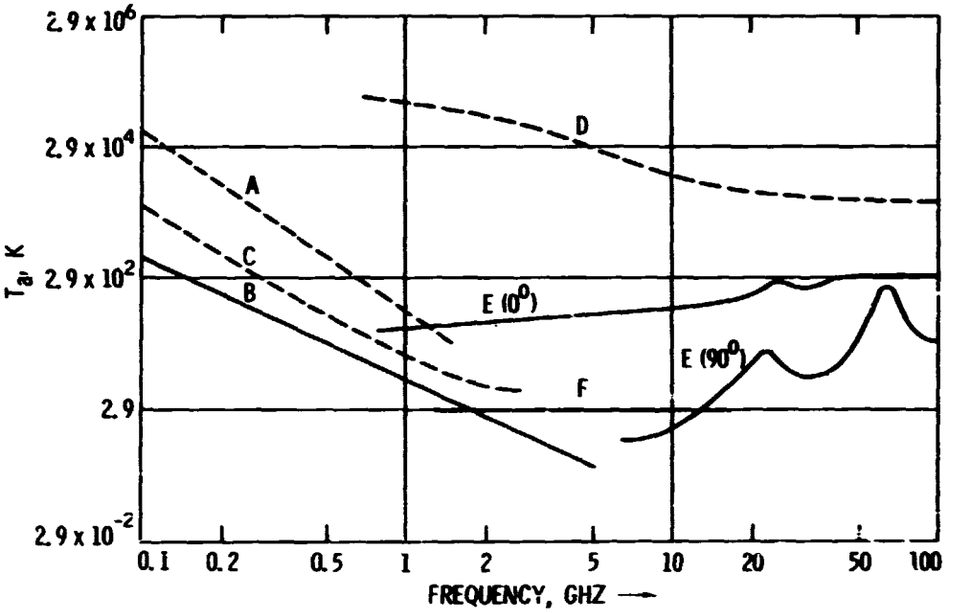

A: ESTIMATED MEDIAN BUSINESS AREA MAN-MADE NOISE
B: GALACTIC NOISE
C: GALACTIC NOISE (TOWARD GALACTIC CENTER WITH INFINITELY NARROW BEAMWIDTH)
D: QUIET SUN (1/2 DEGREE BEAMWIDTH DIRECTED AT SUN)
E: SKY NOISE DUE TO OXYGEN AND WATER VAPOR (VERY NARROW BEAM ANTENNA); UPPER CURVE, 0° ELEVATION ANGLE; LOWER CURVE, 90° ELEVATION ANGLE
F: BLACK BODY (COSMIC BACKGROUND), 2.7 K
: MINIMUM NOISE LEVEL EXPECTED

Fig. 3-3. Worldwide (0.1-100 GHz) minimum external noise levels (solid curves); other noise sources of interest are given by dashed curves (CCIR, 78)

4. Effect of the Atmosphere on Antenna Temperature

The earth's atmosphere (Smith and Waters, 81, 1-45) consists mostly of the dry components oxygen (≈21% by volume), nitrogen (≈78% by volume) and argon (≈1% by volume), and wet components (water vapor, clouds and rain). Water vapor at 100% relative humidity is approximately 1.7% by volume assuming the U.S. Standard Atmosphere, 15°C, at sea level.

A communications link through the atmosphere suffers several forms of degradation (Crane 76, 177-200; Straiton, 75, 595; Damosso, 76, 98; Fogarty, 75, 441; Daywitt, 78, 1-39; Hogg, 59, 1417; Crane, 81, 196-209). The decreased signal-to-noise (SNR) ratio system performance due to atmospheric attenuation and increased noise temperature is discussed further in Sec. 7.

The total loss through the atmosphere (Fig. 4-1) is given by (neglecting scattering[4])

$$L = e^{\tau}, \quad \text{ratio} \quad (\geq 1) \tag{4-1}$$

where

τ = total atmospheric absorption (optical depth), nepers [L(dB) = (10 log e) $\tau \simeq 4.343\tau$]

$$= \int_0^{\ell} \alpha(x)\, dx$$

$\alpha(x)$ = absorption coefficient of the atmosphere at x, nepers/m

x = slant distance along propagation path, m
(x = o at surface, = ℓ at "top"[5] of atmosphere)

ℓ = total atmospheric slant path length, m

---

[4]Scattering should be considered for rain at frequencies above ≈ 10 GHz, and for clouds at frequencies above ≈ 100 GHz (Tsang, 77, 650, Flock, 79, 176)

[5]It is sometimes convenient to integrate from the "top" of the atmosphere to the surface (Waters 76, 142).

From the theory of radiative transfer (neglecting scattering, assuming $hf \ll kT$, see Sec. 20, Stelzried, 81a, 73, Slobin 81a, Chandrasaekhar, 60), the thermal noise temperature defined at the receiving system input is given by

$$T_s' = (T_s/L) + \int_0^{\ell} T(x)\, \alpha(x) e^{-\tau(x)} dx, \text{ K} \qquad (4\text{-}2)$$

where

T_s = source temperature (usually ≈2.7 K, due to the cosmic background noise temperature), K

$T(x)$ = physical temperature of medium at x, K

$\tau(x)$ = attenuation between 0 and x, nepers

$$= \int_0^x \alpha(x')\, dx'$$

Computed clear sky[6] zenith atmospheric attenuation and noise temperature contributions are shown in Figs. 4-4, 5 and Table 4-1 as functions of frequency, surface water vapor density (i.e. absolute humidity), and elevation angle. Microwave absorption is directly proportional to the water vapor density (actually, the total integrated content along the line of sight). For temperate latitudes in summer (20 °C), the average surface water vapor density is about 7.5 g/m^3 (Van Vleck, 51, 647; Bean and Dutton, 68, 269). At saturation (sea level, 20 °C), the density is ≈17 g/m^3; 3-5 g/m^3 may be more appropriate for arid regions such as Goldstone, CA. An approximate measured value of 9 K at 31.4 GHz is obtained from the tipping curve calibrations at Goldstone as shown in Fig. 4-6. The actual value for a particular day depends on the surface water vapor density; this results in the measurement spread shown. Operating frequencies are usually chosen to be well away from the water vapor line (≈22 GHz) and the oxygen line (≈60 and ≈118 GHz). Minimum attenuation occurs with low humidity, low frequency and high elevation angle (Fig. 4-1, Z = 0°).

---

[6]"Clear sky" indicates an atmosphere containing only gaseous constituents (oxygen, nitrogen and water vapor) with no liquid water (rain or clouds).

For a homogeneous, isothermal atmosphere, $\alpha(x) = \alpha_o$, and temperature $T(x) = T_p$. From Eq. 4-2,

$$T_s' = T_s + (1 - 1/L)(T_p - T_s) \tag{4-3}$$

where

$$L = e^{\tau} = e^{\alpha_o \ell}$$

T_p = equivalent atmospheric physical temperature, K
(≈ 260-280 K; Stelzried, 81b, 87)

Atmospheric loss is frequently determined using Eq. 4-3 and measuring T_s' radiometrically,

$$L = 1 + (T_s' - T_s)/(T_p - T_s') \tag{4-4}$$

Atmospheric loss measurements are investigated further in Section 15.

The effect (Ippolito, 81b) of clouds and rain is to both further attenuate the signal and increase the atmospheric noise temperature. The calculated effect of a one- or two-cloud model (Slobin, 81a, 25) is tabulated in Table 4-2 at S, X and K_a bands. This is shown as a function of frequency in Fig. 4-7 for cloud water particle density of 0.5 gm/m^3. Figs. 4-8 to 4-11 show photographs of clouds taken from the area below the JPL Mesa antenna range (R. Clauss, 82). A two-frequency (20.7 and 32.4 GHz) water vapor radiometer observed the approximate increase in noise temperature due to the clouds shown in the circled region of the photographs (Clauss, 82, Slobin, 81c). The range of measured values is indicated in Fig. 4-7. Statistics of cloud noise temperature and attenuation at various sites in the United States, Alaska, and Hawaii are available in Slobin, 82.

Comprehensive treatments of the effects of rain in satellite communications have been published by Hogg (75, 1308-1331), Ippolito (81a, 697-727), Lin (80, 183-228) and Crane, (80, 1717-1733). The attenuation of a microwave signal propagating through rain is given by (Olsen, 76, 318).

$$A = \int_0^L \alpha dx \quad , \text{dB} \tag{4-5}$$

where

α = absorption coefficient, dB/km

L = length of rain cell, km

= specific attenuation of rain cell, dB/ km

$= a\ R^b$

a, b = empirical coefficients

R = rain rate, mm/hour

Table 4-3 tabulates a and b as a function of frequency and rain rate.

The combined effect (Ippolito, 81b) of variations in clouds, rain and clear sky surface water vapor density on the communication link performance is determined empirically. These effects are measured as a function of frequency, geographical location and time of year. Typical statistical multiyear 11-GHz attenuation data is shown in Table 4-4 for various geographical locations. Fig. 4-12 shows the percent of time the zenith X-band atmospheric noise temperature is above the clear sky baseline for Goldstone, CA (data obtained with noise adding radiometers, Sec. 19). Fig. 4-13 shows similar data using a 30^o elevation angle: curve 1, using CCIR data for an arid region, rain only; curve 2, DSS 13, measured X-band data; curves 3, 4 and 5, 810-5 Rev. D data (probably too pessimistic); curve 6, DSS 13 31.4-GHz data. Curve 6, the result of 1500 hours of measured data, taken at Goldstone, DSS 13, during typical winter weather indicates that noise temperature increases due to rain and clouds of more than 30 K occur less than 2% of the time. A comparison of predicted 8.5- and 31.4-GHz confidence levels (for atmospheric loss and noise temperature of the Goldstone region) is shown in Table 4-5 (see Sec. 7 for 8.5- and 31.4-GHz link performance comparison). For this comparison, the 8.5-GHz values are based on the CCIR model (Fig. 4-13) for arid regions; the 31.4-GHz values are based on results of the 1500 hours of measured data together with 396 radiosonde measurements at Edwards Air Force base (Clauss, 82). This comparison is believed to best characterize the effects of the weather upon the 8.5- and 31.4-GHz link performance without the degradation of non-weather effects.

The effects of water collecting on the antenna feed horn cover have been evaluated at X-band (Slobin, 82). Special techniques are required to minimize the resulting increased noise temperature, especially with "weathered" plaster horn cover material (Hoffman, 79).

4. References

1951 Van Vleck, J.H. "Theory of Absorption by Uncondensed Gases", Propagation of Short Radio Waves, (edited by D.E. Kerr), MIT Radiation Laboratory Series, Vol 13 McGraw Hill, N.Y., (1951).

1959 Hogg, D.C., "Effective Antenna Temperatures Due to Oxygen and Water Vapor in the Atmosphere", Journal of Applied Physics, Vol. 30, No. 9, (Sept. 1959), pgs. 1417-1419.

1960 Chandrasekhar,S., Radiative Transfer, Dover Publications, N.Y., (1960).

1968 Bean B.R. and Dutton, E.J., Radio Meteorology, Dover Publications, Inc., N.Y., (1968).

1975 Fogarty, William G., "Total Atmospheric Absorption at 22.2 GHz", IEEE Trans. Ant. and Prop., (May 1975), pgs. 441-444.

1975 Hogg, D.C., "The Role of Rain in Satellite Communications", IEEE Proc., Vol. 63, No. 9, (Sept. 1975), pgs. 1308-1331.

1975 Straiton, Archie W., "The Absorption and Reradiation of Radio Waves by Oxygen and Water Vapor in the Atmosphere", IEEE Trans. Ant. and Prop., Vol. AP-23 (July 1975), pgs. 595-597.

1976 Crane, R.K., "Extinction by Condensed Water", Methods of Experimental Physics, Vol. 12B, Academic Press, (1976).

1976 Damosso, E. D., and S. De Padova, "Some Considerations About Sky Noise Temperature at Frequencies Above 10 GHz", Alta Frequenza, Vol. XLV, No. 2, (Feb. 1976), pgs. 98-106.

1976 Olsen, R.L., et al., "The aR^b Relation in the Calculation of Rain Attenuation", IEEE Trans. on Antennas and Propagation, Vol. AP-26, No. 2, (March 1976), pg. 318.

1976 Waters, J.W., "Absorption and Emission by Atmospheric Gases', Methods of Experimental Physics, Vol. 12B, Academic Press, (1976).

1977 Tsang, L., et al., "Theory of Microwave Emission from a Layer of Cloud or Rain", IEEE Transactions Antennas and Propagation, AP-25, No. 5, (Sept. 1977), pgs. 650-657.

1978 Daywitt, W.C., "Atmospheric Propagation Equations used in the NBS Earth Terminal Measurement System", NBSIR 78-883, NBS, Boulder, Colorado, (April 1978) .

1979 Flock, W. L., Electromagnetics and the Environment: Remote Sensing and Telecommunications, Prentice-Hall, Inc, 1979.

4. References (cont.)

1979 Hoffman, H., "Hydrophobic Coating for Antenna Weather Windows", Microwave Journal, (Oct. 1979), pgs. 43-48.

1980 Lin S. H., et al., "Rain Attenuation on Earth-Satellite Paths - Summary of 10 Year Experiments and Studies", The Bell System Technical Journal, Vol. 59, No. 2, (Feb. 1980), pgs. 183-228.

1980 Crane, R. K., "Prediction of Attenuation by Rain", IEEE Trans. on Communications, Vol. COM-28, No. 9. (Sept. 1980), pgs. 1717-1733.

1981 Crane, R.K., "Fundamental Limitations Caused by RF Propagation", IEEE Proceedings, Vol. 69, No. 2, (Feb. 1981), pgs. 196-209.

1981 Smith, E.K., and Waters, J.W., "Attenuation and Brightness Temperature Due to the Gaseous Atmosphere Using the JPL Radiative Transfer Program - A Comparison with CCIR Values", Jet Propulsion Laboratory, Pasadena, CA, Publication 81-81, (Aug. 15, 1981).

1981 "Deep Space Network/Flight Project Interface Design Handbook" Document 810-5, Rev. D, Vol. 1, Jet Propulsion Laboratory, CA (Oct. 15, 1981) (an internal document).

1981a Ippolito, L.J., "Radio Propagation for Space Communications System", IEEE Proceedings, Vol. 69, No. 6, (June 1981), pgs. 697-727.

1981b Ippolito, L.J., et al., "A Propagation Effects Handbook for Satellite Systems Design", NASA Reference Publication 1082, (December, 1981).

1981a Slobin, S.D., "Microwave Noise Temperature and Attenuation of Clouds at Frequencies Below 50 GHz", Publication 81-46, Jet Propulsion Laboratory, Pasadena, CA (July 1981).

1981b Slobin, S. D. et al, "X-Band Atmospheric Noise Temperature Statistics at Goldstone, DSS 13, 1979 and 1980, and Clear Air Noise Temperature Models for Goldstone," TDA Progress Report 42-64, Jet Propulsion Laboratory, Pasadena, CA, (Aug 15, 1981), pg. 161.

1981c Slobin, S. D., et al, "20.7 and 31.4 GHz Atmospheric Noise Temperature Measurements", TDA Progress Report 42-64, Jet Propulsion Laboratory, Pasadena CA, (Aug. 15, 1981), pg. 132.

1981a Stelzried, C.T., and Slobin, S., "Calculation of Atmospheric Loss From Microwave Radiometric Noise Temperature Measurements", TDA Progress Report 42-62, Jet Propulsion Laboratory, Pasadena, CA (April 1981). pg, 73.

1981b Stelzried, C.T., "Atmospheric Noise Temperature Measurements", TDA Progress Report 42-63, Jet Propulsion Laboratory, Pasadena, CA, (June 1981), pg. 87.

1982 Clauss, R., Franco, H., and Slobin, S., "K_a-Band 64-m Antenna System Performance Estimates for Future DSN Applications," TDA Progress Report 42-71, Jet Propulsion Laboratory, Pasadena, CA, October 15, 1982.

1982 Slobin, S., Franco, M. and Clauss, R., 11 X-band Rain Effects on DSN 64-m Antenna Feed Horns", TDA Progress Report 42-71, Jet Propulsion Laboratory, Pasadena, CA, (August 15, 1982).

1982 Slobin, S. D., "Microwave Noise Temperature and Attenuation of Clouds: Statistics of These Effects at Various Sites in the United States, Alaska and Hawaii", Radio Science, (1982).

1982 Smith, E.K., "Microwave Attenuation and Brightness Temperature Due to Atmospheric Oxygen and Water Vapor", Radio Science (1982).

Table 4-1. Clear sky zenith atmosphere noise temperature as a function of frequency and surface water vapor density (W) for sea level and DSS 14 Goldstone, CA (Slobin, 81b, 161)

Location and altitude	Atmosphere components	2.3 GHz		8.5 GHz		21.0 CHz		32.0 GHz	
	O_2 + W(g/m^3)	T,K	A,dB	T,K	A,Db	T,K	A,dB	T,K	A,dB
Sea level	O_2 + 0.0	2.12	0.035	2.29	0.038	3.23	0.053	6.38	0.106
H = 0.000 km	O_2 + 3.0	2.13	0.035	2.48	0.041	10.30	0.327	9.54	0.154
	O_2 + 7.5	2.15	0.035	2.78	0.045	20.50	0.327	14.29	0.228
	O_2 + 10.0	2.16	0.036	2.94	0.048	25.98	0.417	16.94	0.027
	O_2 + 15.0	2.18	0.036	3.28	0.053	36.52	0.597	22.24	0.355
DSS 14	O_2 + 0.0	1.68	0.028	1.80	0.030	2.54	0.042	5.03	0.083
H = 1.032 km	O_2 + 3.0	1.69	0.028	1.98	0.032	9.95	0.157	7.87	0.127
	O_2 + 7.5	1.70	0.028	2.24	0.036	20.65	0.328	12.14	0.193
	O_2 + 10.0	1.71	0.028	2.39	0.038	26.37	0.423	14.52	0.230
	O_2 + 15.0	1.73	0.029	2.69	0.043	37.40	0.611	19.30	0.306

Table 4-2. Sample cloud models and S-, X-, and K_a-band zenith atmospheric noise temperature contributions (Slobin, 81a, 25)

Case	Lower Cloud				Upper Cloud				Remarks	S-band (2.3 GHz)		X-band (8.5 GHz)		K_a-band (32 GHz)	
	Density g/m	Base km	Top km	Thickness km	Density g/m	Base km	Top km	Thickness km		T(K)	A(dB)	T(K)	A(dB)	T(K)	A(dB)
1	-	-	-	-	-	-	-	-	Clear air	2.15	0.35	2.78	.045	14.29	.228
2	0.2	1.0	1.2	0.2	-	-	-	-	Light, thin clouds	2.16	.036	2.90	.047	15.92	.255
3	-	-	-	-	0.2	3.0	3.2	0.2		2.16	.036	2.94	0.48	16.51	.266
4	0.5	1.0	1.5	0.5	-	-	-	-		2.20	.036	3.55	.057	24.56	.397
5	-	-	-	-	0.5	3.0	3.5	0.5		2.22	.037	3.83	.062	28.14	.468
6	0.5	1.0	2.0	1.0	-	-	-	-	Medium clouds	2.27	.037	4.38	.070	35.22	.591
7	-	-	-	-	0.5	3.0	4.0	1.0		2.31	.038	4.96	.081	42.25	.731
8	0.5	1.0	2.0	1.0	0.5	3.0	4.0	1.0		2.43	.040	6.55	.105	61.00	1.083
9	0.7	1.0	2.0	1.0	0.7	3.0	4.0	1.0		2.54	.042	8.04	.130	77.16	1.425
10	1.0	1.0	2.0	1.0	1.0	3.0	4.0	1.0	Heavy clouds	2.70	.044	10.27	.166	99.05	1.939
11	1.0	1.0	2.5	1.5	1.0	3.5	5.0	1.5		3.06	.050	14.89	.245	137.50	3.060
12	1.0	1.0	3.0	2.0	1.0	4.0	6.0	2.0	Very heavy clouds	3.47	.057	20.20	.340	171.38	4.407

Notes:

1. Cases 2-12 are clear air and clouds combined.
2. Antenna located at sea level.
3. Heights are above ground.
4. No cosmic background or ground contribution considered.
5. T(K) is atmospheric noise temperature at zenith.
6. A(dB) is atmospheric attenuation along vertical path from ground to 30 km above ground.

Table 4-3. Coefficients a and b as a function of frequency and rain rate for calculation of atmospheric rain attenuation (Ippolito, 81a, 701; Olsen, 76, 318)

Marshall-Palmer drop distribution rain temperature 0°C

Frequency, GHz	Coefficient		α, dB/km, for R specified in mm/h		
	a	b	R=10 mm/h	50 mm/h	100 mm/h
2	3.45×10^{-4}	0.891	0.003	0.011	0.021
4	0.00147	1.016	0.015	0.078	0.158
6	0.00371	1.124	0.049	0.30	0.657
12	0.0215	1.136	0.29	1.83	4.02
15	0.0368	1.118	0.48	2.92	6.34
20	0.0719	1.097	0.90	5.25	11.24
30	0.186	1.043	2.05	11.0	22.7
40	0.362	0.972	3.39	16.2	31.8
94	1.402	0.744	7.78	25.8	43.1

Table 4-4. Summary of 11 GHz annual attenuation measurements for various geographical locations (Ippolito, 81a, 707)

Location	Elevation angle	Time period	Attenuation (dB) for given percent outage						
			1%	0.5%	0.1%	0.05%	0.01%	0.005%	0.001%
Waltham, MA	24°	Feb '77 - Jan '78	<1	<1	2.5	4	10.5	14.5	(23)
		Feb '78 - Jan '79	<1	<1	1.5	2.8	8.5	11	15.3
Holmdel, N.J	27°	Jun '76 - Jun '77	<1	<1	3	5	13.5	-	-
		Jun '77 - Jun '78	<1	<1	3	5	13.5	19.5	-
		Jun '78 - Jun '79	<1	<1	2.5	3.6	9.2	12.2	20
Greenbelt, MD	28°	Jul '76 - Jun '77	<1	<1	1.6	3.2	8.8	14.5	>30
		Jul '77 - Jun '78	<1	<1	2.1	3.6	12	18	26.4
		Jul '78 - Jun '79	<1	<1	1.8	3.2	14	21	29.2
Blacksburg, VA	33°	Jan '78 - Dec '78	2	2.7	3.7	4.3	6.8	8.6	13
		Jan '77 - Dec '77	2	2.5	4	5	13	18.5	24
Austin, TX	49°	Feb '78 - Jan '79	<1	1	3	5.5	13	18	23
Munich, Germany	29°	Jan '78 - Dec '78 (91.2% coverage)	3	4	6.8	-	-	-	-
Fucino, Italy	30°	Jan '78 - Dec '78	1	1	2	2.5	4	5.2	12
Lahio, Italy	30°	Jan '78 - Dec '78	1	1	2	2.7	4.8	6.8	13.2
Nederhorst den Berg, Netherlands	27.5°	Aug '75 - Oct '75 Apr '76 - Jun '77 (8100 hrs.)	.6	1	1.5	1.8	3.2	3.8	6
Kashima, Japan	38°	Aug '78 - Jun '79	-	-	2.2	3	5.3	6.5	11
	47°	May '77 - Apr '78	1	1.2	2.5	3.5	6.2	7.5	15.5

Table 4-5. Comparison of Goldstone 8.5 GHz (X-band) and 31.4 GHz (K_a band) predicted confidence level of troposphere loss and noise temperature at 30° elevation angle (R. Clauss, 82)

Confidence level, %		0	50	80	90	95	98	99	99.5
Tropospheric loss, dB	X-band	0.06	0.06	0.08	0.09	0.11	0.13	0.14	0.19
	K_a-band	0.16	0.31	0.41	0.47	0.58	0.72	0.91	1.23
Tropospheric noise Temperature, K	X-band	4	4	5	6	7	8	9	12
	K_a-band	10	19	25	29	35	43	53	69

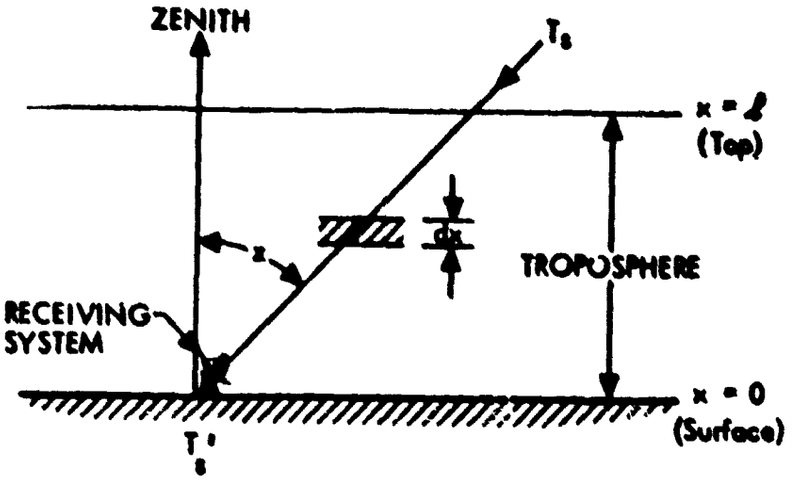

Fig. 4-1. Representation of a receiving system with signal propagating through lossy medium

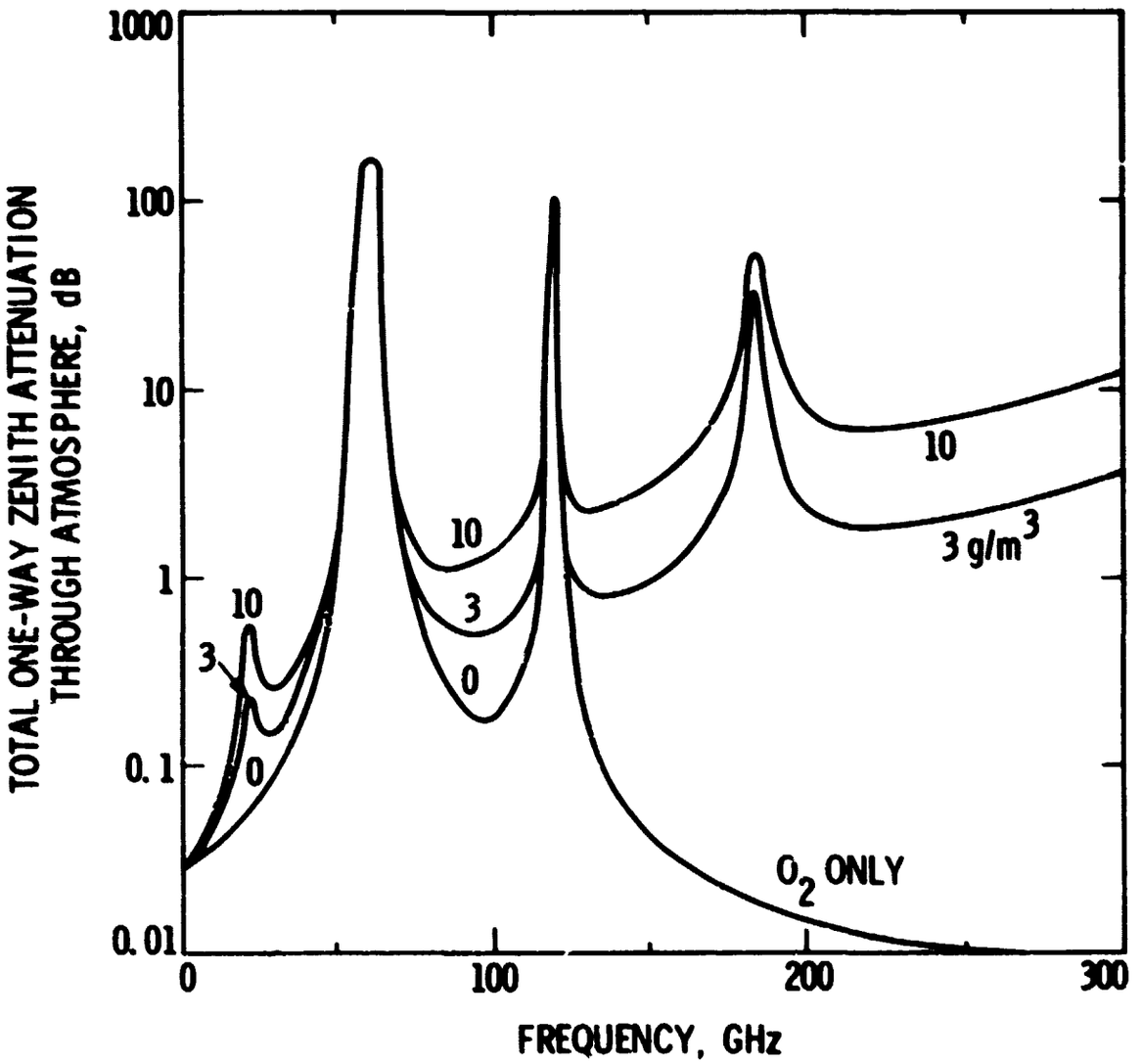

Fig. 4-2. Clear sky zenith atmospheric attenuation as a function of frequency and surface water vapor density (assuming exponential decrease with 2-km scale height; Smith and Waters, 81, 39)

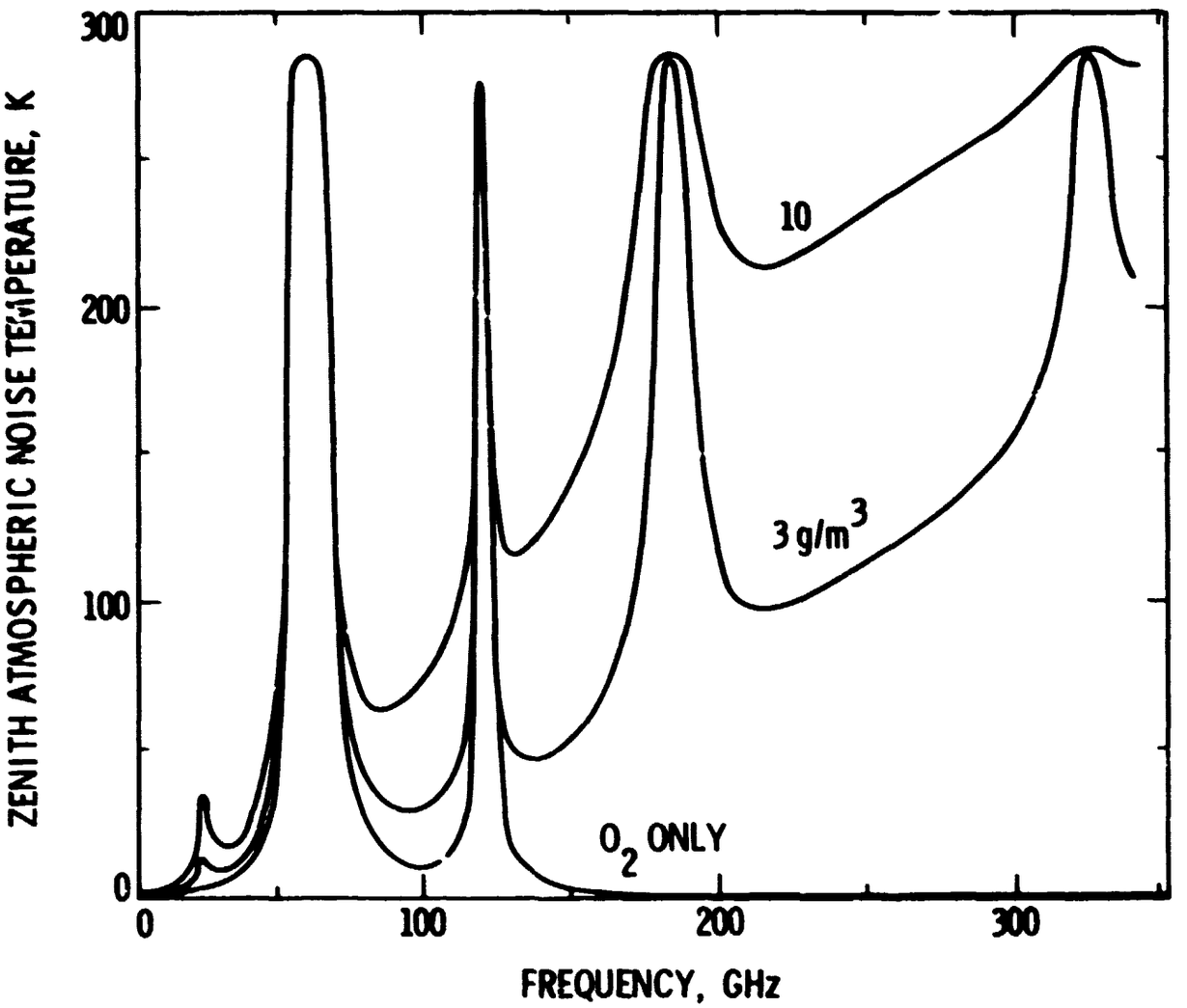

Fig. 4-3. Clear sky zenith atmospheric noise temperature as a function of frequency and surface water vapor density (assuming exponential decay with 2-km scale height; Smith and Waters, 81, 41)

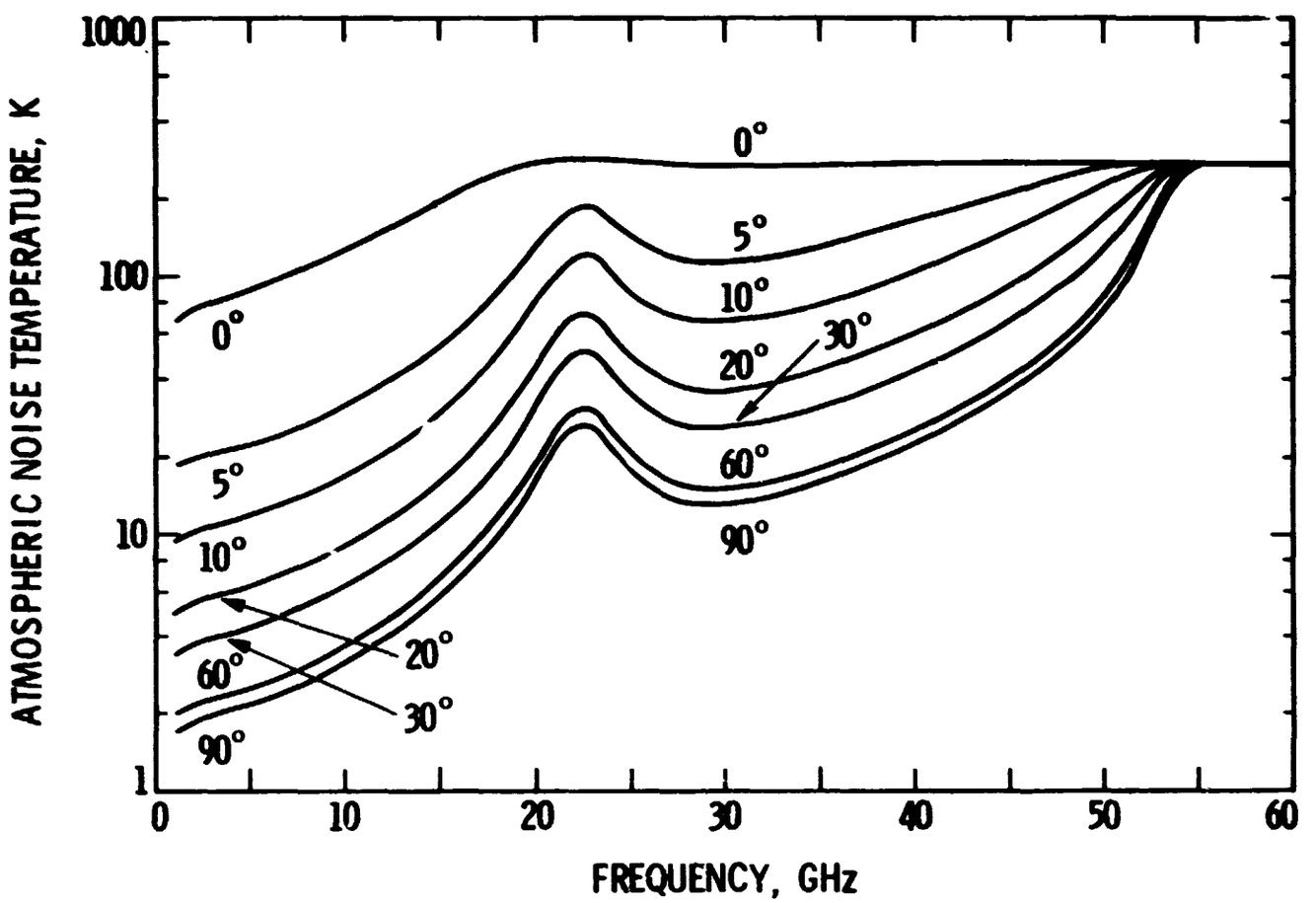

Fig. 4-4. Clear sky atmospheric noise temperature as a function of frequency and elevation angle (7.5 gm/m^3 surface water vapor density, assuming exponential decrease with 2-km scale height; Smith and Waters, 81, 42)

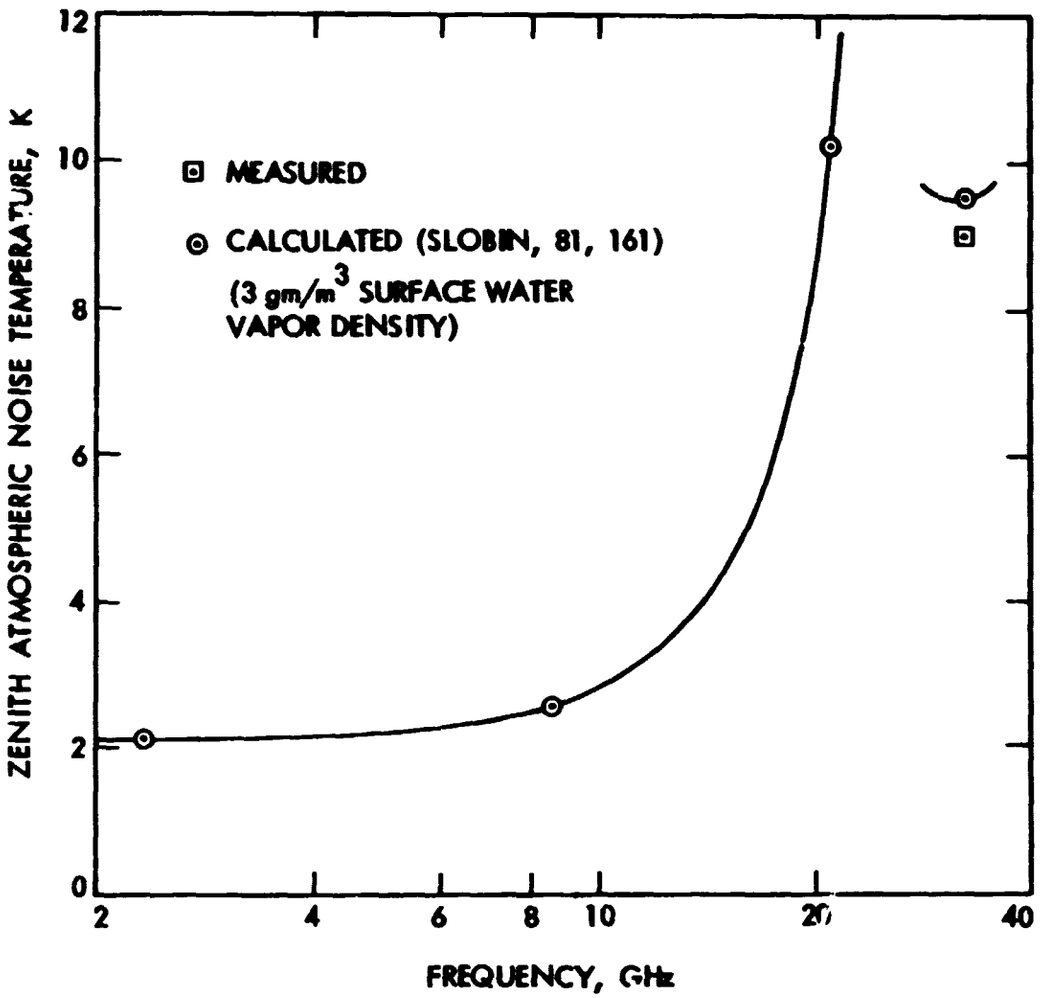

Fig. 4-5. Zenith clear sky atmospheric noise temperature as a function of frequency (Jet Propulsion Laboratory, Goldstone, CA)

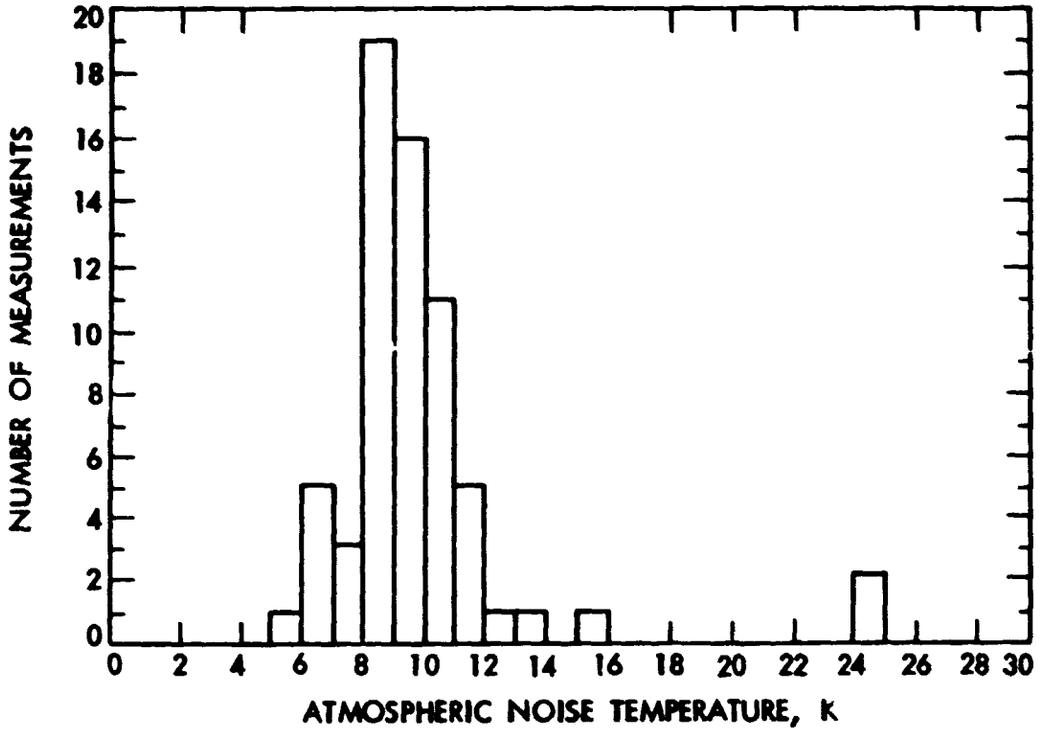

Fig. 4-6. Zenith clear sky atmospheric 31.5 GHz noise temperature measurements (obtained from tipping curve calibrations, Goldstone, CA from March 27-April 29, 1981)

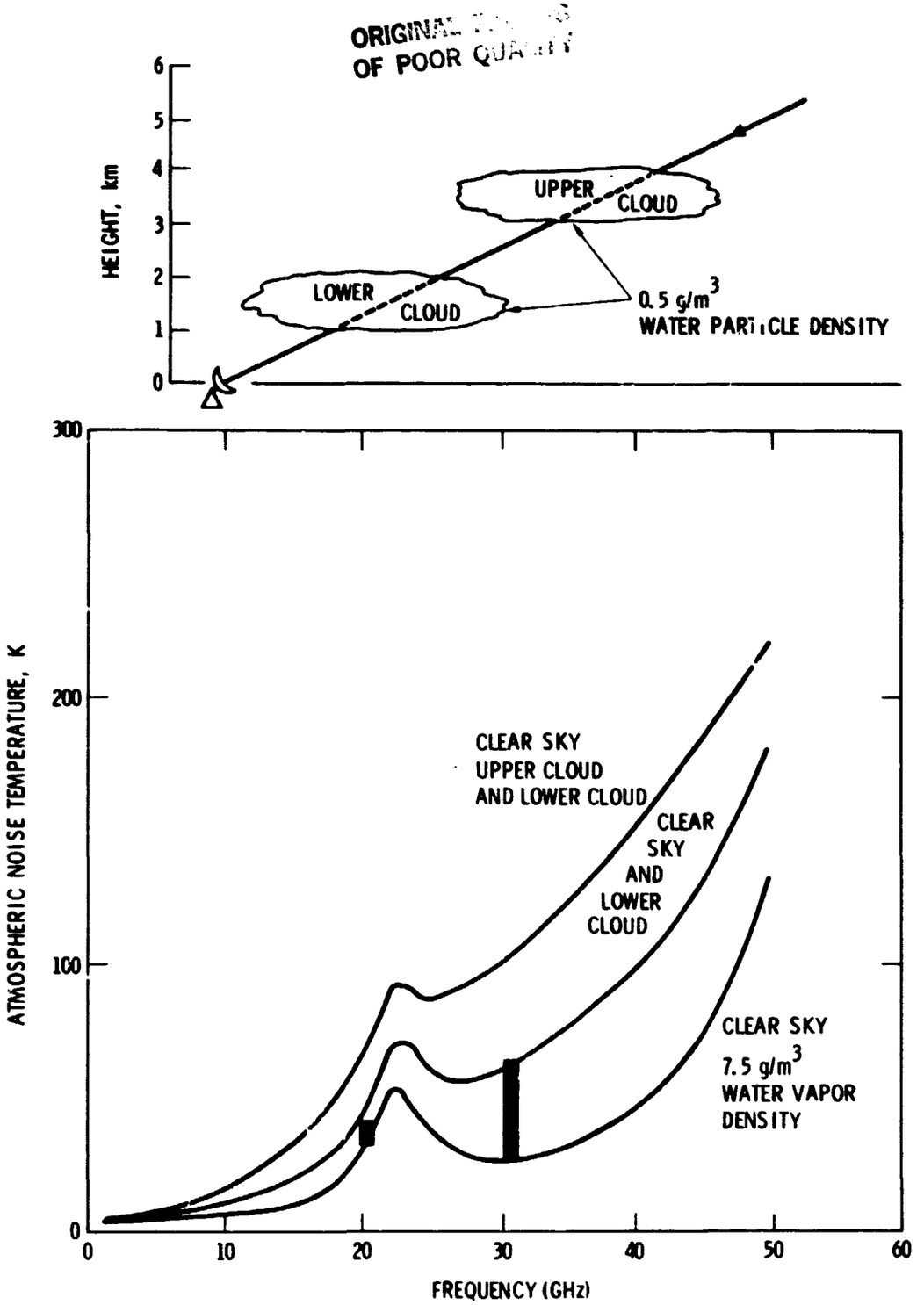

Fig. 4-7. Graph of atmospheric noise temperature vs frequency (assuming 30° elevation angle, clear sky or clear sky and one or two cloud models with 0.5 gm/m^3 cloud water particle density; after Slobin, 81a, 84); the vertical bars at 20.7 and 31.4 GHz represent the ranges of measured noise temperature increase indicated in Figs. 4-8 to 4-11

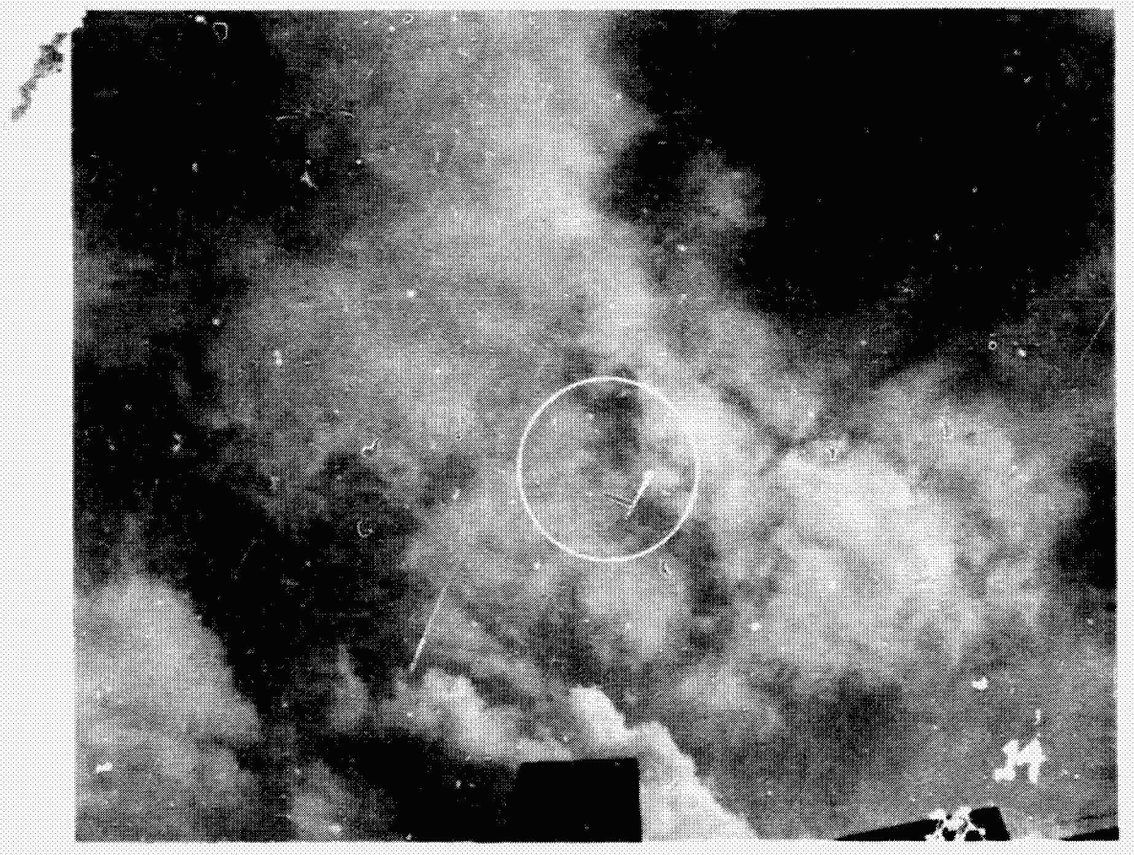

Fig. 4-8. Photograph of clouds observed from below the JPL mesa area. The increase in noise temperature due to the clouds was approximately 0 and 1 K at 20.7 and 31.4 GHz respectively

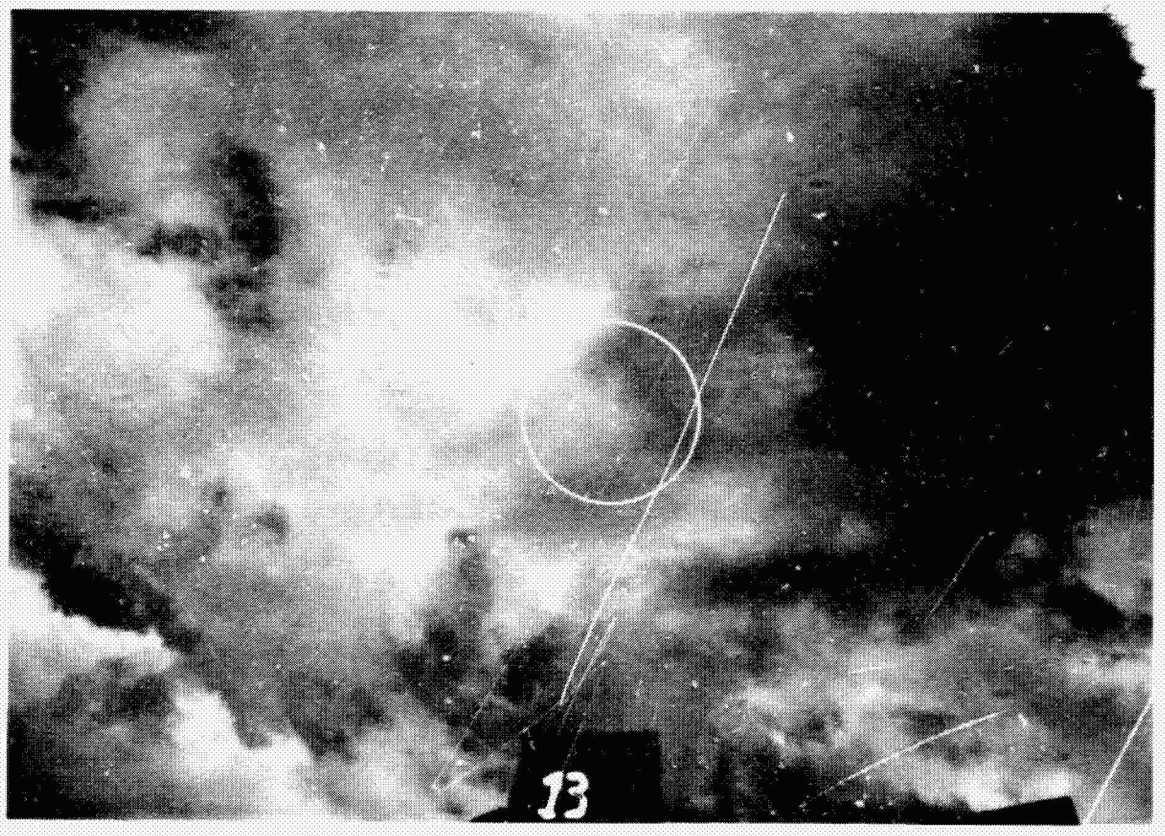

Fig. 4-9. Photograph of clouds observed from below the JPL mesa area. The increase in noise temperature due to the clouds was approximately 1 and 3 K at 20.7 and 31.4 GHz respectively

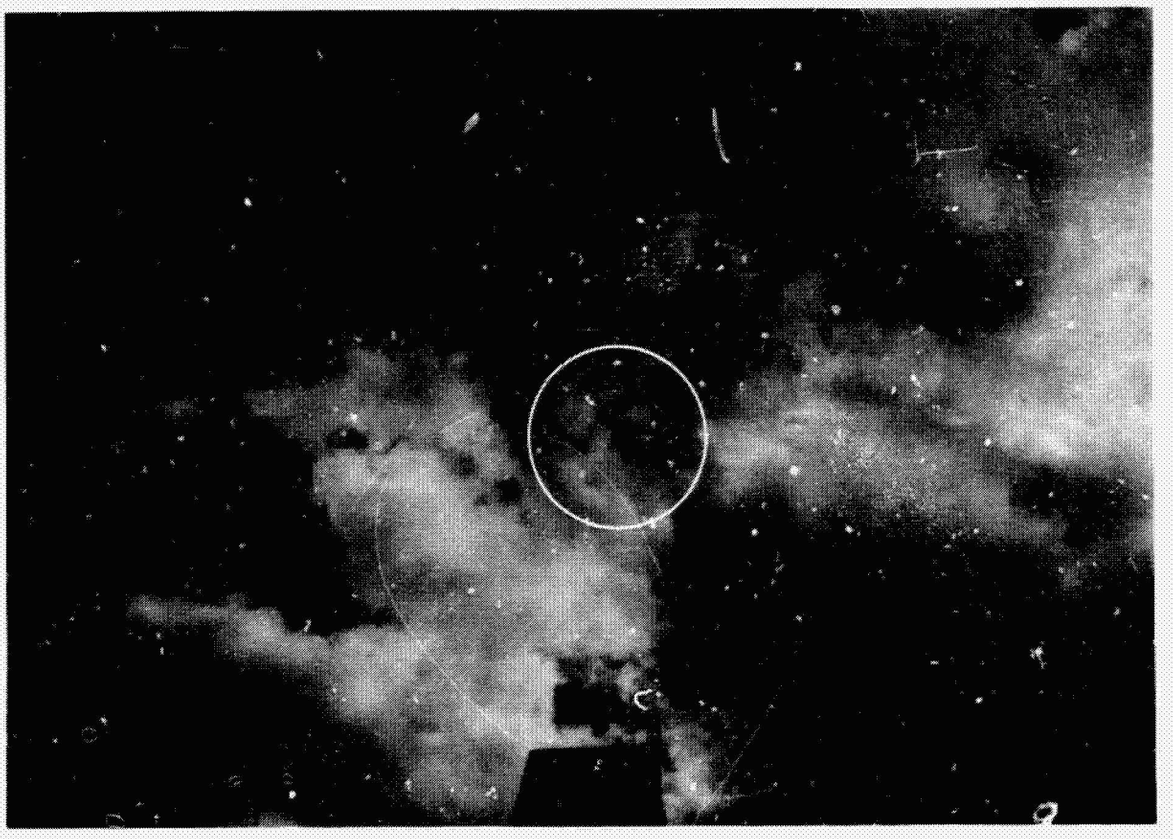

Fig. 4-10. Photograph of clouds observed from below the JPL mesa area. The increase in noise temperature due to the clouds was approximately 4 and 9 K at 20.7 and 31.4 GHZ respectively

Fig. 4-11. Photograph of clouds observed from below the JPL mesa area. The increase in noise temperature due to the clouds was approximately 19 and 38 K at 20.7 and 31.4 GHz respectively

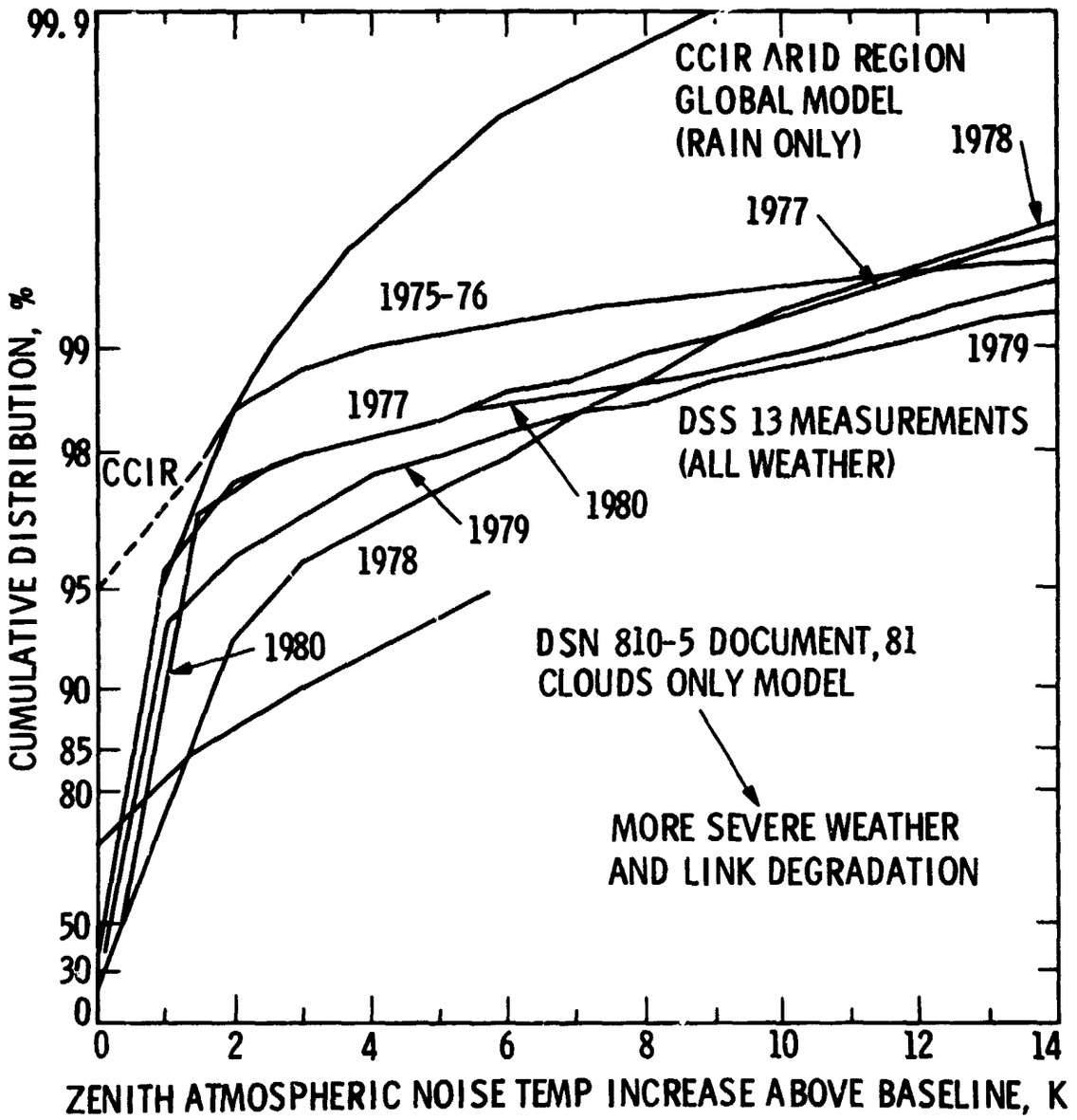

Fig. 4-12. Cumulative distribution of X-band (8.5 GHz), all weather, zenith atmospheric noise temperature increase above quiescent clear sky baseline at DSS 13, Goldstone, CA (Slobin, 81b, 161)

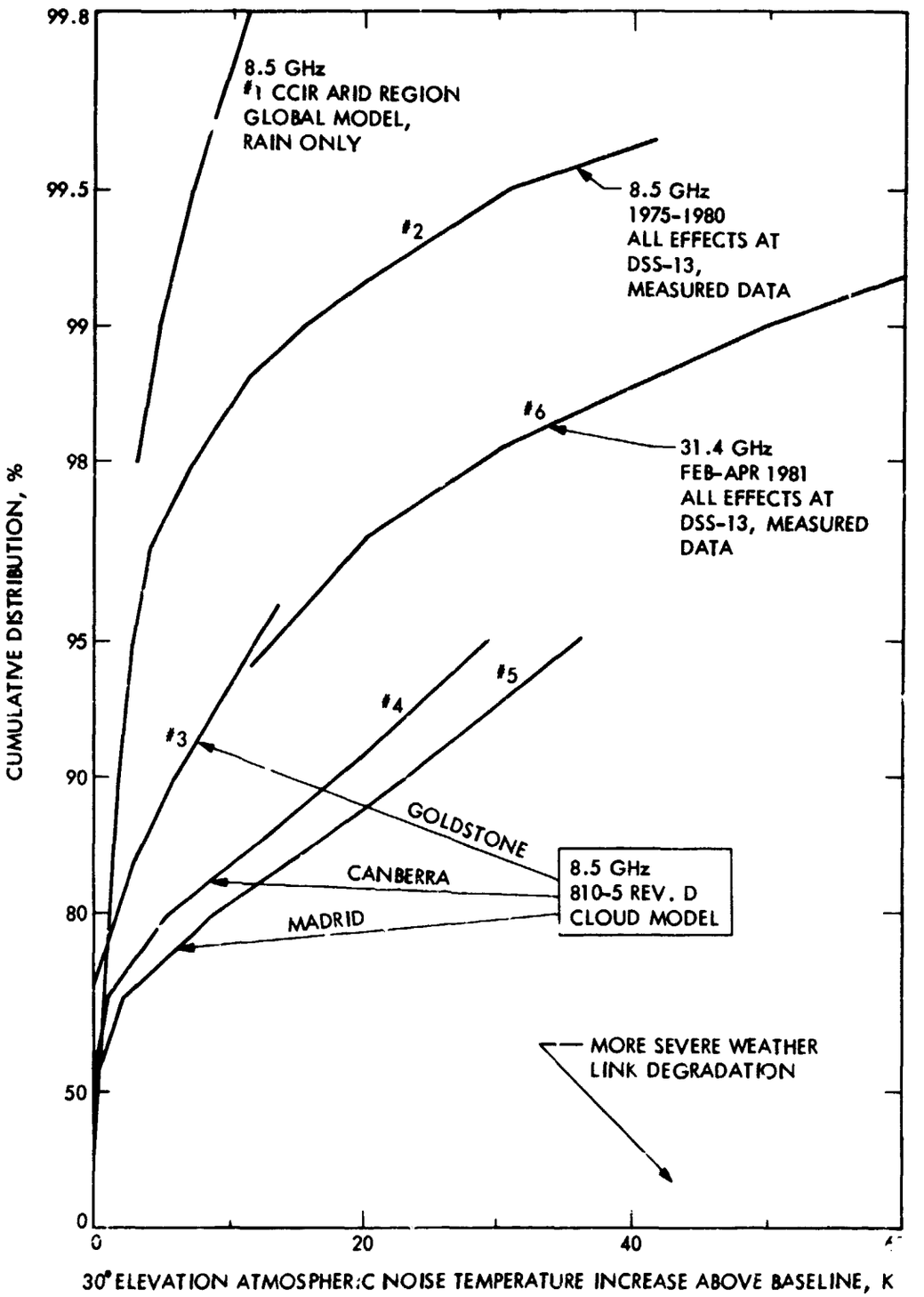

Fig. 4-13. Cumulative distributions of 8.4 and 31.4 GHz, 30° elevation atmospheric noise temperature increase above baseline (Clauss, 82)

5. Amplifier Input Noise Temperature

The noise performance of an amplifier (Haus, 63, 436) can be characterized by its effective input noise temperature T_e. For a single response amplifier (G>>1)[7],

$$T_e = N_{T_o} (T_i = 0\ K)/kBG \tag{5-1}$$

where

$N_{T_o} (T_i = 0\ K)$ = total output noise power of receiver with input termination temperature at 0 K, W

Alternately, T_e can be defined as the input termination temperature of an "ideal" noiseless amplifier with gain G, and bandwidth B which results in the same output noise power as the actual amplifier with an input termination temperature of 0 K.

For a multiple response receiver (Mumford, 68, 45)

$$T_e = N_{T_o} (T_i = 0\ K)/k(B_1G_1 + B_2G_2 + \ldots B_nG_n) \tag{5-2}$$

where

B_n = bandwidth of nth response, Hz

G_n = receiver gain to nth response. ratio

Recent low noise performance parameters of microwave low noise amplifiers are shown in Fig. 5-1 and Table 5-1.

---

[7] T_i = 0 for an "ideal" linear amplifier when hf<<kT and hf/k otherwise (Stelzried, 82, 100).

5. References

1963 Haus, H.A., "Description of the Noise Performance of Amplitiers and Receiving Systems", Proceedings of the IEEE, Vol. 58, Nc. 1, (March 1963), pg. 436.

1968 Mumford, W.W., Noise Performance Factors in Communication Receivers, Horizon House - Microwave, Inc. (1968).

1980 Weinreb, S., "Low-Noisc Cooled GASFET Amplifiers", Electronics Div. Report No. 202, NRAO, Charlottesville, Virginia, (April 1980).

1980 Williams, D. R., Lum W., Weinreb S., "L-Band Cryogenically-Cooled Ga As FET Amplifier", Microwave Journal, Vol. 23, (Oct. 1980), pgs. 73-76.

1981 Lum, W., private communications.

1982 Clauss, R., private communications.

1982 Stelzried, C.T., "Noise Temperature and Noise Figure Concepts: DC to Light", TDA Progress Report, 42-67, Jet Propulsion Laboratory, Pasadena, CA, (Feb. 1982) pg. 100.

Table 5-1. Recent (1981) S- and X-band microwave low noise amplifier noise temperature performance

	Maser[a]	FET[b]	
	Physical temperature, K		
Frequency, GHz	4	77	300
2.3 (S-band)	1.9 K	12 K	60 K
8.5 (X-band)	3.2 K	50 K	220 K

[a] In field use: R. Clauss, 82 Pasadena, CA.
[b] Laboratory: D. Williams, 80 Berkeley, CA.

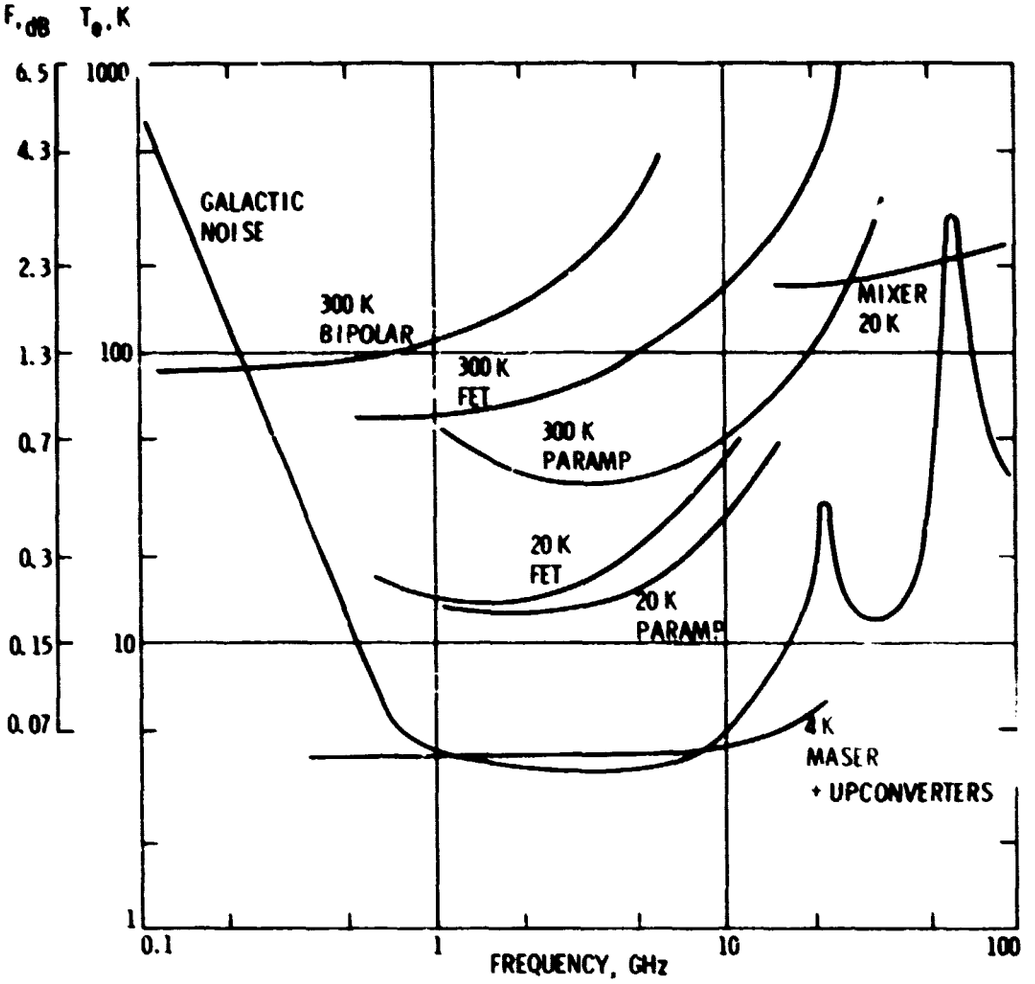

Fig. 5-1. Recent (1980) noise performance for low noise amplifiers as a function of frequency (Weinreb, 80)

6. Input Noise Temperature of Cascaded Amplifiers

Consider an amplifier consisting of two internal amplifiers in cascade (Mumford, 68, 22; Fig. 6-1). Assume $G_1 \gg 1$, $G_2 \gg 1$, $B = B_2 \leq B_1$[8], $G = G_1 G_2$.

We have

$$N_{T_o} = k(T_i + T_e)\, BG \tag{6-1}$$

where

N_{T_o} = total output noise power of combined amplifier, W
T_e = effective input noise temperature of combined amplifier, K
T_i = noise temperature of input termination, K

Also

$$N_{T_o} = k\, T_{e2} BG_2 + k(T_i + T_{e1}) BG_1 G_2 \tag{6-2}$$

Equating Eqs. 6-1 and 6-2 and setting $T_i = 0$,

$$T_e = T_{e1} + (T_{e2}/G_1) \tag{6-3}$$

---

[8]Gain response of the second amplifier is centered within the gain response of the first amplifier.

For multiple amplifiers,

$$T_e = T_{e1} + (T_{e2}/G_1) + (T_{e3}/G_1G_2) + \ldots + (T_{en}/G_1G_2\ldots G_{n-1}) \quad (6\text{-}4)$$

If $B = B_1 < B_2$,

$$T_e = T_{e1} + (T_{e2}B_2/G_1B_1) + \ldots \quad (6\text{-}5)$$

6. References

1968 Mumford, W.W. and Scheibe, E.H., Noise Performance Factors in Communication Systems, Horizon House - Microwave, Inc., (1968).

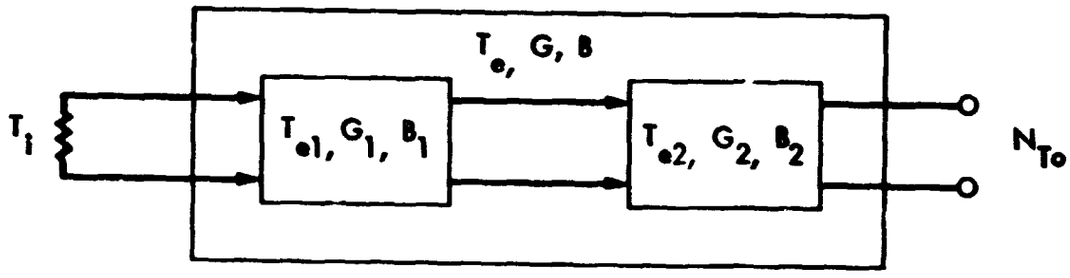

Fig. 6-1. Combined amplifier consisting of two amplifiers in cascade

7. System Operating Noise Temperature

The noise performance of a receiving system is determined by the sum of the input termination temperature and the receiver effective noise temperature. For a single[9] response receiver (G>>1, hf<<kT),

$$T_{op} = N_{T_o} / kBG \qquad (7\text{-}1)$$

where

T_{op} = system operating noise temperature, K

N_{T_o} = total output noise power of the receiving system, W

Also[10] (Haus, 63, 434)

$$T_{op} = T_i + T_e \qquad (7\text{-}2)$$

For an "ideal" receiver[10], $T_e = 0$, and $T_{op} = T_i$.

For a communication receiving system, T_i represents the antenna temperature, T_a. In general, T_i could be a thermal noise standard (Sec. 20) or the output of the source termination at the defined reference plane (Sec. 8).

The signal to noise performance of a linear receiving system is given by,(hf<<kT)

---

[9] The following assumes receivers with a single response; multiple responses require (Mumford 68,33) modification of the equations.

[10] When hf ≠ <<kT, $T_{op} = T_i' + T_e$, where $T_i' = T_i\ (hf/kT_i) / \left(e^{hf/kT_i} - 1\right)$ and T_{op} (ideal) = $T_i + (hf/k)$, (Sec. 2; Stelzried, 82, 100).

$$\left.\begin{aligned} S/N &= S_i G/N_{To} \\ &= S_i/kT_{op}B \\ &= S_i/k(T_i + T_e)B \\ &= S_i/k(T_i + (F-1)T_o)B \end{aligned}\right\} \qquad (7\text{-}3)$$

where

S_i = input signal power, W

For $(0 \leq (hf/kT) \leq \infty)$

$$\left.\begin{aligned} (S/N) &= S_i/kT_{op}B \\ &= S_i/k(T_i' + T_e)B \\ &= S_i/k(T_i' + (F-1)T_o' + FT_q)B \end{aligned}\right\} \qquad (7\text{-}4)$$

and for $hf \gg kT$[11]

$$\left.\begin{aligned} (S/N) &= S_i/(kT_{op}B) \\ &= S_i/kT_eB \\ &= S_i/FkT_qB = S_i/FhfB \end{aligned}\right\} \qquad (7\text{-}5)$$

The performance of a receiving system composed of an "ideal" amplifier ($T_e = T_q$) and a source at the cosmic background temperature (T_i = 2.7 K) is shown in Fig. 7-1 and Table 7-1 (from Stelzried, 82, 100). This demonstrates the loss in sensitivity at very high frequencies relative to low frequencies for a conventional receiving system with an "ideal" linear receiver.

---

[11] A typical infrared detector produces an output voltage proportional to input power. The sensitivity of these detectors is frequently described by their NEP (Noise Equivalent Power, W-Hz$^{1/2}$; Kruse, 62, 268, Gagliardi, 82). For these detectors ($hf \gg kT$), $(S/N) = S_i^2/(NEP)^2B$ referred to the input or voltage signal to noise ratio = VSNR = $S_i(NEP)\sqrt{B}$ referred to the output. For comparison with Table 7-1, an ideal detector at 1 mm has an NEP = 1.9×10^{-19} W$\sqrt{\text{Hz}}$ so that VSNR = $S_i/(1.9 \times 10^{-19})\sqrt{B}$.

It is instructive to consider this relationship for a receiving system degraded by an additional 0.1 dB of input absorption loss (possibly due to atmospheric changes). With high system noise temperatures (T_{op}>>290 K) this degrades S/N by ≈ 0.1 dB due to the additional direct signal attenuation. With low system noise temperatures (T_{op}<<290 K) this has a ver much larger effect due to the increase in T_{op} caused by the added thermal noise contribution. Assume

$$T_{op} = (T_{op})_o + \Delta T_{op}, \tag{7-6}$$

where

T_{op} = system noise temperature assuming atmospheric loss L, K

$(T_{op})_o$ = system noise temperature assuming a baseline atmospheric loss L_o, K

ΔT_{op} = increase in system noise temperature due to loss increase from L_o to L, K

$= (L_o^{-1} - L^{-1})(T_p - T_s)$

T_p = atmosphere equivalent physical temperature for loss L, K

L = atmospheric loss, ratio

L_o = baseline atmospheric loss, ratio

T_s = cosmic background noise temperature, K

The degradation in signal to noise ratio is given by

$$\Delta(S/N) = \Delta A + 10\log\left[T_{op}/(T_{op})_o\right], \text{ dB} \tag{7-7}$$

or

$$\Delta(S/N) = \Delta A + 10\log\left[1 + (T_p - T_s)(1 - 10^{-\Delta A/10})/L_o(T_{op})_o\right], \text{ dB} \tag{7-8}$$

where

ΔA = increased atmospheric absorption, dB

$= (A-A_o)$

$= 10\log (L/L_o)$

$A = 10 \log L$

$A_o = 10 \log L_o$

Fig. 7-2 indicates the degradation of S/N as functions of the baseline system temperature, baseline atmospheric absorption and increase in atmospheric absorption. This analysis technique has been used to compare the confidence performance of 8.5- and 31.4-GHz receiving systems. Table 7-2 shows the link SNR degradation computed using the data from Table 4-5; the resultant performance improvement at 31.4 GHz is due to the higher antenna gain relative to 8.5 GHz. This analysis accounts only for weather effects - all other possible degradations are neglected.

7. References

1962 Kruse, P. W., McGlauchlin, L. D., and McQuistan, K. B., Elements of Infrared Technology: Generation, Transmission, and Detection, J. Wiley and Sons, Inc., N.Y., (1962).

1963 Haus, H.A., "Description of the Noise Performance of Amplifiers and Receiving Systems", Proceedings of the IEEE, Vol. 58, No.3, (March 1963), pg. 436.

1968 Mumford, W.W. and Scheibe, E.H., Noise Performance Factors in Communication Systems, Horizon House - Microwave, Inc., (1968).

1982 Clauss, R., Franco, M. and Slobin, S., "K_a Band Weather Dependent System Performance Estimate for Goldstone", TDA Progress Report 42-70, Jet Propulsion Laboratory, Pasadena, CA, August 15, 1982.

1982 Gagliardi, R. M., Private communication

1982 Stelzried, C.T., "Noise Temperature and Noise Figure Concepts: DC to Light", TDA Progress Report 42-67, Jet Propulsion Laboratory, Pasadena, CA, (Feb. 1982), pgs. 100-110.

Table 7-1. Tabulation of the sensitivity of an "ideal" receiver ($T_e = T_q$) with an input source temperature of 2.7 K as a function of frequency

Parameter	Frequency (GHz) (Wavelength)					
	0.0	8.5 (3.5 cm)	32 (9.4 mm)	300 (1 mm)	3000 (0.1 mm)	300,000 (1 um)
T_i', K	2.7	2.5	2.0	0.1	0.0	0.0
$T_e(=T_q)$, K	0.0	0.4	1.5	14.4	144.0	14,400
T_{op}, K	2.7	2.9	3.5	14.5	144.0	14,400
S_i, dbm/Hz[a] (w/Hz)	-194.3 (3.73×10^{-23})	-194.0 (4.00×10^{-23})	-193.1 (4.83×10^{-23})	-187.0 (2.00×10^{-22})	-177.0 (1.99×10^{-21})	-157.0 (1.99×10^{-19})

[a] S_i is the input signal power required for (S/N) = 1. Since the energy of a photon is hf, $S_i = (T_{op}/T_q)$, photons /sec-Hz. Therefore $S_i \simeq 7$, 2 and 1 photons/sec-Hz for this system at 8.5, 32 and > 300 GHz respectively

Table 7-2. Comparison of Goldstone 8.5 GHz (X-band) and 31.4 GHz (K_a band) predicted confidence level of link SNR loss and receiving system SNR improvement at 30° elevation angle

Confidence level, %	0	50	80	90	95	98	99	99.5
Link SNR loss caused by the atmosphere, K_a-band relative to X-band, dB[a]	0.89	2.21	2.90	3.31	3.86	4.51	5.20	6.14
Link SNR improvement, K_a-band relative to X-band, dB[b]	10.62	9.30	8.61	8.20	7.65	7.00	6.31	5.37

[a]R. Clauss, 82, assuming baseline system noise temperatures of 72 K with 4 K atmospheric contribution at 30° elevation angle for X-band and 26 K with 10 K atmospheric contribution at 30° angle for K_a-band.

[b]This improvement accounts for atmospheric loss and noise temperature; antenna sizes and efficiencies and transmitted powers are assumed equal for both X- and K_a-bands.

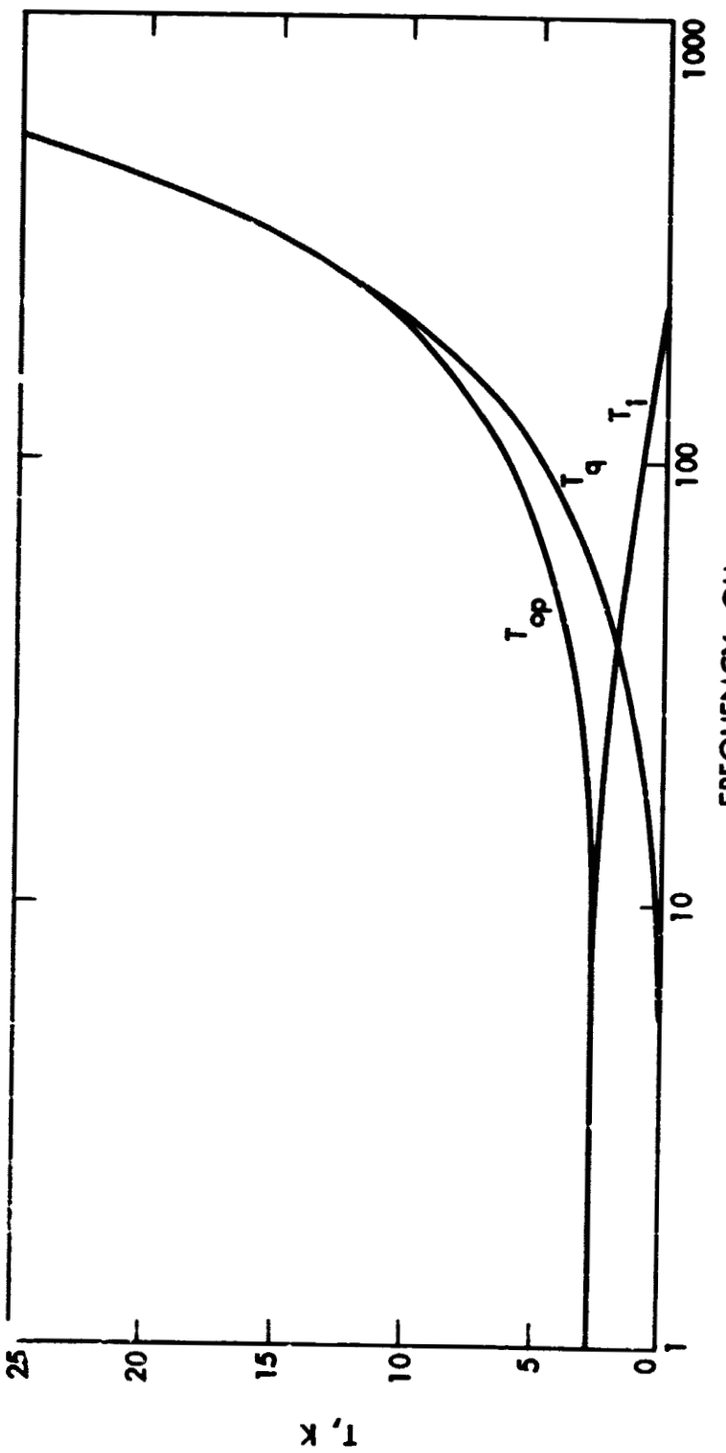

Figure 7-1. T_i', T_q', and T_{op} vs frequency using an "ideal" receiver ($T_e = T_q$) with an input source temperature of 2.7 K.

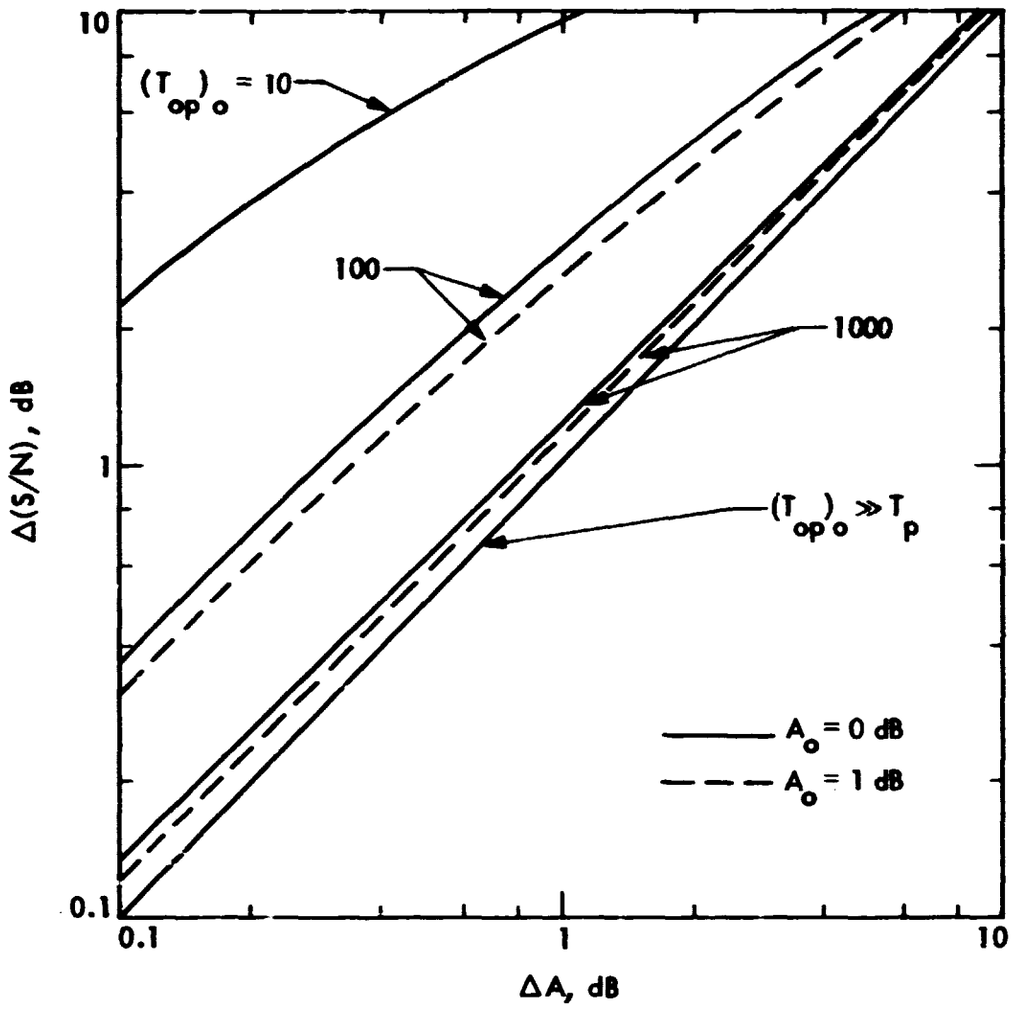

Fig. 7-2. (S/N) degradation vs atmospheric absorption increase as a function of the baseline system noise temperature $(T_p - T_s)$ = 280 K.

8. Shifting the Reference Plane of Cascaded Amplifiers

The previous concepts of noise temperature (T_i, T_e and T_{op}) are applicable to a defined reference plane in a typical receiving system. Assuming a linear receiving system and $hf \ll kT$, the signal to noise (Eq. 7-3) ratio is invariant regardless of the chosen reference plane. Then (Fig. 8-1)

$$(T_{op})_2 = (T_{op})_1 / L \tag{8-1}$$

and

$$(T_{op})_3 = G(T_{op})_2 \tag{8-2}$$

where

$(T_{op})_n$ = T_{op} defined at reference plane n, K
= $(T_i)_n + (T_e)_n$
L = attenuator loss, ratio ($L \geq 1$; assumed "matched")

$(T_i)_n$, $(T_e)_n$ = T_i and T_e defined at reference plane n, K

Also (Mumford, 68, 19)

$$(T_i)_2 = \left[(T_i)_1 / L\right] + (1 - 1/L)\, T_P \tag{8-3}$$

where

T_P = physical temperature of attenuator, K

With Eqs. 5-1 and 7-2,

$$(T_e)_2 = \left[(T_e)_1 / L\right] - (1 - 1/L)\, T_P \tag{8-4}$$

Also (Eq. 8-3),

$$(T_i)_1 = L(T_i)_2 + (L - 1)\, T_p \tag{8-5}$$

and

$$(T_e)_1 = L(T_e)_2 - (L - 1)\, T_p \tag{8-6}$$

The output signal to noise ratio is ($hf \ll kT$)

$$(S/N)_o = (S_i)_n / k(T_{op})_n B \tag{8-7}$$

where

$(S_i)_n$ = signal power at the receiving system reference plane n, W

The reference plane chosen in a particular receiving system is usually dictated by physical constraints; the JPL Deep Space Network has historically chosen the reference plane at the receiver input.

The above techniques can be used to transfer T_i, T_e, or T_{op} defined at any given reference plane to any other chosen reference plane. However, T_i, T_e and T_{op} must all be defined at the same reference plane.

8. References

1968 Mumford W. W. and Scheibe, E. H., Noise Performance Factors in Communication Systems, Horizon House-Microwave, Inc., Dedham, Mass. (1968).

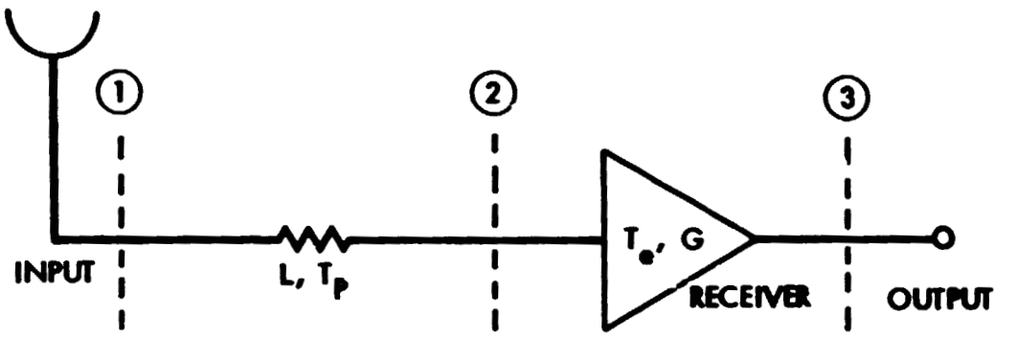

Fig. 8-1. Receiving system representation

9. Relationship of Noise Figure to Noise Temperature

The definition (Haus, 63, 434) of an amplifier noise figure is (neglecting quantum effects; hf<<kT),

$$F = N_{T_o} (T_i = T_o)/k\, T_o\, BG \tag{9-1}$$

where

N_{To} $(T_i=T_o)$ = total output noise power of the receiver with the input termination at T_o, W

$T_o = 290$ K

From Eqs. 7-1, 7-2 and 9-1[12],

$$F = 1 + T_e/T_o \tag{9-2}$$

or

$$T_e = (F - 1)\, T_o \tag{9-3}$$

In terms of F,

$$T_{op} = T_i + (F - 1)\, T_o \tag{9-4}$$

For an "ideal" amplifier (hf<<kT), $T_e = 0$ and $F = 1$ (see Sec. 2).

---

[12] When hf $\not<<$ kT, quantum effects cannot be ignored. Then, it is proposed (Stelzried, 82, 100) that $F = (1 + T_e/T_o')/(1 + T_q/T_o')$ where $T_o' = T_o(hf/kT_o)/(e^{hf/kT_o}-1)$ and $T_q = (hf/k)$. Then, for an "ideal" receiver, $T_e = (hf/k)$ and $F = 1$.

9. Reference

1963 Haus, H.A., "Description of the Noise Performance of Amplifiers and Receiving Systems", Proceedings of the IEEE, (March 1963), pg. 434.

1982 Stelzried, C.T., "Noise Temperature and Noise Figure Concepts: DC to Light", TDA Progress Report 42-67, Jet Propulsion Laboratory, Pasadena, CA, (Feb. 1982), pgs. 100-111.

10. Measurements of Antenna Temperature

The evaluation of antenna noise temperature T_a is usually an intermediate measurement. For example, we have

$$T_{op} = T_a + T_e \tag{10-1}$$

where

T_a = antenna temperature, K

Separate measurements of T_a and T_e can be used to obtain T_{op}. T_a has multiple contributors,

$$T_a = T_s + T_{atm} + T_g + \ldots \tag{10-2}$$

where

T_s = cosmic noise background temperature, K
T_{atm} = atmospheric contribution to antenna noise temperature, K
T_g = ground contribution (due to antenna spillover, etc.; Otoshi, 67, 143) to antenna noise temperature, K

T_s is determined (Penzias, 65, 419-421; Otoshi, 75, 174) from

$$T_s = T_a - T_{atm} - T_g - \ldots \tag{10-3}$$

Antenna noise temperature T_a can be measured using matched thermal noise standards. Switching sequentially between the thermal noise standards and the antenna (Fig. 10-1, $hf \ll kT$, matched antenna and thermal noise standards, linear receiving system),

$$T_a = T_C + (T_H - T_C)(Y_2 - 1)/(Y_1 - 1) \qquad (10\text{-}4)$$

where

$Y_1 = P_H/P_C$, ratio
$Y_2 = P_A/P_C$, ratio
P_A = receiver output power when switched to antenna, W
P_H = receiver output power when switched to T_H, W
P_C = receiver output power when switched to T_C, W
T_H = thermal noise temperature of calibration source T_H, K
T_C = thermal noise temperature of calibration source T_C, K

Y_1 and Y_2 can be determined directly from power meter measurements or with a precision attenuator by adjusting for equal output levels when the receiver input is switched between the appropriate noise sources. The thermal noise standards (see Sec. 20) T_H and T_C are usually calibrated by measuring the transmission line insertion loss. The physical temperatures of the terminations are monitored with thermometers or maintained at a constant temperature by submersion in a boiling liquid, such as liquid nitrogen (boiling temperature 77.36 K at 760 mm Hg). It is usually convenient to select one of the terminations to be at ambient temperature due to the ease of construction and low sensitivity to errors in waveguide loss calibrations.

It is sometimes convenient (Franco, 81, 80), to use a square law detector ($V_{output} \propto T_{op}$) and voltmeter to interface with an automated computer system. For this configuration,

$$T_a = T_C + \frac{T_H - T_C}{V_H - V_C} (V_A - V_C) \qquad (10\text{-}5)$$

where

V_A = receiver output voltage when switched to antenna, V
V_H = receiver output voltage when switched to T_H, V
V_C = receiver output voltage when switched to T_C, V

Antenna temperature can also be found using

$$T_a = T_{op} - T_e \tag{10-6}$$

where T_{op} (Sec. 12) and T_e (Sec. 11) are measured separately. Assuming the errors in T_{op} and T_e are independent, the error in T_a is

$$\delta T_a = \sqrt{(\delta T_{op})^2 + (\delta T_e)^2} \tag{10-7}$$

where

δT_{op} = measurement error of T_{op}, K
δT_e = measurement error of T_e, K

A technique for measuring antenna temperature (or an unknown termination temperature) is illustrated in Fig. 10-2 which requires only one thermal noise standard T_C and a precision attenuator, frequently (Otoshi, 71, 843) a rotary vane attenuator. This technique has the advantage of eliminating receiver linearity errors (Sec. 24). Adjusting L for equal output noise levels (assuming $T_a \ll T_C$)

$$T_a = LT_C - (L - 1)\, T_P \tag{10-8}$$

where

T_p = physical temperature of L, K

Another technique (Schuster, 62, 786) for measurement of T_a which requires one thermal noise standard and a noise source is shown in Fig. 10-3. For this technique,

$$T_a = T_C + T_N(Y_1 - 1)/(Y_2 - 1) \tag{10-9}$$

where

$Y_1 = (P_A/P_C)$, ratio

$Y_2 = (P_{CN}/P_C)$, ratio

P_A = receiver output power, when switched to antenna, (noise source turned off), W

P_C = receiver output power, when switched to T_C, (noise source turned off), W

P_{CN} = receiver output power, when switched to T_C (noise source turned on), W

T_N = increase in system noise temperature when noise source turned on, K

This technique requires calibration of T_N, which can be accomplished by use of another thermal noise standard or by the method discussed in Sec. 12 using a single ambient termination applicable if $T_e \ll T_C$

It is frequently desirable to measure the change in antenna temperature. From Sec. 3,

$$\Delta T_a = T_s A_e A_s/(R\lambda)^2 \tag{3-3}$$

or

$$\Delta T_a = SA_e/2k \tag{3-4}$$

Antenna efficiency is given by

$$\eta = A_e/A_p \tag{10-10}$$

$$= 2k\Delta T_a/SA_p$$

where

A_p = antenna physical area, m^2

Figure 10-4 shows antenna efficiency (1972) vs elevation angle and frequency for the DSS 14 (Goldstone) 64-m antenna. The 15.3-GHz (K_u-band) measurements were performed using a noise adding radiometer (Sec. 19) and the planets Jupiter and Saturn for calibration sources.

10. References

1962 Schuster, D., Stelzried, C.T., and Levy, G.S., "The Determination of Noise Temperatures of Large Paraboloidal Antennas", Inst. of Radio Engineer Antennas and Propagation, AP-10, No. 3, (May 1962), pg. 286.

1965 Penzias, A.A., and Wilson, R.W., "A Measurement of Excess Antenna Temperature at 4080 Mc/s", Astro Phys. J., Vol. 142, No. 1, (July 1965), pgs. 419-421.

1967 Otoshi, T.Y. and Stelzried, C.T., "Computer Programs for Antenna Feed System and Design Analysis" (Ludwig, A.C., ed), Tech. Report No. 32-979, Jet Propulsion Lab, Pasadena, CA, (April 1967), pg. 143.

1971 Otoshi, T.Y. and Stelzried, C.T., "A Precision Compact Rotary Vane Attenuator", IEEE Trans on Microwave Theory and Techniques, Vol. MTT-19, No. 11, (Nov. 1971), pg. 843.

1975 Otoshi, T.Y. and Stelzried, C.T., "Cosmic Background Noise Temperature Measurement at 13-cm wavelength". IEEE Transactions on Instruments and Measurement, Vol. 24, No. 2, (June 1975), pg. 174.

1981 Franco, M.M., Slobin, S.D., Stelzried, C.T., "X-band Narrow Beam Radiometer for DSS-13", TDA Progress Report 42-66, Jet Propulsion Laboratory, Pasadena, CA, (Dec. 1981), pg. 80.

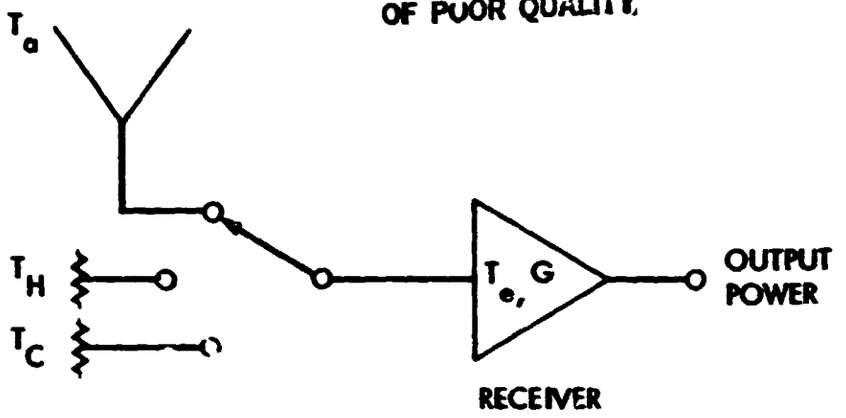

Fig. 10-1. Receiving system configuration for measuring antenna noise temperature using two thermal noise standards

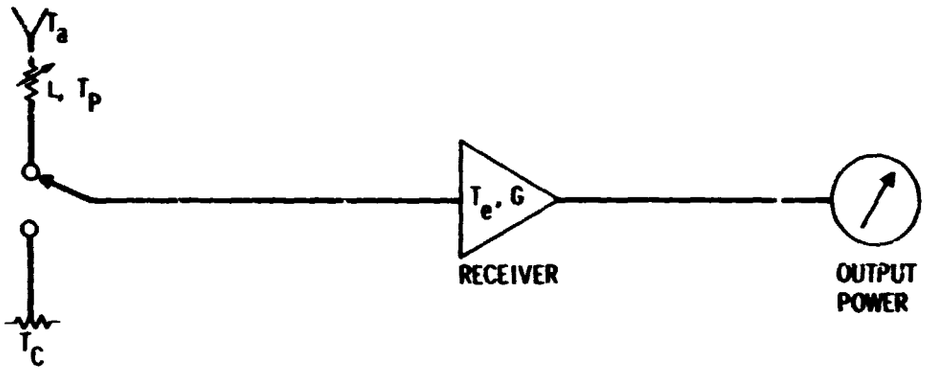

Fig. 10-2. Configuration for measuring antenna noise temperature using one thermal noise standard and a precision attenuator

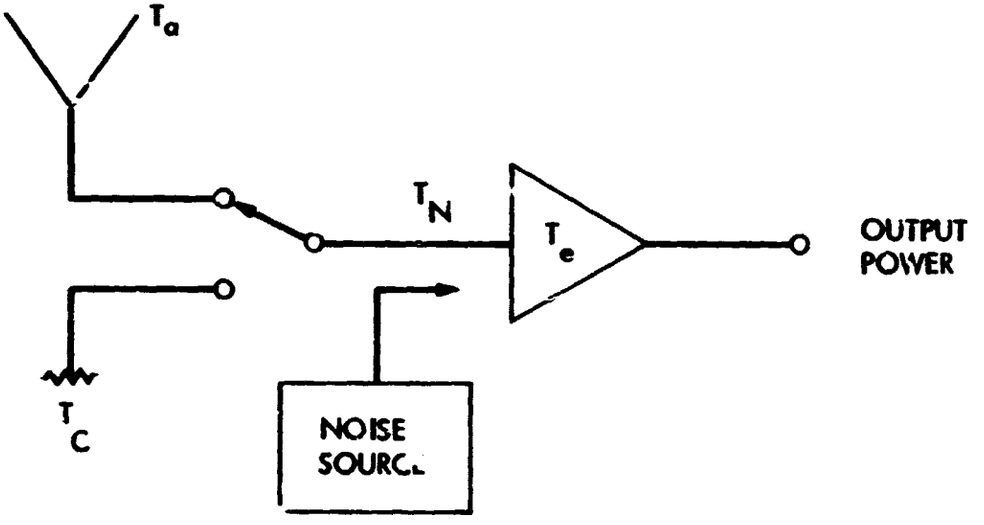

Fig. 10-3. Configuration for measuring antenna noise temperature using a thermal noise standard and a noise source

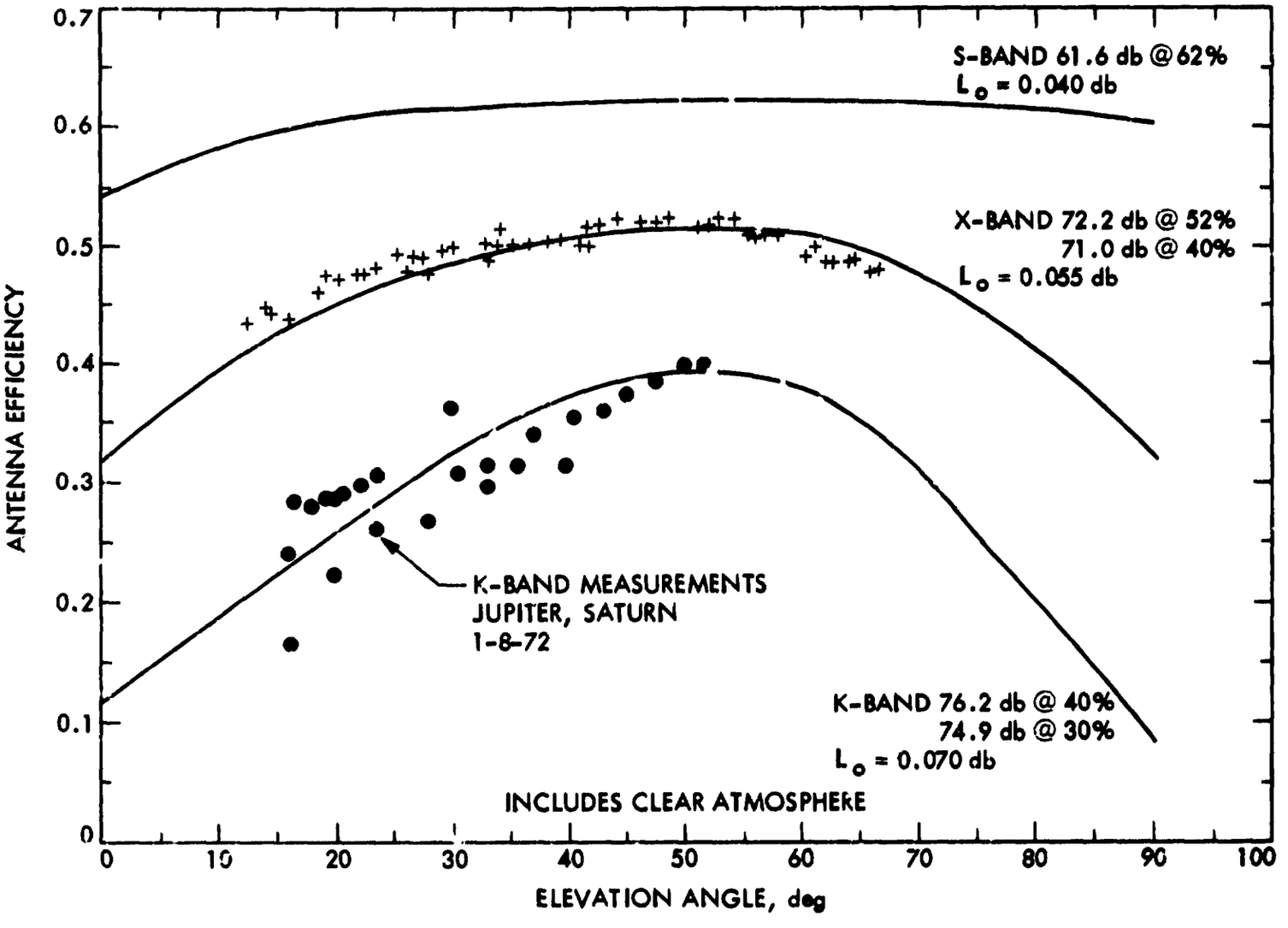

Fig. 10-4. Antenna efficiency vs elevation angle and frequency for the Goldstone, CA, DSS 14 64-m antenna (L_o is the zenith atmospheric loss)

11. Measurement of Receiver Input Noise Temperature

Receiver noise temperature (Mumford, 68, 58; Arthur, 74, 1-188) can be evaluated with thermal noise standards or auxiliary noise sources (gas-discharge tubes, noise diode, etc.). These measurements require careful attention to instrumentation detail such as "matched" thermal noise standards and "linear" amplifiers.

Switching (Stelzried, 82, 100; Wait, 73b, 25; Wait, 73a, 1-25) between the thermal noise standards (Fig. 11-1; $hf \ll kT$, P_H and P_C defined in Sec. 10)[13]

$$T_e = (T_H - YT_C)/(Y - 1) \qquad (11\text{-}1)$$

where

$$Y = (P_H/P_C), \text{ ratio}$$

It is sometimes convenient to use a calibrated noise source (Fig. 11-2) to calibrate the receiver noise temperature. Turning the noise source on and off,

$$T_e = \left[T_N/(Y - 1)\right] - T_i \qquad (11\text{-}2)$$

---

[13] If $hf \not\ll kT$, verify that T_H and T_C are properly calibrated (Stelzried, 82, 100); accounting for quantum noise does not impact the measurement technique or the equations; it simply sets a lower limit [$T_q = (hf/k)$ for a linear amplifier] to the value obtainable for T_e using a linear amplifier.

11. References

1968 Mumford, W.W. and Scheibe, E.H., Noise Performance Factors in Communication Systems, Horizon House - Microwave, Inc., (1968).

1973a Wait, D.F., "Measurement of Amplifier Noise," The Microwave Journal, Vol. 16, No. 1, (Jan. 1973), pg. 25.

1973b Wait, D.F., "Considerations for the Precise Measurement of Amplifier Noise," NBS Technical Note 640, NBS, (Aug. 1973).

1974 Arthur, M.G., and Anson, W.J., The Measurement of Noise Performance Factors: A Metrology Guide, U.S. Dept. of Commerce, NBS Monograph 142, Supt. of Doc. Cat. No. C13.44:142, Stock No. 0303-01290, (1974).

1982 Stelzried, C.T., "Noise Temperature and Noise Figure Concepts: DC to Light", TDA Progress Report 42-67, Jet Propulsion Laboratory, Pasadena, CA, (Feb. 1982), pgs. 100-111.

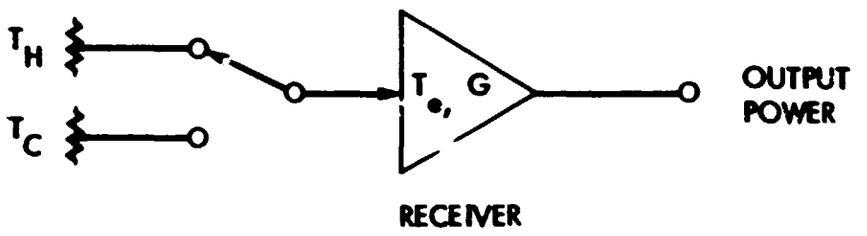

Fig. 11-1. Configuration for measuring receiver noise temperature using two thermal noise standards

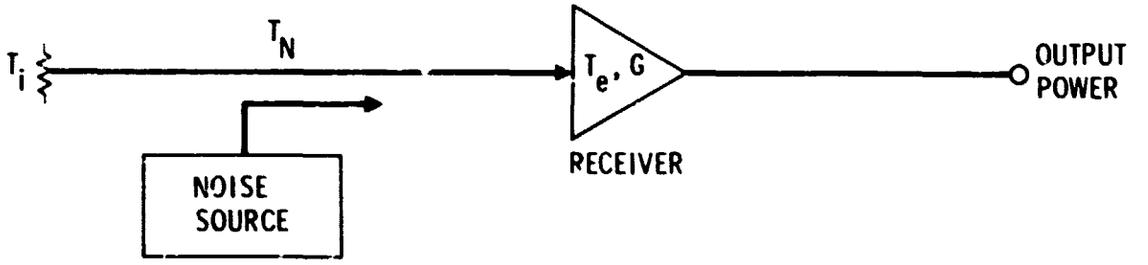

Fig. 11-2. Configuration for measuring receiver noise temperature using a noise source

12. Measurement of System Temperature

Using Eq. 7-2,

$$T_{op} = T_a + T_e \tag{12-1}$$

System temperature can be obtained from the measurement results of Secs. 10 and 11 of antenna and receiver noise temperatures. More directly, using the concepts of Sec. 10 (Fig. 10-1; P_A, P_C and P_H defined in Sec. 10),

$$T_{op} = (T_H - T_C)/(Y_2 - Y_1) \tag{12-2}$$

where

$$Y_1 = (P_C/P_A), \text{ ratio}$$

$$Y_2 = (P_H/P_A), \text{ ratio}$$

Thermal terminations at liquid helium (Fig. 12-1) and liquid nitrogen temperatures were used to determine the noise temperature of a maser system terminated in a liquid helium cooled termination. This 2.3-GHz maser system has a noise temperature of 15 K (Clauss, 64, 619).

Although, in general, calibration terminations at two different temperatures are required to solve for T_{op}, T_a, or T_e, it is sometimes convenient to use a single termination (Stelzried, 71, 41). This technique requires that $T_e \ll T_H$ for reasonable accuracy.

Switching between T_H and the antenna (Fig. 12-2)

$$T_{op} = (T_H + T_e)/Y \tag{12-3}$$

where

$$Y = (P_H/P_A)$$

For this calibration technique, the physical temperature of the standard termination T_H (usually an ambient termination) is monitored for T_H; T_e is considered known (from a previous laboratory measurement before installation in an operating receiving system). Assuming $T_e << T_H$, it is seen that a fairly large error in T_e does not have much effect on the measurement error of T_{op}. For example, if T_H = 295 K, T_e = 5 K, and Y = 10, then T_{op} = 30 K. A 100% error in T_e (i.e. T_e really 10 K) results in T_{op} = 31 K (an error of only 3.3%). This technique of monitoring system noise temperature using a single ambient reference is used by the JPL Deep Space Network with good results at a tremendous cost savings. A simplified technique for evaluating T_{op} using an aperture ambient termination is illustrated in Figs. 12-3 and 12-4. The noise temperature contributions for this 8.5-GHz system is shown in Table 12-1.

A summary of the JPL Goldstone maser receiving system's measured noise performance is given in Table 12-2.

T_{op} is commonly measured by providing a noise source T_N (Fig. 12-5). T_{op} is given by

$$T_{op} = T_N (Y - 1) \tag{12-4}$$

where

$Y = (P_{AN}/P_A)$, ratio
P_A = receiver output power, noise source off, W
P_{AN} = receiver output power, noise source on, W

The initial calibration of T_N can be performed by determination of T_{op} by some other means, such as switching between thermal noise standards; then (Stelzried, 80, 98)

$$T_N = (T_{op})_K/(Y - 1) \tag{12-5}$$

where

$(T_{op})_K$ = known system operating noise temperature, K

12. References

1964 Clauss, R. C., Higa, W. H., Stelzried, C.T., Wiebe, E.R., "Total System Noise Temperature: 15K", IEEE Trans. on Microwave Theory and Technique, Vol. MTT-12, No. 6, (Nov. 1964), pg. 619.

1971 Stelzried, C.T., "Operating Noise-Temperature Calibrations of Low-Noise Receiving Systems", Microwave Journal, Vol. 14, No. 6, (June 1971), pg. 41.

1980 Stelzried, C.T., "Noise Adding Radiometer Performance Analysis", TDA Progress Report 42-59, Jet Propulsion Laboratory, CA, (Oct. 15, 1980), pg. 98.

1980 Clauss, R. C., private communication

Table 12-1. Noise temperature performance of 8.5-GHz JPL horn-maser receiving system located on the ground (Clauss, 80)

Parameters	Noise temperature (K)
T_{op}	10.5 (measured)
T_M	3.5 (measured)
T_{COSMIC}	2.5 (measured)
$T_{HORN + ATMOSPHERE}$	4.5 (implied)

Table 12-2. Summary of JPL Goldstone, CA, maser receiving systems noise temperature performance (1972); T_e evaluated in the laboratory and T_{op} evaluated with the single ambient termination technique, Eq. 12-3

System	Freq (GHz)	T_{op} (K)	T_e (K)	T_M [b] (K)
Goldstone 64-m antenna	2.3	15.6	4.3	4.1
"	8.5	20.0	6.1	6.0
"	15.3	27.0	8.5	8.4
Minimum horn/maser[a]	2.3	10.7	4.3	4.2
"	8.5	12.4	6.1	6.0
"	15.3	18.5	8.7	8.4

[a]System located on ground.

[b]T_M = noise temperature of maser amplifier only.

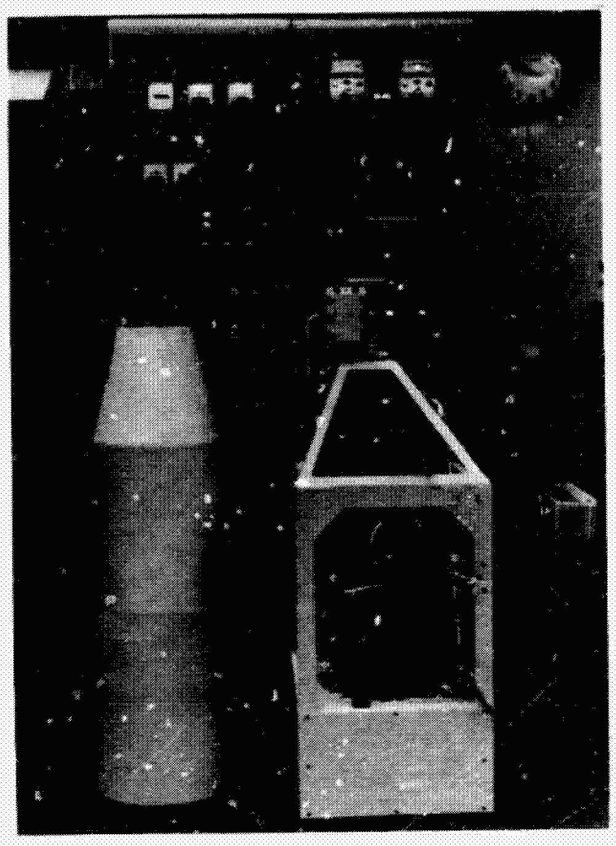

Fig. 12-1. Photograph of traveling wave maser system consisting of a liquid helium cooled termination and a 2.3-GHZ maser

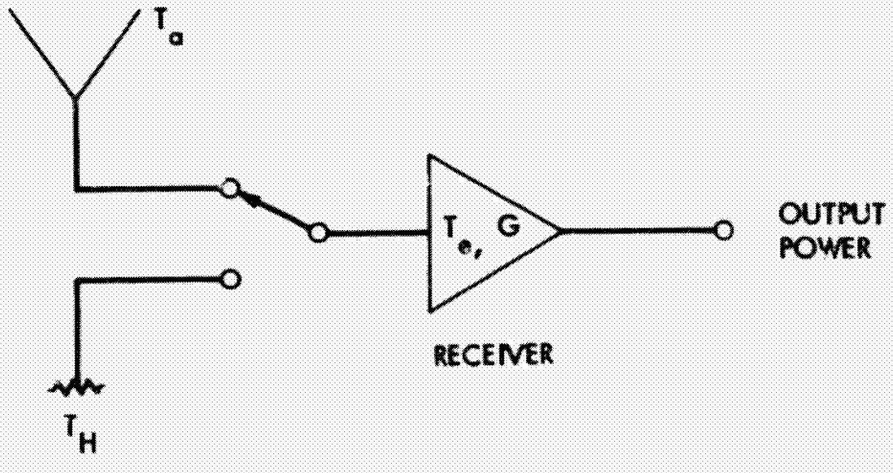

Fig. 12-2. Configuration for measuring system noise temperature using a single thermal noise standard

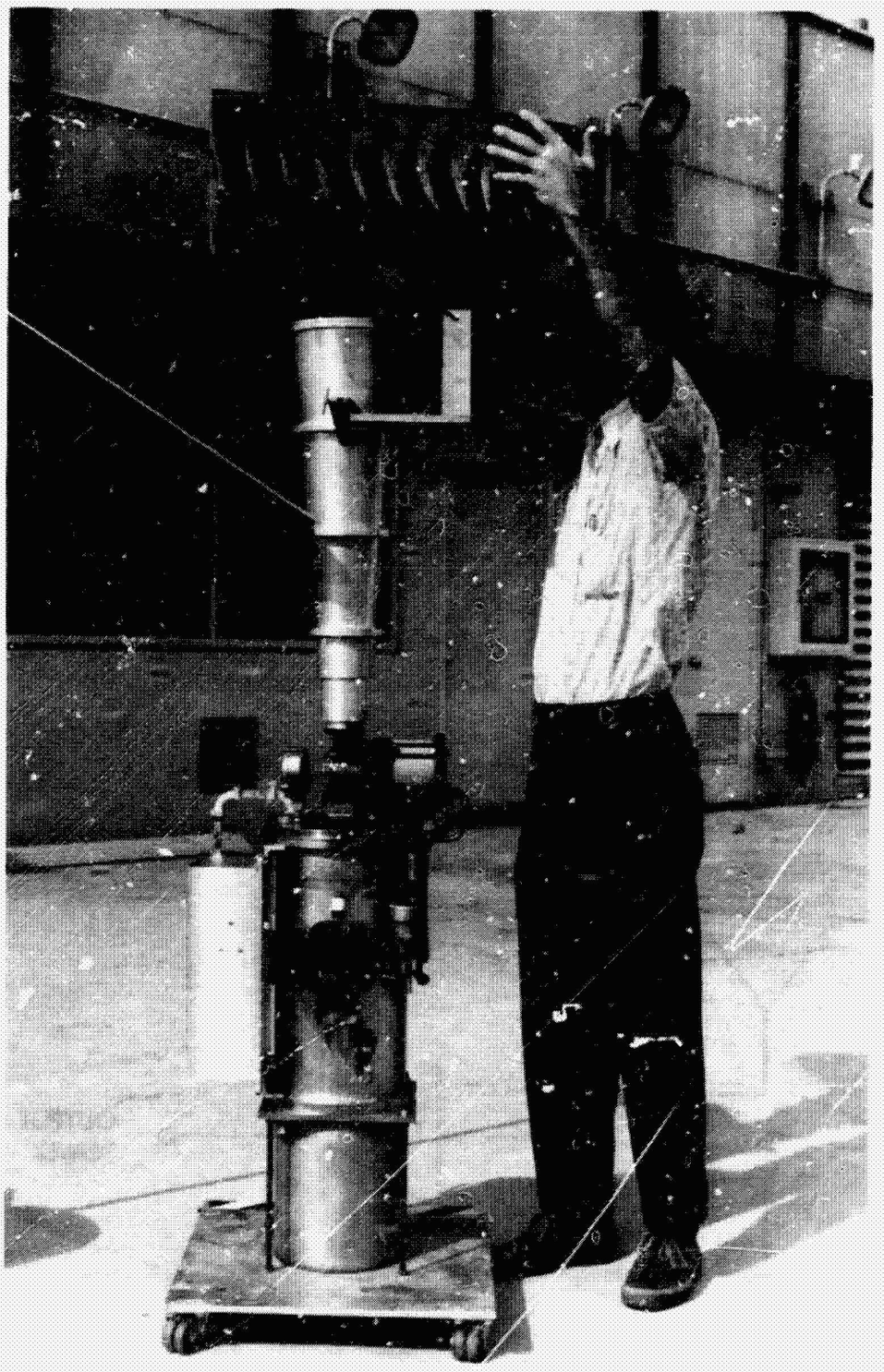

Fig. 12-3. JPL 8.5-GHz horn-maser receiving system noise temperature measurement system; T_{op} is evaluated by switching between the sky and an aperture ambient termination

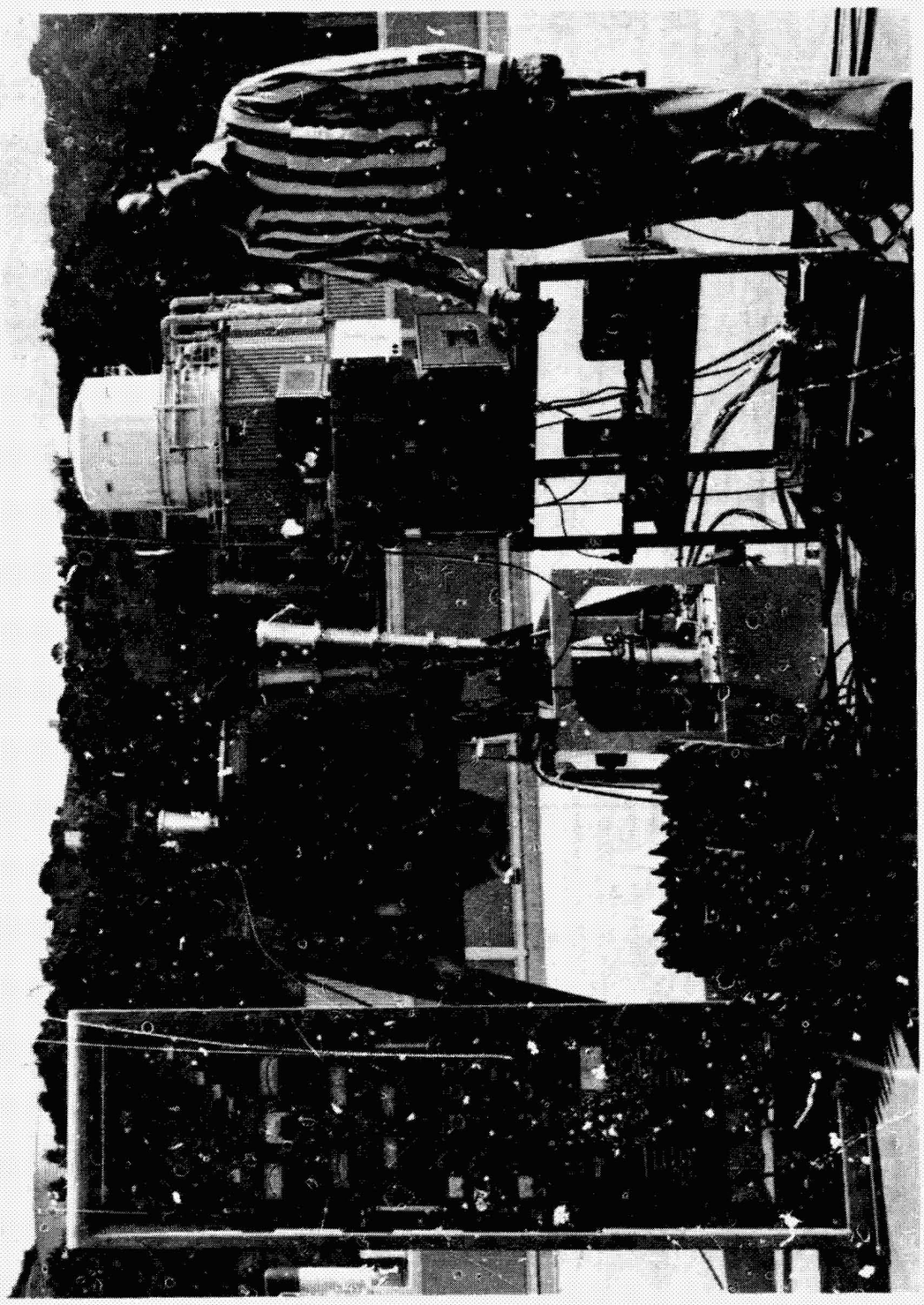

Fig. 12-4. JPL 8.5 GHz horn-mater receiving system showing noise measuring instrumentation

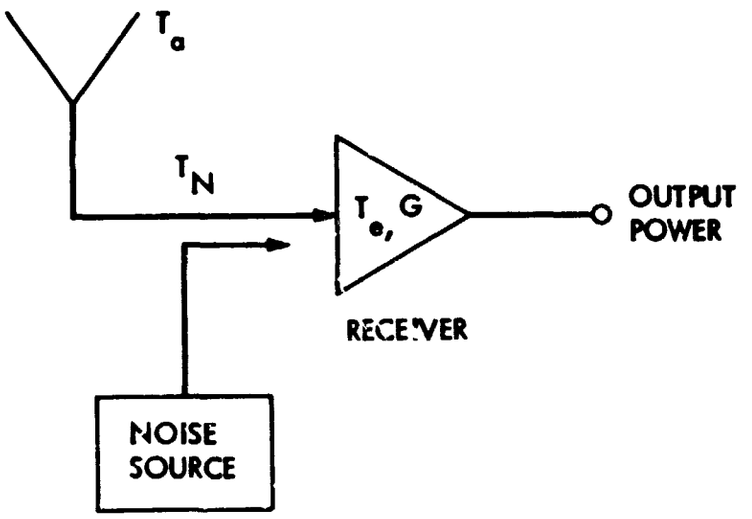

Fig. 12-5. Representation of receiving system with calibration noise source T_N

13. Measurement of G/T

For typical communcications links (Fig. 13-1) the receiving system output signal to noise ratio is

$$(S/N)_0 = \frac{P_T\, G_T\, G_R\, G_A/L_S}{k\, T_{op}\, B\, G_A} \qquad (13\text{-}1)$$

where

P_T = transmitter power, W
G_T = transmitter antenna gain, ratio
G_R = receiver antenna gain, ratio
G_A = amplifier gain, ratio
L_S = space loss, ratio
$= (4\pi R/\lambda)^2$
R = antenna separation, m
λ = wavelength, m

Inspection of Eq. 13-1 indicates that a figure of merit (Wait, 77, 49, Lawton, 82) for the ground system is

$$M = G/T \qquad (13\text{-}2)$$

where $G = G_R$ and $T = T_{op}$ is understood. M can be determined indirectly by separate determinations of G_R and T_{op} (Sec. 7). However, there is usually[14] considerable advantage to a direct measurement using radio star sources. Consider the receiving system shown in Fig. 13-2. Moving the antenna beam on and off the source,

$$(G/T) = 8\pi k\, (Y - 1)/k_1 k_2 \lambda^2 S \qquad (13\text{-}3)$$

[14]The JPL Deep Space Network does not use this technique due to the scheduling difficulty of routine performance monitoring.

C-2

where

$Y = (P_{ON}/P_{OFF})$, ratio

P_{ON} = receiver output power when on source, W

P_{OFF} = receiver output power when off source, W

k_1 = atmospheric transmission factor, ratio (≤ 1; Daywitt, 78, 1-39; Sec. 4)

k_2 = radio star shape factor, ratio (≤ 1; Kanda, 76, 173)

$= \int T(\mu) P(\Omega) d\mu / \int T(\Omega) d\Omega$

The error sources k_1, k_2 and others (such as antenna pointing, radiometer bandwidth and radio star polarization) have been analyzed (Daywitt, 76, 1-17; Daywitt, 77, 1-25; Kanda, 76, 173). As an example, a brightness temperature contour for Cassiopeia A is shown in Fig. 13-3. The correction k_2 for Cassiopeia A is obtained using this contour and the antenna pattern with the definition of k_2 above. It has been shown (Kanda, 76, 177) that Cassiopeia A can be treated as a uniform disk of about 4.6' diameter for antennas with a half-power beam width greater than about 4.6'.

Recent accurately calibrated radio star flux values for 2.3-GHz (S-band) and 8.4-GHz (X-band) are available (Klein, 76, 1078; Turegano, 80, 46). Radio star flux values are also available for a wider range of frequencies (Baars, 77, 99).

The communication link performance can be evaluated for a given ground system with known G/T using Eq. 13-1. G/T is a useful specification for a ground system contract (Wait, 77, 49). Tradeoffs can be made between receiver and antenna performance to meet an overall system specification. For very large antennas, T_{op} should be designed as low as possible due to the high cost of large antenna structures. Table 13-1 shows the figure of merit (expressed in dB).

$$M(dB) = 10 \log (G/T) \qquad (13\text{-}4)$$

for the JPL Deep Space Network receiving systems from pre-1960 to post-1980. The 26-m antennas with mixer receivers were updated with maser amplifiers (servicing maser, Figs. 13-4 and 13-5) in 1960. The present (1982) 64-m antennas have very low noise masers with reliable cryogenic refrigerators. Further improvement in G/T will be obtained at higher frequencies and increased aperture using array techniques.

13. References

1970 Rosenberg, I., "Distribution of Brightness and Polarization in Cassiopea A at 5 GHz", Royal Astron. Soc. Monthly Notices, Vol. 151, No. 1, (1970), pgs. 109-122.

1976 Daywitt, W.C., "Error Equations used in the NBS Precision G/T Measurement System", NBSIR - 842, Boulder, Colorado,(Sept. 1976).

1976 Kanda, M., "An Error Analysis for Absolute Flux Density Measurements of Cassiopeia A", IEEE Trans. on Instrumentation and Measurement, Vol IM-25, No. 3,(Sept. 1976), pgs. 173-182.

1976 Klein, M. J. and Stelzried, C. T., "Calibration Radio Sources for Radio Astronomy: Precision Flux Density Measurements at 2295 MHz", The Astronomical Journal, Vol. 81, No. 12, (Dec 1976), pg. 1078.

1977 Baars, J. W. M., et al, "The Absolute Spectrum of Cas A; An Accurate Flux Density Scale and a Set of Secondary Calibrators", Astron. Astrophys., Vol. 61, (1977), pgs. 99-106.

1977 Daywitt, W.C., "Error Equations Used in the NBS Earth Terminal Measurement System", NBSIR 78-869, Boulder, Colorado, (December 1977), pgs. 1-25.

1977 Wait, D.F., "Satellite Earth Terminal G/T Measurements", Microwave Journal, Vol. 20, No. 4 (April 1977), pg. 49.

1978 Daywitt, W.C., "Atmospheric Propagation Equations Used in the NBS Earth Terminal Measurement System", NBSIR 78-883, Boulder, Colorado, (April 1978).

1980 Turegano, J. A., Klein M. J., "Calibration Radio Sources for Radio Astronomy: Precision Flux Density Measurements at 8420 MHz", Astron. Astrophy., Vol. 86, (June 1, 1980), Pg. 46.

1982 Lawton, W.M., "What is G_R/T_N?", IOM 314.5-582, Jet Propulsion Laboratory, Pasadena, CA, (February 16, 1982) (an internal document).

Table 13-1. Summary of JPL DSN receiving system figure of merit (G/T) performance

System	Receiving system figure of merit (dB)	Improvement over 1960 (dB)
pre 1960 26-m antenna 960 MHz T_{op} = 2000 K	13	-
1960 26-m antenna 960 MHz T_{op} = 72 K	27	14
1970 64-m antenna 2300 MHz T_{op} = 25 K	47	34
post 1980 64-m antenna 31 GHz T_{op} = 25 K	71 (optimistic)	58 (optimistic)

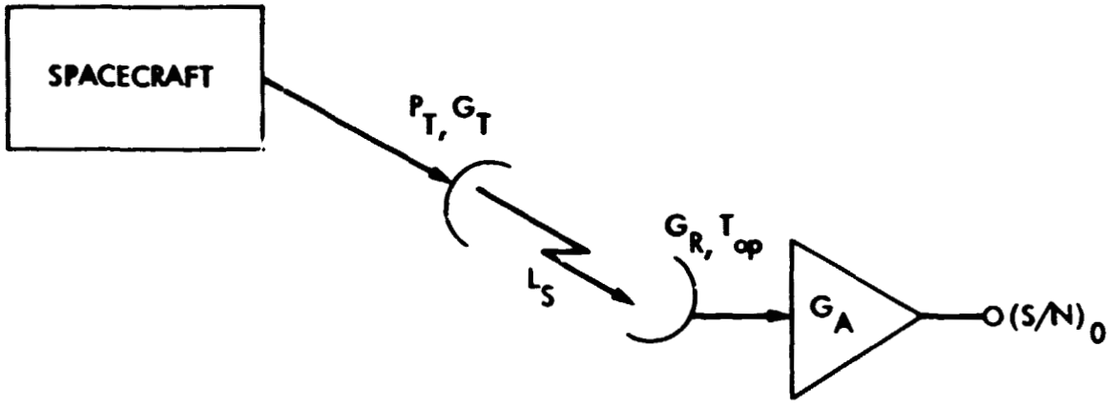

Fig. 13-1. Representation of typical deep space communications link

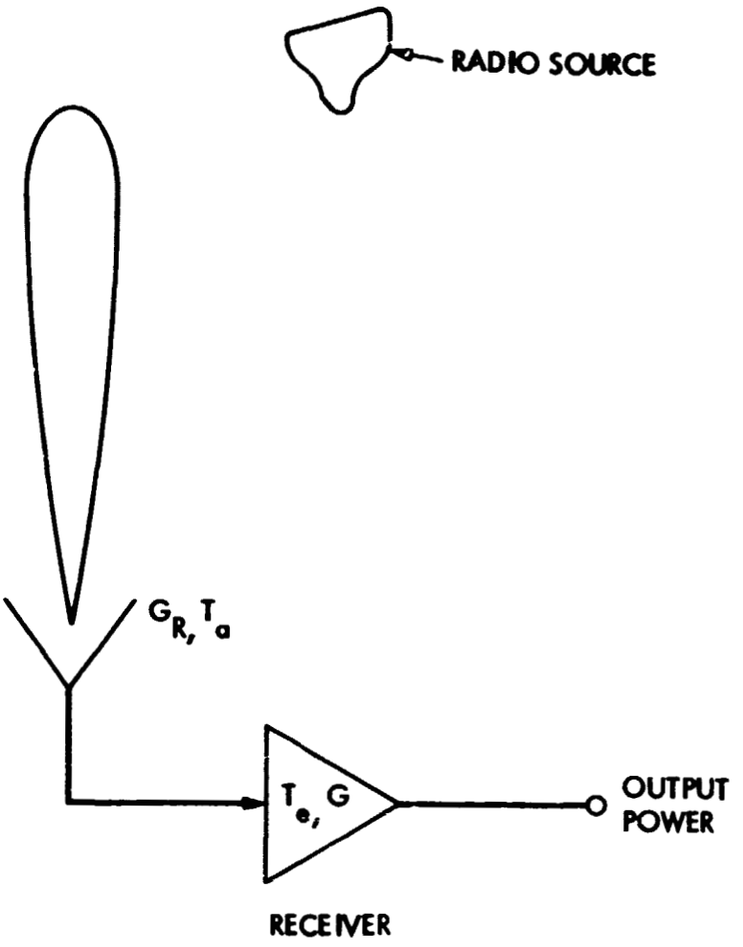

Fig. 13-2. Representation of receiving system configuration for G/T calibrations

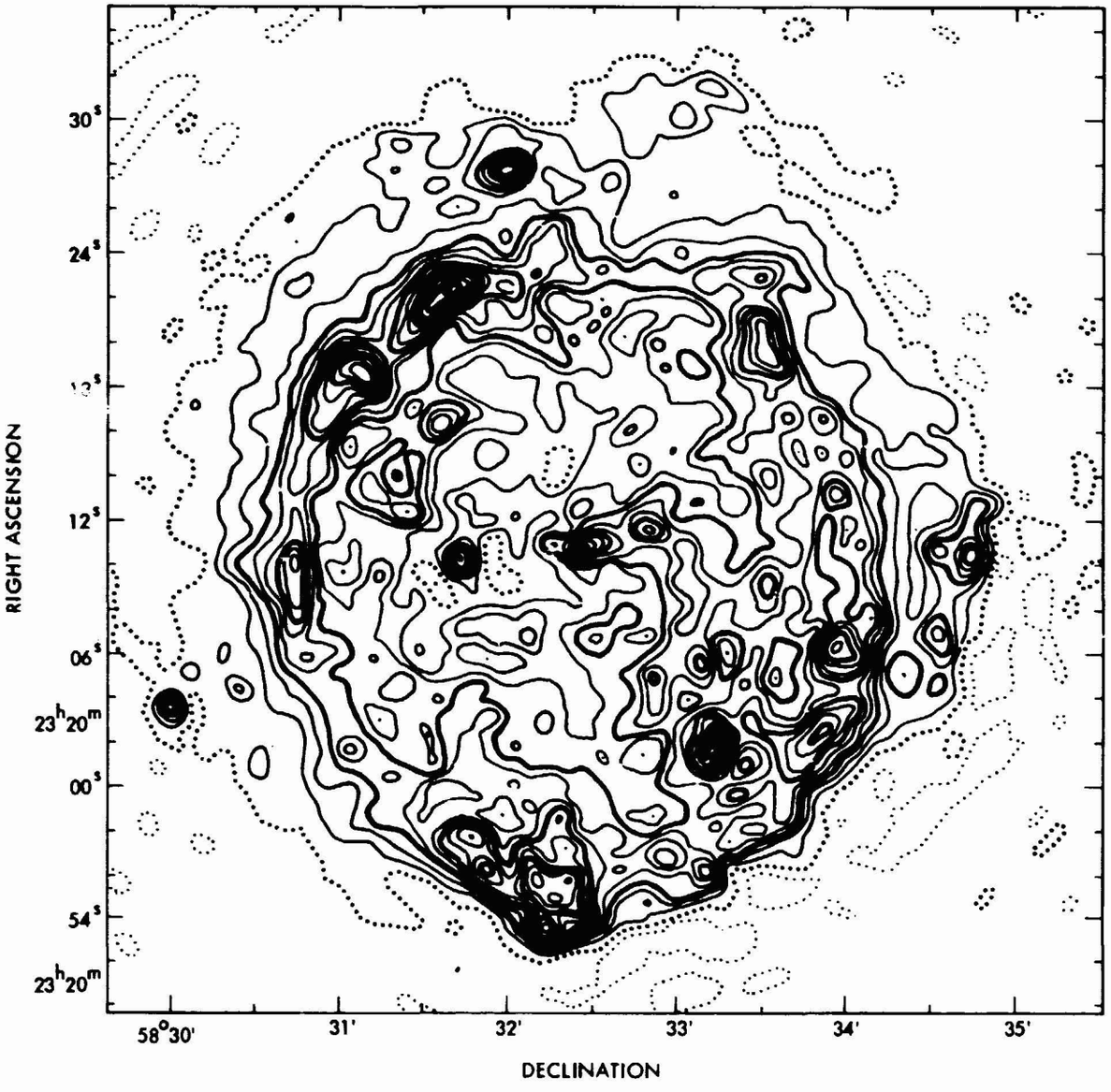

Fig. 13-3. Brightness temperature contour map of Cassiopeia A (coordinates for Epoch AD 1950.0, after Rosenberg, 70, 109-122)

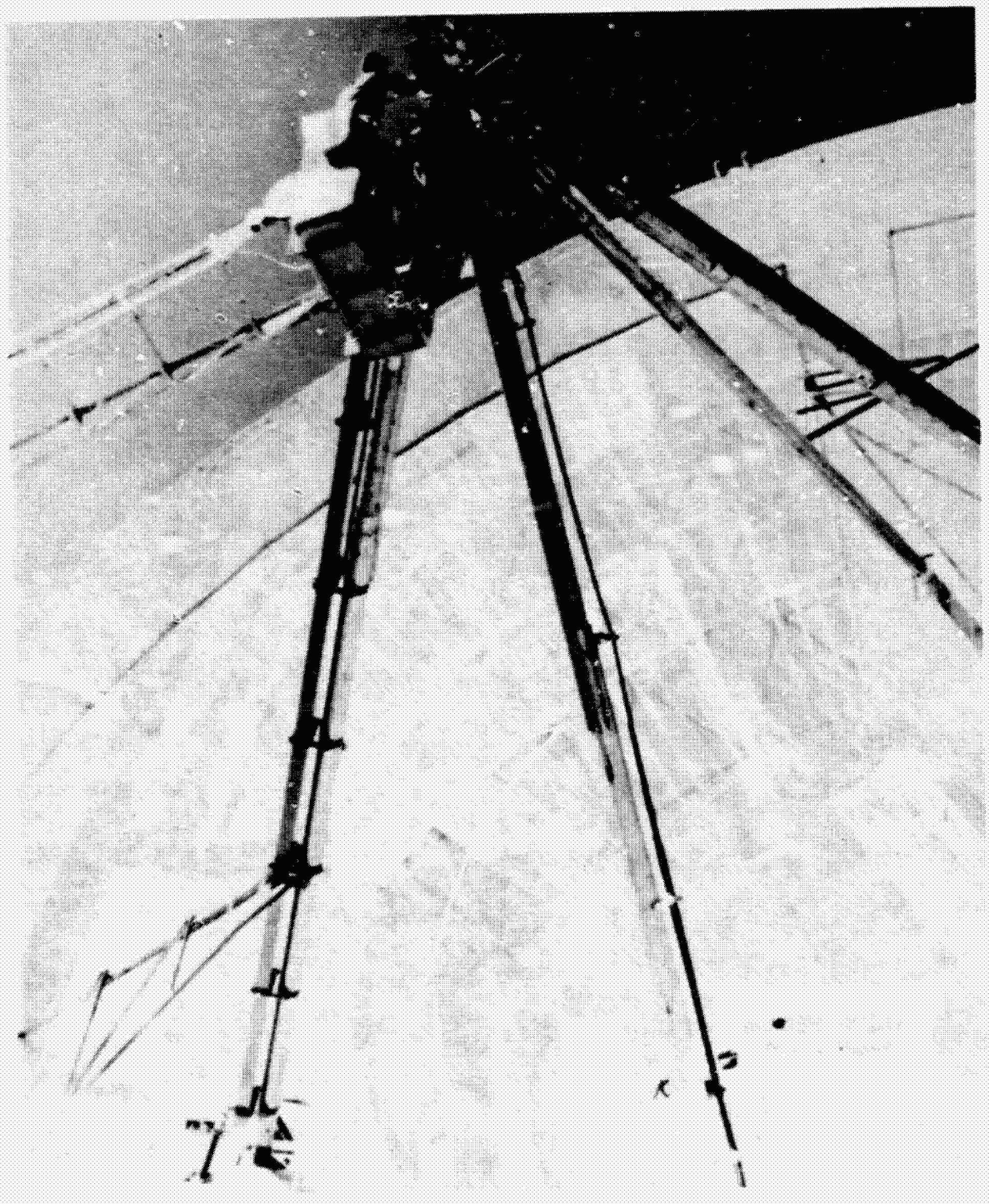

Fig. 13-4. Photograph of 1960 960-MHz liquid-helium-cooled maser amplifier installed on 26-m antenna (JPL DSS 11 Goldstone, CA)

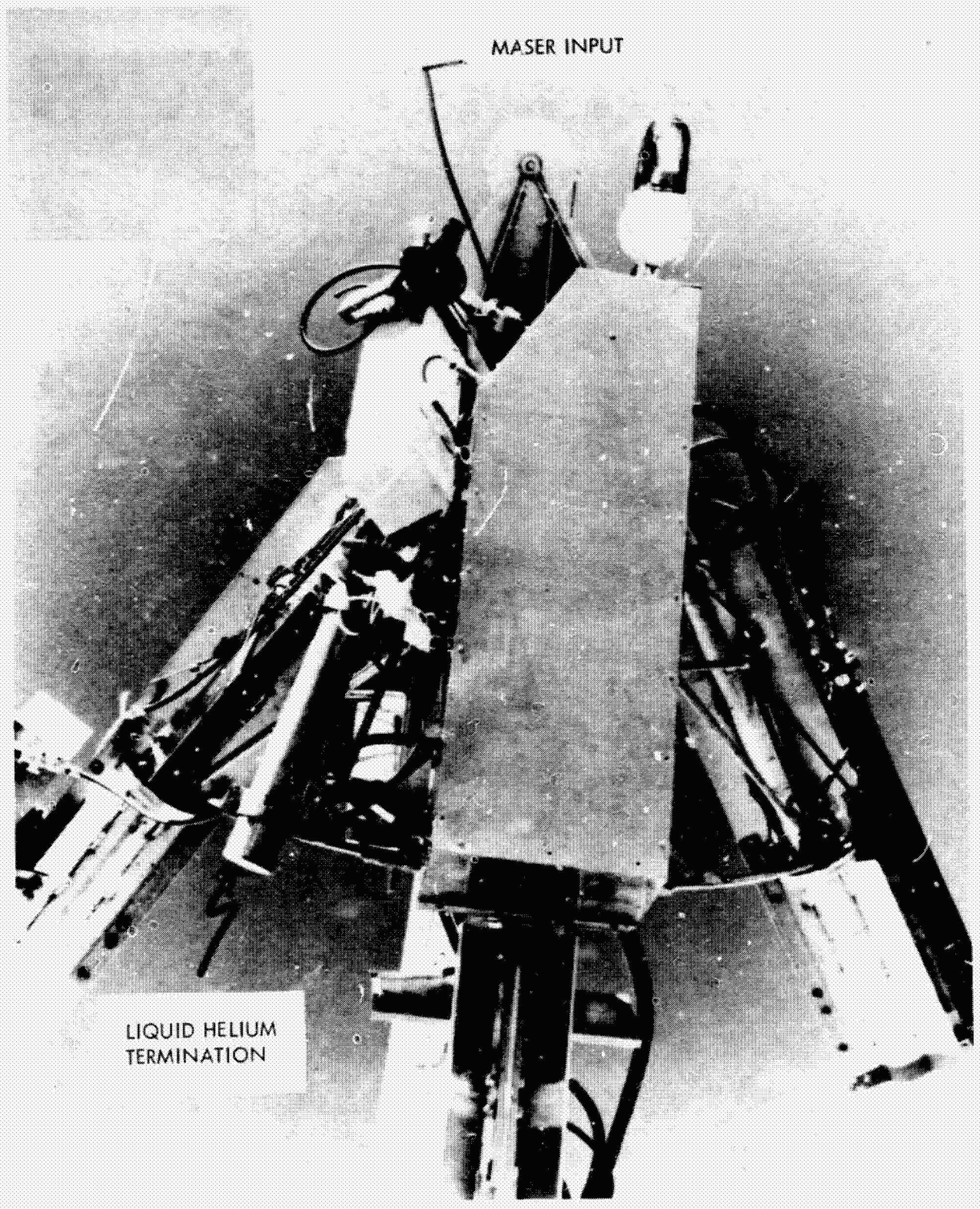

Fig. 13-5. Close-up photograph of 1960 960-MHz maser amplifier installation on 26-m antenna (JPL, DSS 11, Goldstone, CA)

14. Measurement of Flux Density of Radio Stars

Knowledge of the flux density (Baars, 77, 99; Klein 76, 1078; Juancey 82) of radio stars can be used to evaluate antennas or receiving system (previous Sec.) performance. Alternately, a receiving system with known antenna gain can be used for flux density calibration of radio stars (Baars 73,461; Freiley 77). Referring to Fig. 13-2, the increase in antenna temperature obtained when the radio source is in the beam vs not in the beam is given by (Y as defined in Sec. 13)

$$\Delta T_a = T_{op}(Y - 1) \tag{14-1}$$

where

T_{op} = system operating noise temperature (off source), K

The source temperature T_s or flux density S is evaluated using Eqs. 3-3 or 3-4. T_{op} can be evaluated as before (Sec. 12). Then (using terms as defined in Sec. 3)

$$S = 2k\ \Delta T_a/A_e \tag{14-2}$$

One of the best methods (minimizing antenna gain and atmospheric loss calibrations; Klein, 76, 1078) is to use a previously calibrated reference radio source. Then, the flux density of the unknown source is

$$S = S_R\ \Delta T_a/(\Delta T_a)_R \tag{14-3}$$

where

S_R = flux density of reference radio source, $J\text{-}m^2$

$(\Delta T_a)_R$ = increase in antenna temperature due to reference radio source, K

14. References

1973 Baars, J.W.M., "The Measurement of Large Antennas with Cosmic Radio Source", IEEE Transactions Antenna and Propagation, AP-21, No. 4, (July 1973), pg. 461.

1976 Klein, M. and Stelzried, C.T., "Calibration of Radio Sources for Radio Astronomy: Precision Flux-Density Measurements at 2295 MHz", The Astronomical Journal, Vol. 81, No. 12, (Dec. 1976), pg. 1078.

1977 Baars, J.W.M., et al., "The Absolute Spectrum of Case A; An Accurate Flux Density Scale and a Set of Secondary Calibrators," Astrm. Astrophys., Vol. 61, (1977), pgs. 99-106.

1977 Freiley, A.J., et al., "Absolute Flux Density Calibration of Radio Sources: 2.36 Hz", Technical Memorandum 33-806, Jet Propulsion Laboratory, Pasadena, CA, (Dec. 1, 1977).

1982 Juancey, D. L., Batty, M. J., Gulkis, S., Savage, A., "2.3 GHz Accurate Positions and Optical Identifications for Selected Parkes Radio Sources", Astronomical Journal, submitted for publication, (1982).

15. Measurement of Transmission Loss

It is shown in Sec. 7 that the receiving system sensitivity of a low noise system can be degraded severely, even with a relatively small amount of transmission line loss. Transmission line loss can be measured very precisely (Stelzried, 66, 98). These direct techniques require precision transmission lines that are well matched with precision connectors or waveguide flanges. Fig. 15-1 shows a photograph of typical instrumentation components used for these measurements. Fig. 15-2 shows a WR 430 waveguide flange being hand lapped prior to precision insertion loss calibrations. Verification by the National Bureau of Standards indicates that these calibration techniques are accurate to better than 0.001 dB (Otoshi, 70, 406).

Radiometric techniques are useful where these conditions are not realizable such as in bulk material (Seidel, 68, 625; Stelzried, 69, 172). The increase in system temperature (Fig. 15-3) is given by

$$(\Delta T_{op}) = (1 - L_m^{-1})\,(T_m - T_{atm} - T_s/L) \tag{15-1}$$

where

L = atmospheric loss, ratio (≥ 1)
L_m = transmission loss of lossy material, ratio (≥ 1)
T_m = physical temperature of lossy material, K
T_s = cosmic background noise temperature, K (≈ 2.7 K)
T_{atm} = atmospheric noise temperature contribution, K

Then

$$L = 1/\left[1 - (\Delta T_{op})_m/(T_m - T_{atm} - T_s/L)\right] \tag{15-2}$$

It is frequently convenient to perform a radiometer "tipping measurement" to determine T_{atm} and the atmospheric loss. Assuming a flat earth (Fig. 4-1) with a stratified atmosphere

$$L = L_z^{\sec Z} \tag{15-3}$$

where

Z = zenith angle

L, L_z = atmospheric loss at zenith angle Z and zenith respectively, ratio, (L, $L_z \geq 1$)

For the "tipping" measurement, the system temperature (T_{op}) is measured at zenith and Z. Assuming an antenna with no sidelobes and an infinitely narrow beamwidth,

$$\Delta T_{op} = \left(L_Z^{-1} - L_Z^{-\sec Z} \right) \left(T_p - T_s \right) \tag{15-4}$$

For many applications, it is convenient to measure ΔT_{op} between $Z = 0$ and 60^o. Then (see Stelzried. 8 , for additional terms in the expansion),

$$T_{atm} = \Delta T_{op} = \left[L_z(dB)/4.343 \right] (T_p - T_s) + \ldots \tag{15-5}$$

so that

$$L_z(dB) = \left[4.343\ \Delta T_{op}/(T_p - T_s) \right] + \ldots \tag{15-6}$$

This measurement, performed near the water vapor resonance (≈22 GHz), is convenient for monitoring atmospheric water vapor content in the antenna beam line of sight with a "water vapor radiometer".

Two frequency water vapor radiometers are frequently used to monitor the water vapor and liquid in the troposphere. The increased loss through the troposphere due to the water content is given by (Stelzried, 82)

$$\left.\begin{aligned} \tau = \left[L(dB)/4.343\right] = \left[(T-T_s)/(T_p-T_s)\right] \\ -(B/A)\left[(T-T_s)/(T_p-T_s)\right]^2 + \ldots \end{aligned}\right\} \quad \text{nepers} \qquad (15\text{-}7)$$

where (T_p and (B/A) defined precisely in Stelzried, 82)

T = measured increased noise temperature, K

T_p = troposphere physical temperature, K

$(B/A) \approx -(1/2)$

This loss consists of a stable oxygen component τ_0 assumed known and water vapor and liquid components τ_V and τ_L, assumed unknown,

$$\tau = \tau_V + \tau_L + \tau_0, \text{ nepers} \qquad (15\text{-}8)$$

This can be evaluated by measurements of τ_1 and τ_2 at two frequencies f_1 and f_2.

At frequencies f_1 and f_2, from Eq. (15-3)

$$\tau_1 \approx \left[(T_1 - T_s)/(T_p - T_s)\right] + (1/2)\left[(T_1 - T_s)/(T_p - T_s)\right]^2 + \ldots, \text{ nepers} \qquad (15\text{-}9)$$

and

$$\tau_2 \approx \left[(T_2 - T_s)/(T_1 - T_s)\right] + (1/2)\left[(T_2 - T_s)/(T_p - T_s)\right]^2 + \ldots, \text{ nepers} \qquad (15\text{-}10)$$

and from Eq. (15-8),

$$\tau_1 = \tau_{V1} + \tau_{L1} = \tau_{01}, \text{ nepers} \qquad (15\text{-}11)$$

and

$$\tau_2 = \tau_{V2} = \tau_{L2} + \tau_{02}, \text{ nepers} \qquad (15\text{-}12)$$

The total precipitable water vapor through the tropospheric line of sight is

$$\left.\begin{aligned} M_V &= \tau_{V1}/k_{V1} \\ &= \tau_{V2}/k_{V2} \end{aligned}\right\} \text{ cm} \qquad (15\text{-}13)$$

and the total precipitable water liquid is

$$\left.\begin{aligned} M_V &= \tau_{L1}/k_{L1} \\ &= \tau_{L2}/k_{L2} \end{aligned}\right\} \text{ cm} \qquad (15\text{-}14)$$

where

k_V, k_L = proportionality constants relating precipitable water to attenuation, nepers/cm

Also

$$\left.\begin{aligned} \tau_{V2}/\tau_{V1} &= k_{V2}/k_{V1} \\ &= k_V \end{aligned}\right\} \qquad (15\text{-}15)$$

and

$$\left.\begin{aligned} \tau_{L2}/\tau_{L1} &= k_{L2}/k_{L1} \\ &= k_L \end{aligned}\right\} \qquad (15\text{-}16)$$

Combining and solving for M_V and M_L, in terms of T_1 and T_2 assuming all constants are "known",

$$\left.\begin{aligned} M_V = {} & a_1(T_1 - T_s) + a_2(T_1 - T_s)^2 \\ & + a_3(T_2 - T_s) + a_4(T_2 - T_s)^2 + a_5 \end{aligned}\right\} \text{ cm} \qquad (15\text{-}17)$$

and

$$\left.\begin{aligned} M_L = {} & b_1(T_1 - T_s) + b_2(T_1 - T_s)^2 \\ & + b_3(T_2 - T_s) + b_4(T_2 - T_s)^2 + b_5 \end{aligned}\right\} \text{ cm} \qquad (15\text{-}18)$$

where

$$a_1 = -k_L/kk_{V1}(T_p - T_s) \qquad b_1 = k_V/kk_{L1}(T_p - T_s)$$

$$a_2 = a_1/2(T_p - T_s) \qquad b_2 = b_1/2(T_p - T_s)$$

$$a_3 = 1/kk_{V1}(T_p - T_s) \qquad b_3 = -1/kk_{L1}(T_p - T_s)$$

$$a_4 = a_3/2(T_p - T_s) \qquad b_4 = b_3/2(T_p - T_s)$$

$$a_5 = 1(\tau_{02} - k_L\,\tau_{01})/kk_{V1} \qquad b_5 = (\tau_{02} - k_V\,\tau_{01})/kk_{L1}$$

$$k = k_v - k_L$$

This allows monitoring of M_V and M_L from measurements of T_1 and T_2. S. C. Wu 78, 67, has investigated optimum frequency selection. The constants in Eqs. (15-13) and (15-14) can either be evaluated from the definitions above or from direct tropospheric calibrations (from radiosonde balloons, etc.). At frequencies f_1 = 20.6 GHz and f_2 = 31.6 GHz (Stelzried, 82)[15],

$$\left.\begin{aligned} M_V = {} & 0.11\,(T_1 - T_s) + 0.00020\,(T_1 - T_s)^2 \\ & - 0.048\,(T_2 - T_s) - 0.000086\,(T_2 - T_s)^2 \\ & - 0.064\,\cos Z \end{aligned}\right\} \text{ cm} \qquad (15\text{-}19)$$

---

[15] Hogg, 80, 281, has $M_V \simeq 0.11\,T_1 - 0.053\,T_2 - 0.18$ and $M_L \simeq a - 0.0011T_1 + 0.0027T_2 - 0.17$ appropriate for the zenith climatology of Denver, CO. The biggest difference between these expressions is the constant term for M_L (accounting for $T_s \simeq 2.7$ K).

and

$$M_L = \left.\begin{aligned} &-0.0016(T_1-T_s) - 0.0000023(T_1-T_s)^2 \\ &+ 0.0027(T_2-T_s) + 0.0000048(T_2-T_s)^2 \\ &- 0.013 \cos Z \end{aligned}\right\} \text{ cm} \qquad (15\text{-}20)$$

The increase in propagation path length due to both the precipitable water vapor and liquid is (Flock, 81, 71)

$$\Delta\ell = 6.48\, M_V + 1.45\, M_L, \text{ cm} \qquad (15\text{-}21)$$

or, in terms of T_1 and T_2

$$\Delta\ell = \left.\begin{aligned} &0.71\,(T_1 - T_s) + 0.0013\,(T_1-T_s)^2 \\ &- 0.31\,(T_2-T_s) - 0.00056(T_2-T_s)^2 \\ &-0.43 \cos Z \end{aligned}\right\} \text{ cm} \qquad (15\text{-}22)$$

Inspection of the above equations indicates that most of the tropospheric delay is due to the water vapor and very little from the liquid water. The primary effect of the liquid water is to alter the noise temperature measurements.

If it is required that the constants of Eqs. (15-17) and (15-18) be determined from direct radiometer calibrations, the constants a_2, a_4, b_2 and b_4 might best be determined analytically.

Figure 15-4 shows a comparison of the Jet Propulsion Laboratory water vapor radiometer system with the Socorro, New Mexico, Very Large Array (7-km baseline VLBI) tropospheric delay measurements.

Single frequency water vapor radiometers can be used to monitor clear sky water vapor in the troposphere. Simple "tipping" measurements (Eq. 15-4) can be used for continuous calibrations. Although the single frequency water vapor radiometer will perform well in clear sky conditions, serious degradation occurs during cloudy weather. Some applications allow the selection of good data, while discarding poor data.

15. References

1966 Stelzried, C.T., et al., "A Precision DC Potentiometer Microwave Insertion Loss Test Set", IEEE Trans. on Inst. and Meas., Vol. IM-15, No. 3, (Sept. 1966), pg. 98.

1968 Seidel, B.L., and Stelzried, C.T., "A Radiometric Method for Measuring the Insertion Loss of Radome Materials", IEEE Trans. on Microwave Theory and Techniques, Vol. MTT-16, No. 9, (Sept. 1968), pg. 625.

1969 Stelzried, C.T., and Otoshi, T.Y., "Radiometric Evaluation of Antenna-Feed Component Losses," IEEE Transactions on Instr. and Meas., Vol. IM-18, No. 3, (Sept. 1969), pgs. 172-183.

1970 Otoshi, T.Y., Stelzried C.T., Yates B.C. and Beatty, A.W., "Comparisons of Waveguide Losses Calibrated by the DC Potentiometer Techniques," IEEE Trans. on Microwave Theory and Techniques, (July. 1970), pg. 406.

1978 Wu, S.C., "Frequency Selection and Calibration of a Water Vapor Radiometer", DSN Progress Report 42-43, Jet Propulsion Laboratory, Pasadena, CA, (Feb. 15, 1978), pgs. 67-81.

1980 Hogg, D.C., "Ground-Based Remote Sensing and Profiling of the Lower Atmosphere Using Radio Wave Lengths", IEEE Trans. on Antennas and Propagation, Vol. AP-28, Nov. 2, (March 1980), pgs. 281-283.

1981 Flock, W.L., "Effects of the Gaseous and Liquid Water Content of the Atmosphere on Range Delay and Doppler Frequency", TDA Progress Report 42-63, Jet Propulsion Laboratory, Pasadena, CA, (June 15, 1981), pgs. 71-86.

1982 Stelzried, C.T. "Application of Radiative Transfer Theory to Microwave Transmission Medium Calibrations", TDA Progress Report 42-69, Jet Propulsion Laboratory, Pasadena, CA (June 15, 1978).

1982 Resch G., Hogg, D., and Napier, P., "Correction of Interferometer Phases Using Water Vapor Radiometer", Radio Science (submitted, 1982).

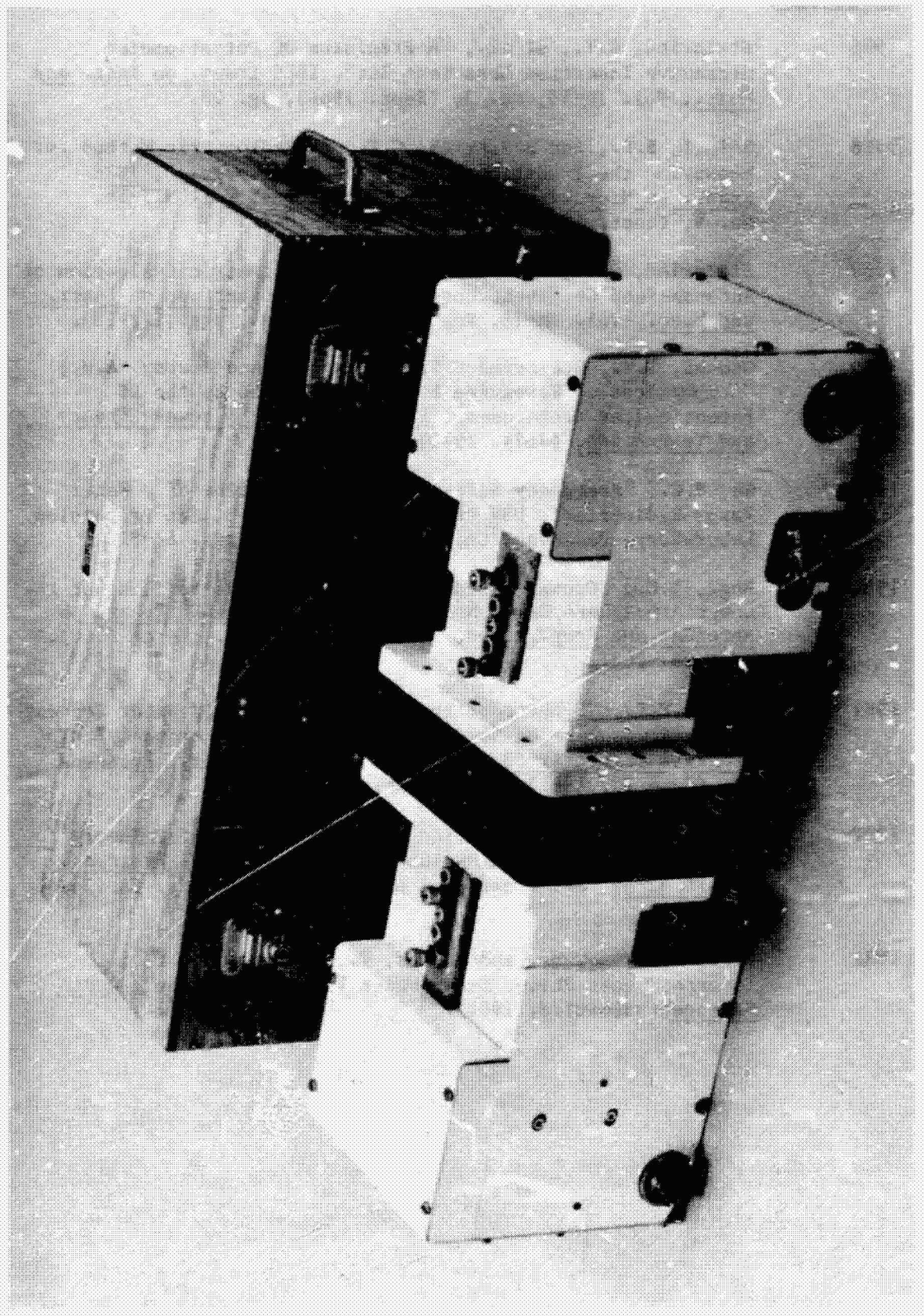

Fig. 15-1. Photograph of WR 430 waveguide insertion test set calibration components

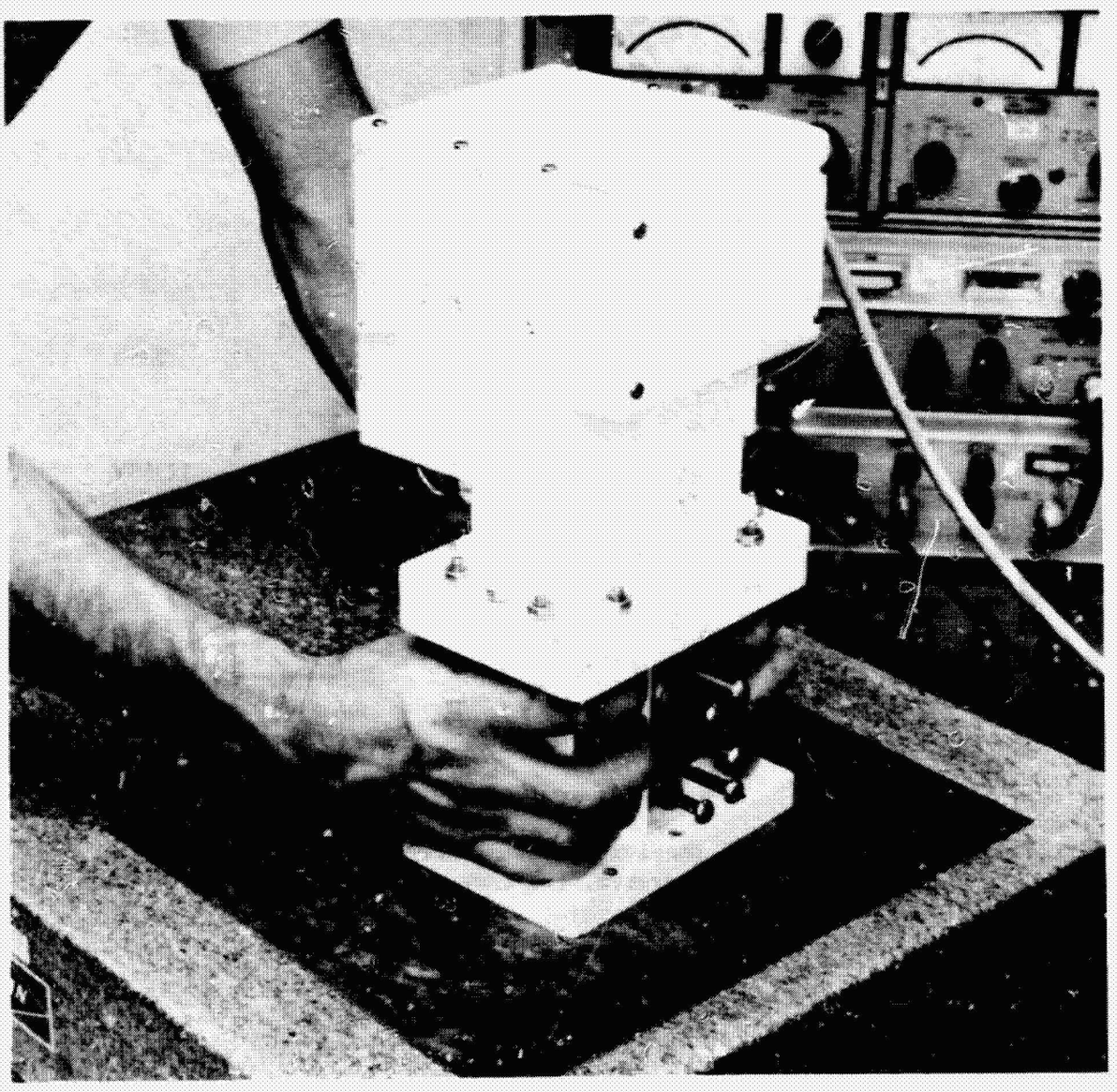

Fig. 15-2. Photograph of WR 430 waveguide flanges being hand lapped prior to precision insertion loss calibrations

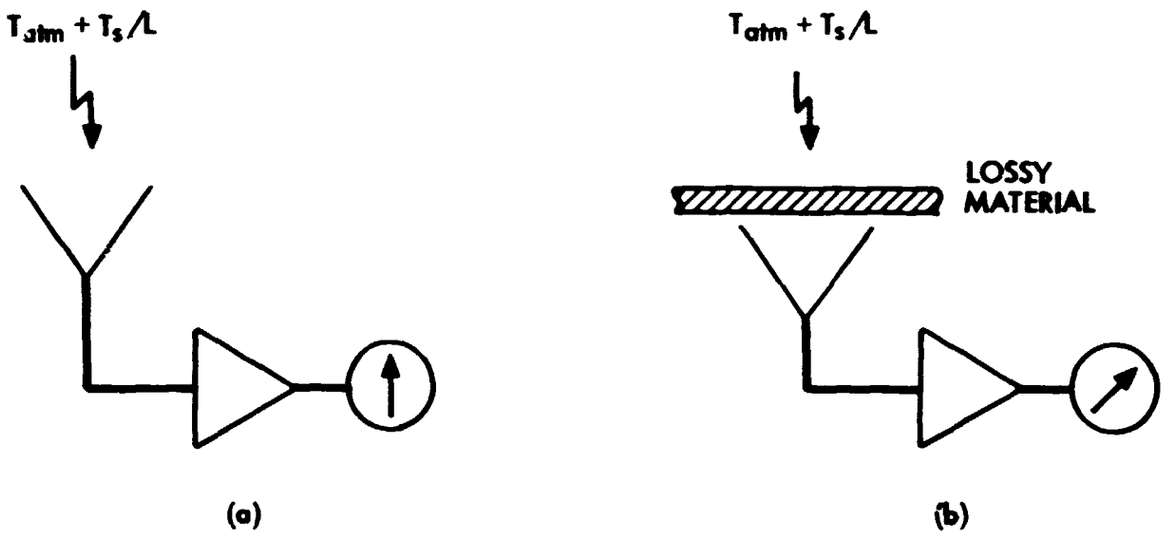

Fig. 15-3. Representation of receiving system used to evaluate lossy material; (a) basic receiving system, (b) same as (a) except lossy material placed over antenna

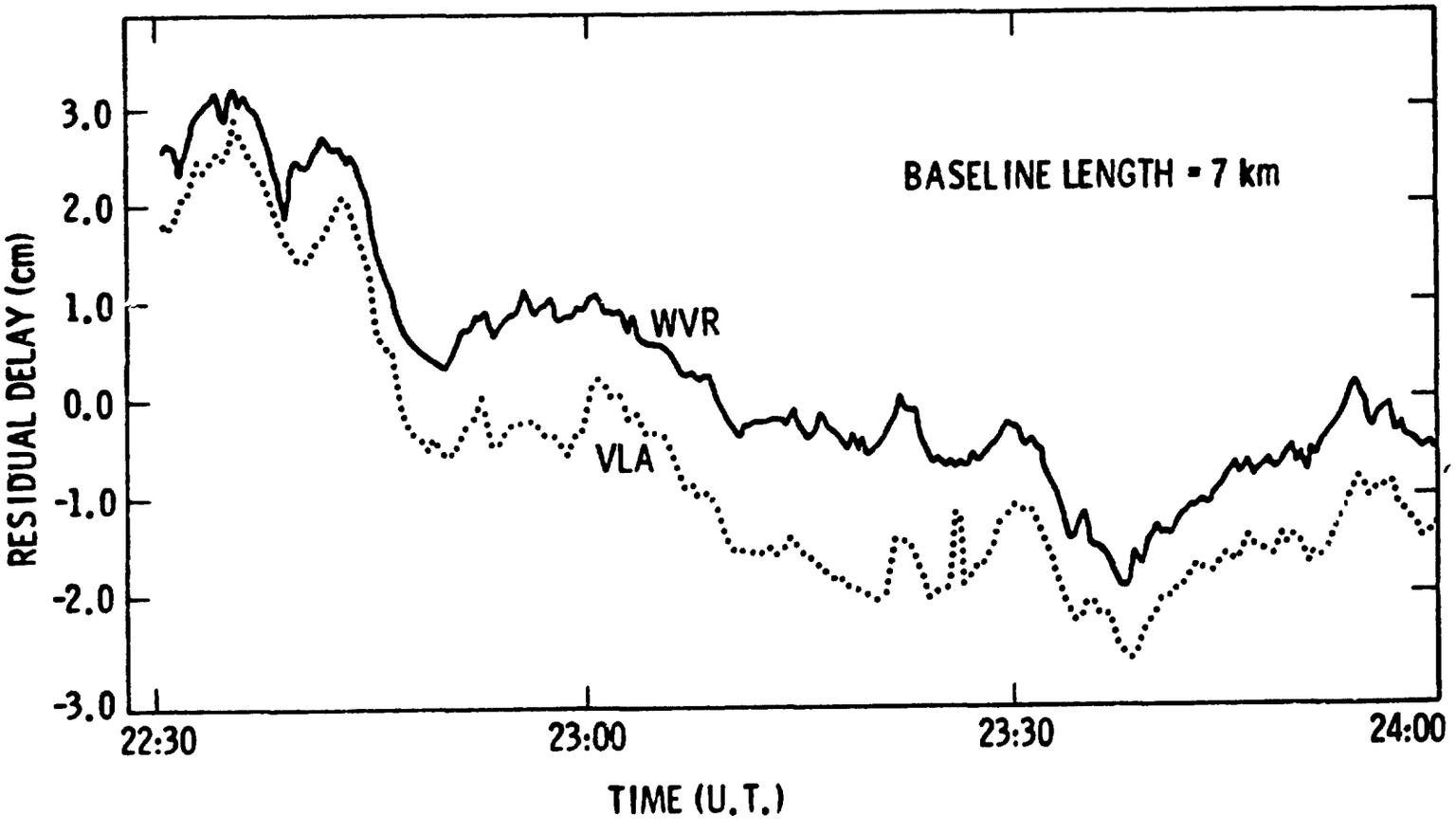

Fig. 15-4. Comparison of a JPL water vapor radiometer and the New Mexico Very Large Array (7-km baseline VLBI) tropospheric delay measurements (July 23, 1981; G. Resch, 82)

16. Noise Temperature Measurements

A wide variety of techniques and instrumentation is required and available for noise temperature measurements. Ideally, a measurement system is designed and assembled to perform the required measurements to the accuracy required with minimum expense and difficulty. Due to the inherent difficulty in most noise temperature measurements, obtaining more accuracy (see Secs. 22 through 25) than required, usually results in a waste of time and resources. Many times, the technique used is forced by the equipment available. Resourcefulness, experience and attention to detail are mandatory.

17. Total Power Radiometer

The total power radiometer is the simplest and potentially the most sensitive of all microwave radiometers. As shown in Fig. 17-1 it consists of the input source termination (or antenna) followed by amplification G and a square law detector. The output noise voltage is given by

$$E_o = k\, T_{op}\, B\, G \tag{17-1}$$

where

T_{op} = system operating noise temperature, K

$= T_i + T_e$

Solving for T_{op},

$$T_{op} = (E_o/kBG) \tag{17-2a}$$

$$= aE_o \tag{17-2b}$$

where

a = scale factor, K/Volt

The radiometer scale factor a can be determined with the use of thermal noise standards (Section 20) or other calibration techniques (Baars, 73). T_{op} is determined by measuring E_o. Assuming "perfect" amplification, the measurement resolution, or minimum detectable signal, of a total power radiometer is given by (Krauss, 66, 244)

$$(\delta T_{op})_{min} = T_{op}/\sqrt{\tau B} \tag{17-3}$$

where

τ = integration time, seconds

This is the standard by which all other radiometer types are compared (Colvin, 61). Gain instability is a serious problem with total power radiometers which other radiometers attempt to circumvent, usually with a resultant loss in

sensitivity. To account for gain and bandwidth instability Eq. 17-2a is differentiated and the instabilities treated as random variables (Price, 65, 210). Then, with Eq. 17-3

$$\delta T_{op} = T_{op}\sqrt{(1/\tau B) + (\delta G/G)^2 + (\delta B/B)^2} \qquad (17\text{-}4)$$

where

$(\delta G/G)$ = radiometer amplification gain instability, ratio.

$(\delta B/B)$ = radiometer bandwidth instability, ratio

The consequences of amplifier gain and bandwidth instabilities depend on the radiometer application. Slow drifts can usually be removed from the baseline of single radio source scan measurements. However, measurement of the galactic background temperature profile is difficult with such a system. For most total power radiometer applications, the gain instability of Eq. 17-4 dominates and

$$\delta T_{op} \approx T_{op}\left|\delta G/G\right| \qquad (17\text{-}5)$$

This explains the requirement for various other radiometer types discussed in subsequent sections used to reduce or circumvent the effect of gain instability.

17. Reference

1961 Colvin, R. S., "A Study of Radio-Astronomy Receivers," Publication No. 18A, Stanford Radio Astronomy Institute, Stanford, CA, (October 31, 1961).

1966 Kraus, J.D., Radio Astronomy, McGraw-Hill, N.Y., (1966).

1976 Price, R. M., "Radiometers", Methods of Experimental Physics, Academic Press, N.Y., (1976), pg. 201.

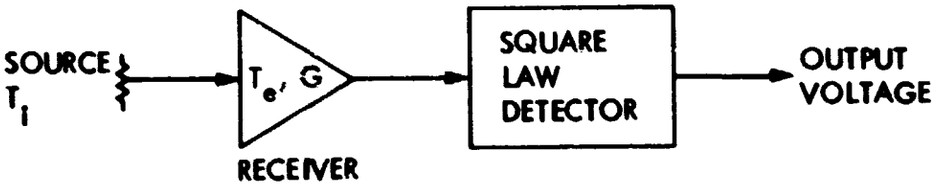

Fig. 17-1. Representation of total power radiometer

18. Dicke Radiometer

The Dicke radiometer (Dicke, 46, 268) was possibly the earliest microwave radiometer scheme to successfully reduce the effects of radiometer gain instability. This radiometer is still in wide usage with minor variations (Wait, 67, 127) due primarily to its simplicity.

The receiver input is rapidly switched between the source input termination (or antenna) and reference termination (Fig. 18-1). The receiver output is switched synchronously by the switch controller resulting in an output voltage

$$E_o = k\,(T_i - T_R)\,BG \tag{18-1}$$

where

T_i = antenna or unknown input termination temperature, K
T_R = reference termination temperature, K

Then

$$T_i = (E_o/kBG) + T_R \tag{18-2a}$$
$$= aE_o + b \tag{18-2b}$$

where

a = scale factor, K/volt
b = bias constant, K

The radiometer constants a and b are determined in the same manner as for the total power radiometer (Sec. 17).

The effect of amplification instability is proportional to $(T_i - T_R)$ instead of T_{op} as in a total power radiometer. Differentiating Eq. 18-2a, using Eq. 17-3 with (1/2) for each switch position and assuming random instabilities

$$\delta T_i = \sqrt{\left[2(T_{op})_i^2/\tau B\right] + \left[2(T_{op})_R^2/\tau B\right] + (T_i - T_R)^2\left[(\delta G/G)^2 + (\delta B/B)^2\right]} \quad (18\text{-}3)$$

If the radiometer is "balanced" ($T_i \approx T_R$),

$$\left(\delta T_i\right)_{min} = 2T_{op}/\sqrt{\tau B} \quad (18\text{-}4)$$

Eqs. 18-3 and 4 are applicable for square wave modulation. Other modulation schemes or signal filtering (Colvin, 51) result in a slightly increased instability.

The advantage of a Dicke radiometer relative to a total power radiometer is degraded unless $T_i \approx T_R$. Various modifications to the basic Dicke scheme such as the Kyle-Vonburg method (Ryle, 48) are used to further improve performance (Kraus, 66, 248-254). Another method is the beam "nodding" radiometer (Slobin, 70, 439) where the antenna pointing serves as the switch. The antenna beam is rapidly pointed on and off the source. Of course, balancing is only obtained for "weak" sources.

An actual radio source calibration measurement for most radiometers requires separate on and off source measurements. The radio source temperature is then given by

$$T_s = (T_A)_{on} - (T_A)_{off} \quad (18\text{-}5)$$

where

$(T_A)_{on}$ = antenna temperature measured with antenna beam pointed on source, K

$(T_A)_{off}$ = antenna temperature measured with antenna beam pointed off source, K

Assuming random measurement instabilities

$$\delta T_s = \sqrt{(\delta T_A)^2_{on} + (\delta T_A)^2_{off}} \tag{18-6}$$

Then, for the "ideal" total power radiometer, ignoring amplifier gain instabilities and assuming a "weak" source

$$\left(\delta T_s\right)_{min} = T_{op} \sqrt{(1/\tau_1 B) + (1/\tau_2 B)} \tag{18-7}$$

where

τ_1, τ_2 = radiometer measurement times on and off source

For $\tau_1 = \tau_2 = \tau$

$$\left(\delta T_s\right)_{min} = T_{op} \sqrt{2/\tau B} \tag{18-8}$$

Eqs. 18-6 and 18-7 are doubled for the balanced Dicke radiometer. Potentially, the beam nodding radiometer can provide superior performance to the conventional Dicke radiometer since the radiometer is always "looking" at either the source or the sky. Bias errors can be removed by alternating the "on" and "off" source antenna beam positions. This observing strategy provides near ideal performance.

18. References

1946 Dicke, R.H., "The Measurement of Thermal Radiation at Microwave Frequencies", The Review of Scientific Instruments, Vol. 17, No. 7, (July 1946), pg. 268.

1948 Ryle, M., and Vonberg, D.D., Proc. Roy. Soc. Longon Ser. A, Vol. 193, (1948), pg. 98.

1961 Colvin, R. S., "A Study of Radio-Astronomy Receivers," Publication No. 18A, Stanford Radio Astronomy Institute, Stanford, CA, (October 31, 1961).

1966 Kraus, J.D., Radio Astronomy, McGraw-Hill, N.Y., (1966).

1967 Wait, D.F., "The Sensitivity of the Dicke Radiometer", Journal of Research, NBS, Vol. 71C, No. 2, (1967) pg. 127.

1970 Slobin, S.D., Rusch, W.V.T., Stelzried, C.T. and Sato, T., "Beam Switching Cassegrain Feed System and Its Application to Microwave and Millimeter Wave Radio Astronomical Observations", The Review of Scientific Instruments, Vol. 41, No. 3, (March 1970), pgs. 439-445.

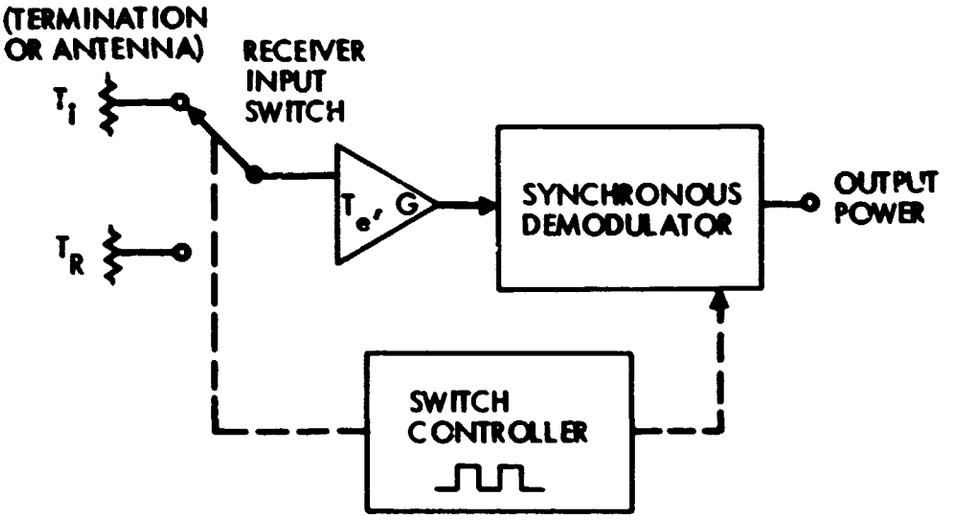

Fig. 18-1. Representation of Dicke radiometer

19. Noise Adding Radiometer

Very low noise receiving systems cannot tolerate the loss normally found in Dicke radiometer receiver input switches (≈ 0.1 dB loss increasing the system noise temperature ~6-7 K; see Secs. 7 and 20). The noise adding radiometer (Fig. 19-1) is particularly advantageous for this type of receiving system. The switch and reference termination of the Dicke radiometer is replaced in the noise adding radiometer by a transmission coupler and noise source. Square-wave-modulated noise at the receiver input is injected through the transmission line coupler. Then (Ohm, 63, 2047)

$$T_{op} = T_N/(Y - 1) \tag{19-1}$$

where

$Y = (P_{AN}/P_A)$, ratio
T_N = excess noise at receiver input from noise[16] source, K
P_{AN} = receiver power output, noise source on, W
P_A = receiver power output, noise source off, W

T_N can be calibrated with thermal noise standards or with a single ambient load termination (Stelzried, 71) applicable to systems with very low noise temperatures.

For this radiometer scheme (Batelaan, 70, 66-69)

$$\delta T_{op} = 2T_{op}\,(1 + T_{op}/T_N)\,/\sqrt{\tau B} \tag{19-2}$$

This approaches the performance of a Dicke radiometer if (T_{op}/T_N). T_{op}/T_N is usually reduced to about 0.1, limited by the receiver dynamic range. If the modulation rate for T_N is high enough (10 Hz is satisfactory for many systems), this system is virtually immune to gain changes without a requirement for "balancing."

---

[16] This is gererally a commercial, solid-state, fast-switching noise source using a stabilized power supply installed in a temperature-stabilized oven (Kanda, 77, 676).

Eq. 19-2 assumes that the noise source T_N is perfectly stable. Noise temperature bias errors are caused by incorrect calibration of T_N and receiver nonlinearity (Stelzried, 80, 98).

Noise adding radiometer performance is illustrated in Fig. 19-2. In this example, two noise adding radiometers are operating simultaneously at 2.3 and 8.5 GHz. This figure shows standard "drift" curves obtained by "locking" the antenna and letting the radio source drift through the antenna beam with the earth's rotation. Noise temperature measurement resolution of 10^{-4} K during cosmmic background measurements has been reported by Carpenter, 73, L61 using a noise adding radiometer on the Goldstone, CA 64-m antenna.

19. References

1963 Ohm, E.A. and Snell, W.W., "A Radiometer for a Space Communications Receiver", Bell Syst. Tech. J., 42, (1963) pg. 2047.

1970 Batetaan, P.D., Goldstein, R.M., and Stelzried, C.T., "A Noise-Adding Radiometer for Use in the DSN", Space Programs Summary 37-65, Vol. II, Jet Propulsion Laboratory, Pasadena, CA, (Sept. 30, 1970), pg. 66.

1970 Nicolson, G.D., "A Gain-Stabilized Maser Radiometer for 13 cm", IEEE Trans. Microwave Theory and Techniques, MTT-18, (1970), pg. 169.

1973 Carpenter, R.L. Gulkis S. and Sato, T., "Search for Small-Scale Anisotropy in the 2.7 K Cosmic Background Radiation at a Wavelength of 3.56 Centimeters", The Astrophysical Journal, Vol. 182, (June 1, 1973), pg. L61.

1973 Reid, M.S., et al., "Low Noise Mircowave Receiving Systems in a Worldwide Network of Large Antennas", IEEE Proceedings, Vol. 61, No. 9, (Sept. 1973) pg. 1330.

1973 Wallace, K.B., "Noise Diode Evaluation", Technical Report 32-1526, Vol. III, Jet Propulsion Laboratory, Pasadena, CA, (April 15, 1973), pg. 121.

1976 Kanda, M., "An Improved Solid-State Noise Source", IEEE Transition on Microwave Theory and Technique, MTT-24, No. 12 (Dec. 1976), pg. 990.

1977 Kanda, M., "A Statistical Measure for the Stability of Solid State Noise Sources", IEEE Transactions on Microwave Theory and Techniques, Vol. MTT-25, No. 8, (Aug 1977) pg. 676.

1980 Stelzried, C.T., "Noise Adding Radiometer Performance Analysis", TDA Progress Report 42-59, Jet Propulsion Laboratory, Pasadena, CA, (Oct. 15, 1980), pg. 98.

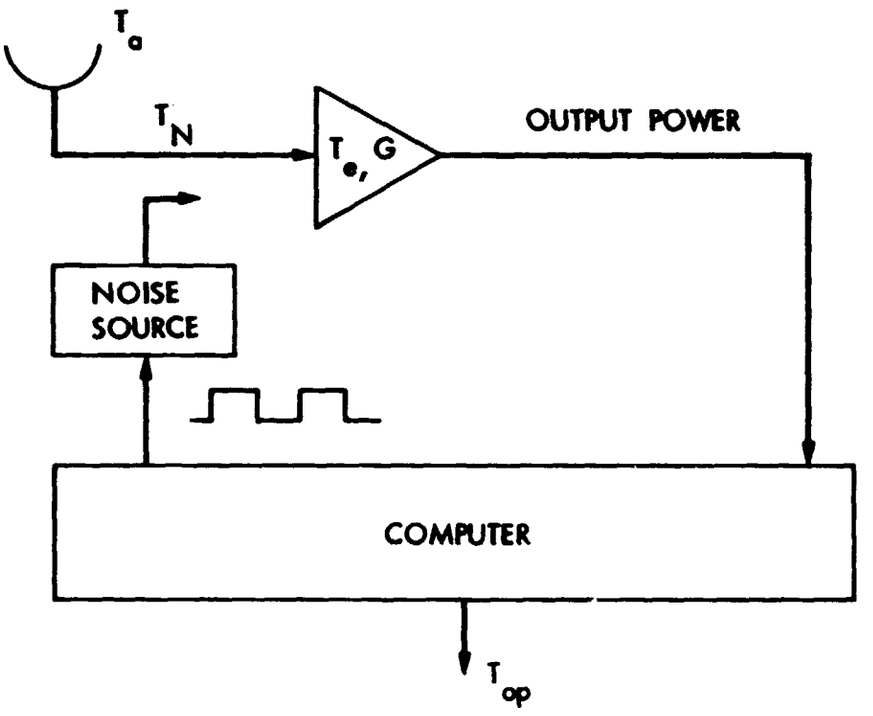

Fig. 19-1. Noise adding radiometer configuration

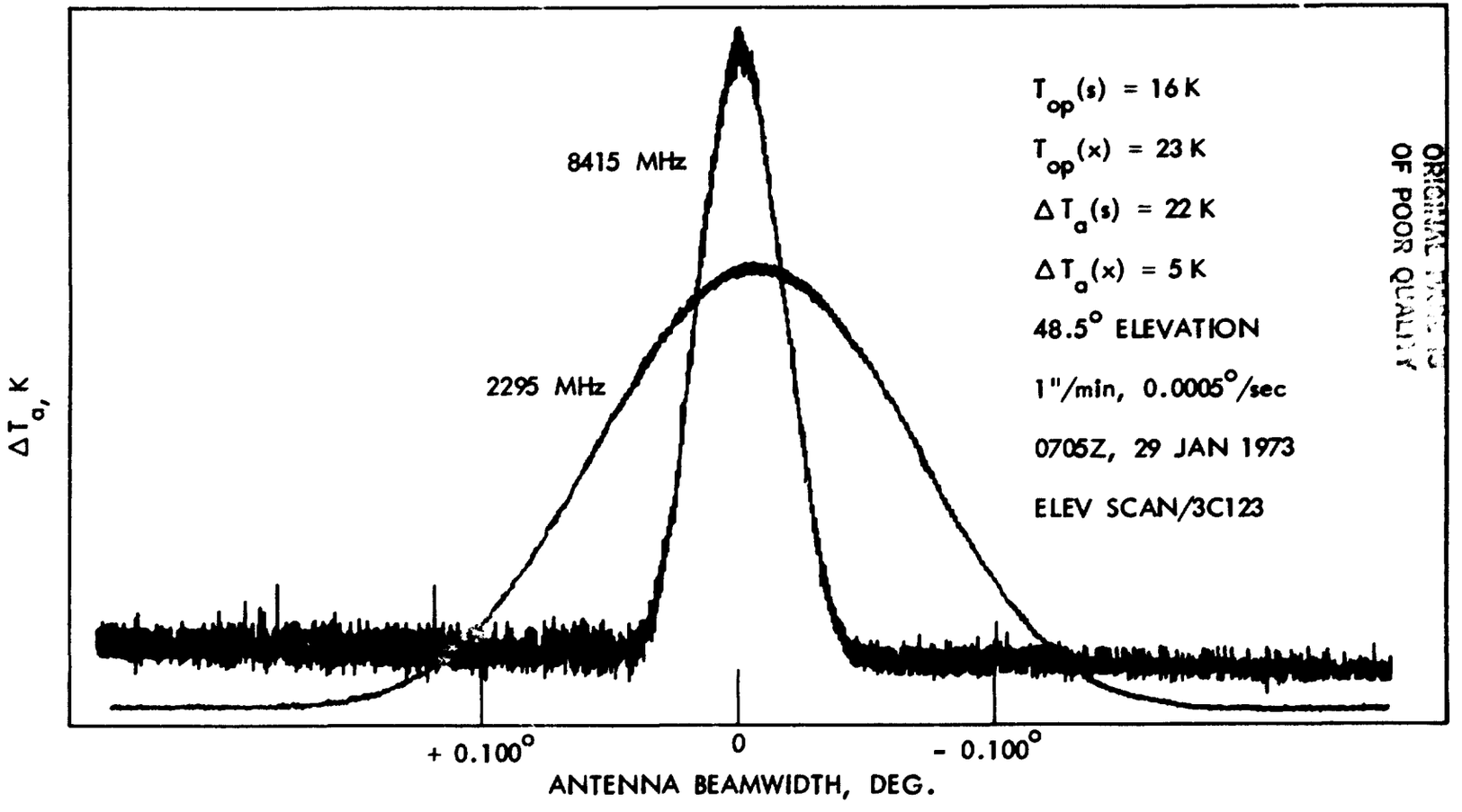

Fig. 19-2. Noise adding radiometer; simultaneous drift scan of 3C123 radio source through the 2.3-GHz and 8.5-GHz beams of the DSS 14 reflex feed (DSS 14 Goldstone, CA, 64-antenna)

20. Thermal Noise Standards

Thermal noise standards (Stelzried, 68, 646; Trembath, 68, 709; Daywitt, 72, 1-148; Yokoshima, 77, 1-140) provide the foundation for absolute radiometer noise temperature calibrations. A typical (Fig. 20-1) thermal noise standard consists of a matched source termination at temperature T_s (as determined with a thermometer or by immersing the termination in a boiling liquid such as liquid helium (Stelzried, 61, 1224) or liquid nitrogen (Figs. 20-2 and 20-3). The transmission line is required to thermally isolate the output connector from the source termination.

The total loss through the transmission line (Fig. 20-1) is given by (assume "matched", $hf \ll kT$, Stelzried 82; the following is also applicable to the atmosphere, Sec. 4)

$$L = e^{\tau}, \text{ ratio } (\geq 1) \qquad (20\text{-}1)$$

where

τ = total transmission line absorption [$L\ (dB) = (10 \log e)\ \tau$]

$$= \int_0^{\ell} \alpha(x)\, dx$$

$\alpha(x)$ = absorption coefficient of the transmission line at x, nepers/m

x = distance along the transmission line, m ($x = 0$ at output = ℓ at source[17])

ℓ = total path length, m

[17] It is sometimes convenient to integrate from the source to the output.

From the theory of radiative transfer (neglecting reflections; Chandrasekhar, 60), the thermal noise temperature defined at the output is

$$T_s' = (T_s/L) + \int_o^{\ell} T(x)\ \alpha\ (x)\ e^{-\tau(x)} dx,\ K \qquad (20\text{-}2)$$

where

T_s = source thermal noise temperature, K

$T(x)$ = physical temperature of medium at x, K

$\tau(x)$ = absorption between 0 and x, nepers

$$= \int_o^{x} \alpha\ (x')dx'$$

This can be integrated directly or solved stepwise (Stelzried, 61, 1224). For small transmission loss, Eq. (20-2) can be approximated by expanding $e^{-\tau}$ and $e^{\tau(x)}$ in power series.

$$T_s' \simeq T_s + A\tau + B\ \tau^2 + C\ \tau^3 + \ldots \qquad (20\text{-}3)$$

A, B and C can be solved and treated as "constants" assuming the physical temperature and loss distributions of the transmission line are known. For a transmission medium composed of discrete sections ($\ell = n\Delta x$ and $x = i\Delta x$) and assuming uniform loss, $\alpha(x) = \alpha_o$ and $\tau = \alpha_o \ell$, usually applicable to thermal noise standards[18],

$$A = T_p - T_s \qquad (20\text{-}4)$$

where

T_p = average physical temperature of the transmission medium, K

$$= \frac{1}{\ell}\int_o^{\ell} T(x)dx = \frac{1}{n}\sum_{i=1}^{n} T_i$$

---

[18] See Sec. 4 for nonuniform loss.

and

$$B = -\left[\frac{1}{2\ell^3}\int_0^{\ell} xT(x)dx - (T_s/2)\right] = -\left[\frac{1}{n^2}\sum_{i=1}^{n} iT_i - (T_s/2)\right] \qquad (20\text{-}5)$$

$$C = \frac{1}{2\ell^3}\int_0^{\ell} x^2T(x)dx - (T_s/6) = \frac{1}{2n^3}\sum_{i=1}^{n} i^2T_i - (T_s/6)$$

The last terms of Eq. (20-3) are small and provide an indication of the number of terms required and the accuracy of the power series expansion. Only 1 or 2 terms are required for most applications. In many applications, it is suitable to use two terms with $(B/A) = -(1/2)$.

Consider the solution of Eq. (20-3) for a linear physical temperature distribution, $T(x) = T_1 + (T_2-T_1)x/\ell$ (applicable to a thermal noise standard consisting of a source at temperature T_s and a transmission line with a linear temperature distribution between T_1 and T_2). We have

$$A = (T_1 + T_2 - 2T_s)/2$$

$$B = (T_1 + 2T_2 - 3T_s)/6 \qquad (20\text{-}6)$$

$$C = (T_1 + 3T_2 - 4T_s)/24$$

resulting in

$$T_s' \simeq T_s + L(dB)/4.343\ (T_1 + T_2 - 2T_s)/2$$
$$- L(dB)/4.343^2\ (T_1 + 2T_2 - 3T_s)/6 \qquad (20\text{-}7)$$
$$+ L(db)/4.343^3\ (T_1 + 3T_2 - 4T_s)/24 + \ldots$$

in agreement with Stelzried, 68, 648 (Case 4).

The error in T_s' due to an error in L(dB) is (using the first two terms of Eq. (20-3))

$$\delta T_s' \simeq 0.23\ (T_p-T_s)\ \delta L(dB) \qquad (20\text{-}8)$$

This relationship is useful for estimating the required[19] accuracy for loss calibrations; for $\delta T_s' < 0.1$ K, it is necessary that L(dB) <0.0015 dB (assumes $(T_p - T_s) \approx 290$ K).

Similarly, the error in T_s' due to an error in T_p ($T_s << T_p$) is given by

$$\delta T_s' \approx 0.23026 \, (\delta T_p) \, L(dB) \qquad (20\text{-}9)$$

For $\delta T_s' < 0.1$ K it is necessary to monitor T_p within ≈ 4 K (assumes L(dB) ≈ 0.1dB).

The model sophistication necessary for calibration depends on the accuracy requirement of the output noise temperature.

For some applications it may be necessary to measure the temperature distribution along the transmission line and compute the noise temperature at the output with an iterative technique. This technique can account for non-uniform transmission line loss with an overall accuracy of better than 0.2 K for a 78.1 K liquid-nitrogen-cooled termination calibrated at 2.3 GHz (Stelzried, 68, 650).

---

[19]Precision transmission line loss measurement error has been reported at less than 0.001 dB (Stelzried, 70, 23). Precision calibrations require that special care be taken with matching (Sec. 23) and the use of precision connectors or waveguide flanges. Loss calibrations can also be performed with the "short circuit" method (Engen, 69, 1-23; Beatty, 65, 642; Otoshi, 70, 406; Yokoshima, 77, 1-140; Yokoshima, 76, 138).

20. References

1960 Chandrasekhar, S., Radiative Transfer, Dover Publications, N.Y., (1960).

1961 Stelzried, C.T., "A Liquid Helium Cooled Coaxial Termination," IRE Proceedings, Vol. 49, No. 7, (July 1961), pg. 1224.

1965 Beatty, R. W., "A Two-Channel Nulling Method for Measuring Attenuation Constants of Short Sections Of Waveguide and the Losses in Waveguide Joints," Vol. 53, No. 6, Proc. IEEE, (June 1965), pg. 642.

1968 Stelzried, C.T., "Microwave Thermal Noise Standards", IEEE Trans. on Microwave Theory and Techniques, Vol. MTT-16, No. 9, (Sept 1968), pg. 646.

1968 Trembath, C.L., et al., "A Low-Temperature Microwave Noise Standard", IEEE Trans. on Microwave Theory and Techniques, Vol. MTT-16, No. 9, (Sept. 1968), pg. 709.

1969 Engen, G. F., "An Introduction to the Description and Evaluation of Microwave Systems Using Terminal Invariant Parameters", National Bureau of Standards Monograph 112, NBS Monogr. 112, Boulder, Colorado, Library of Congress No. 77-601820, (October 1969).

1970 Otoshi, T.Y., Stelzried, C.T., Yates, K. C., Beatty, R. W., "Comparisons of Waveguide Losses Calibrated by the DC Potentiometer, AC Ratio Transformer, and Reflectometer Techniques", Proc. IEEE, MTT-18, No. 7, (July 1970), pg. 406.

1970 Stelzried, C.T., "Precision Microwave Waveguide Loss Calibrations", IEEE Transactions on Instrumentation and Measurement, Vol. IM-19, No. 1 (Feb. 1970), pg. 23.

1972 Daywitt, W.C. et al., "WR 15 Thermal Noise Standard", NBS Technical Note 615, National Bureau Standards, Boulder, Colorado, (March 1972).

1976 Yokoshima, I., "Direct Measurement Techniques of Transmission Line Corrections for Thermal Noise Standards", IEEE Trans. Instrum. and Meas., Vol IM-25, (June 1976), pg. 138.

1977 Yokoshima, I., "Microwave Noise Standards", Researches of the Electrotechnical Laboratory No. 770, UDC 621.391, 822, 098.6: 621.3.029.6, Chiyoda-Ku, Tokyo, Japan, (Nov., 1977).

1982 Stelzried, C.T., "Application of Radiative Transfer Theory to Microwave Transmission Medium Calibrations", TDA Progress Report 42-69, Jet Propulsion Laboratory, Pasadena, CA, (June 15, 1982).

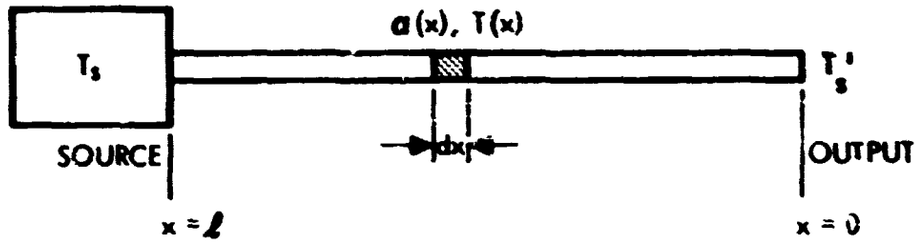

Fig. 20-1. Representation of a thermal noise standard consisting of a source and a lossy transmission line

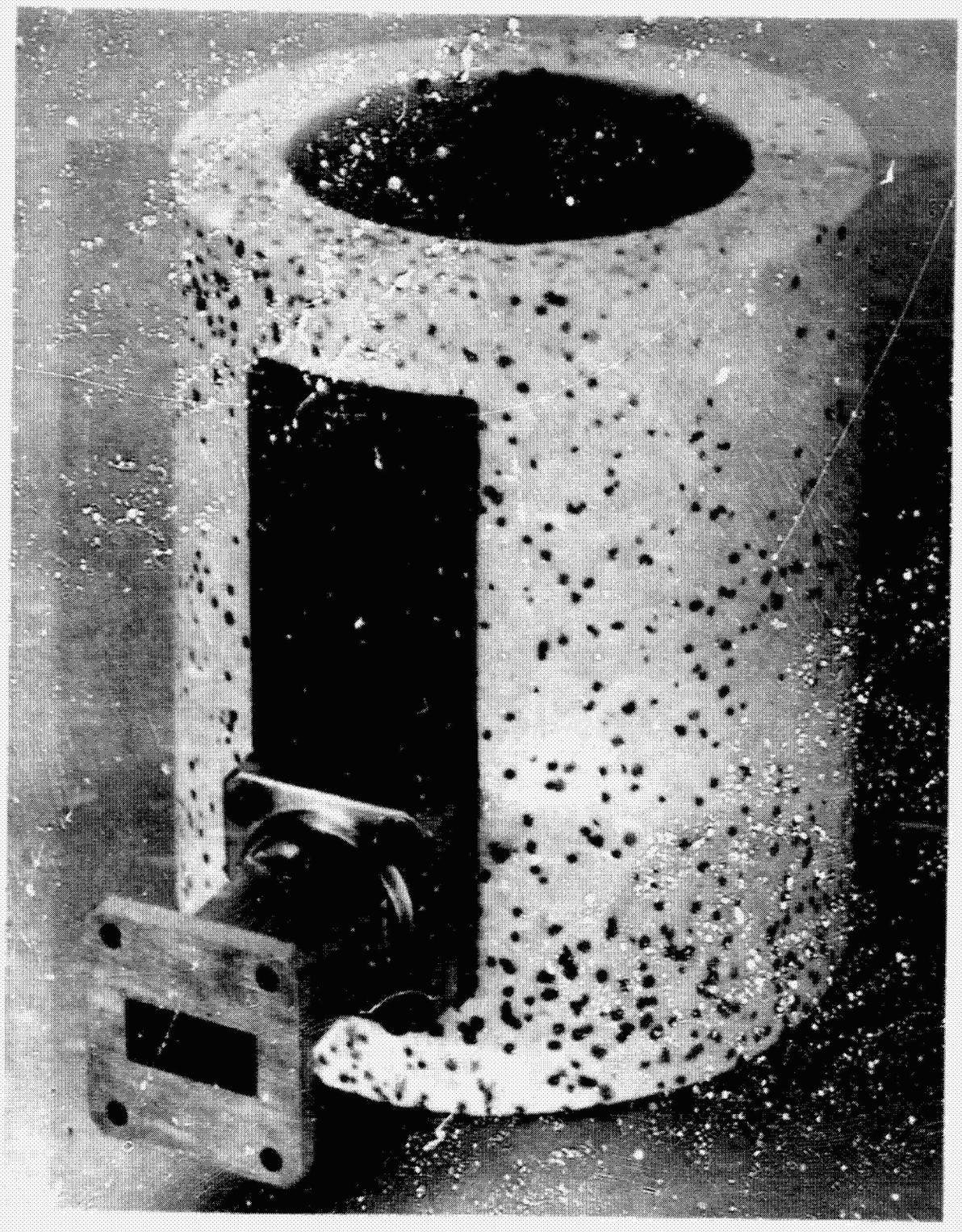

Fig. 20-2. Photograph of liquid-nitrogen-cooled X-band microwave thermal noise standard

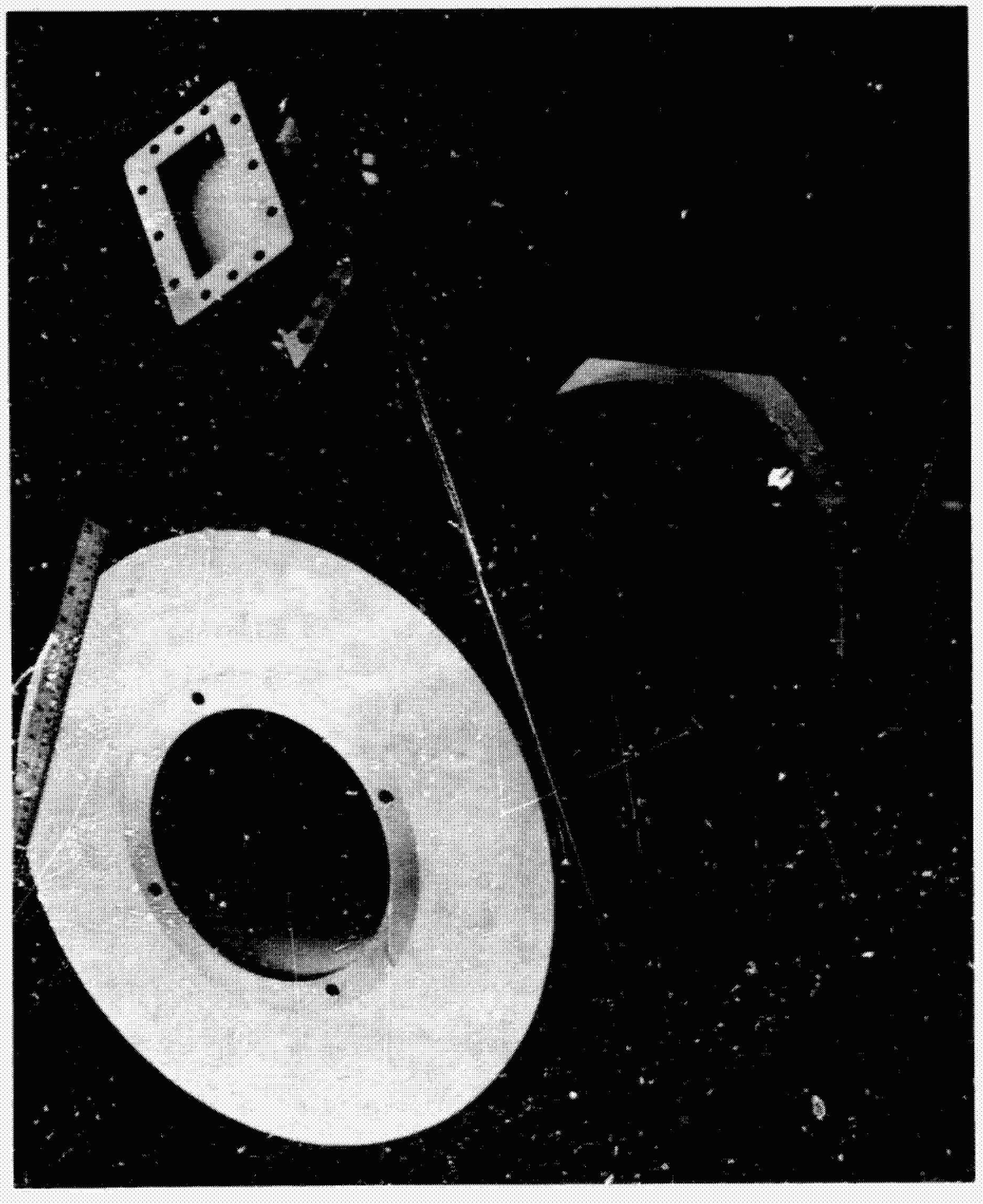

Fig. 20-3. Photograph of liquid-nitrogen-cooled S-band microwave thermal noise standard

21. Noise Measuring Instrumentation

Considerable time and effort can be invested in noise measurements. The required instrumentation can be fabricated as required by the experimenter. However, the wide availability of commercial noise instrumentation can reduce this time investment in many cases.

This equipment includes microwave antennas, thermal noise standards (cryogenically cooled, ambient and hot), transmission line components (supplied with precision match and loss calibrations) and precision measurement instrumentation. Typical manufacturers include: Maury Microwave Corporation (Cucamonga, CA), Airborne Instrument Laboratories (Deer Park, Long Island, NY) Weinschel Engineering (Gaithersburg, MD), Scientific Atlanta Inc (Atlanta, GA), Merrimac Inds. Inc (West Caldwell, NJ), Microlab/FXR, (Livingston, NJ), Rhode and Schwarz (Fairfield, NJ), Telonic/Berkeley (Laguna Beach, CA), Hewlett-Packard Co. (Palo Alto, CA), Narda Microwave Corp. (Plainview, NJ), and Coax Devices (Chelsea, MA).

22. Measurement Resolution Error

The measurement resolution of noise temperature calibrations can be analyzed from the radiometer equation appropriate to the system analyzed. Consider the typical configuration for measuring receiver noise temperature (Fig. 11-1). From Sec. 11

$$T_e = (T_H - YT_C)/(Y - 1) \tag{22-1}$$

where

$$Y = P_N/P_C$$

The measurement resolution of T_e is determined by the measurement resolution of Y,

$$\delta T_e/R = \left|\partial T_e/\partial Y\right| \delta Y/R \tag{22-2}$$

where

$\delta Y/R$ = measurement resolution of Y

$$= \sqrt{(\partial Y/\partial P_H)^2 \, (\delta P_H)^2 + (\partial Y/\partial P_C)^2 \, (\delta P_C)^2}$$

$$\left|\partial T_e/\partial Y\right| = (T_H - T_s')/(Y - 1)^2$$

$$= (T_{op})_C^2/(T_H - T_C)$$

$$(\partial Y/\partial P_H)^2 = 1/P_C^2$$

$$(\partial Y/\partial P_C)^2 = P_H^2/P_C^4$$

$$^{20}(\delta P_H)^2 = P_H^{\,2}\left[(1/\tau B) + (\delta G/G)^2\right]$$

$$^{20}(\delta P_C)^2 = P_C^{\,2}\left[(1/\tau B) + (\delta G/G)^2\right]$$

$(T_{op})_H$ = system noise temperature when switched to T_H, K

$(T_{op})_C$ = system noise temperature when switched to T_C, K

This results in

$$\delta T_e/R = \frac{(T_{op})_H\,(T_{op})_C}{(T_H - T_C)}\sqrt{(2/\tau B) + 2(\delta G/G)^2} \qquad (22\text{-}3)$$

For $\delta G \to 0$

$$(\delta T_e/R)_{min} = \frac{(T_{op})_H\,(T_{op})_C}{(T_H - T_C)}\sqrt{2/\tau B} \qquad (22\text{-}4)$$

This technique is applicable to other configurations. As examples, for antenna noise temperature calibrations (Fig. 10-1) (Franco, 81, 80), the measurement resolution of T_a is given by

$$(\delta T_a/R) = \sqrt{(T_{op})_a^2 + \left(\frac{T_C - T_a}{T_H - T_C}\right)^2 (T_{op})_H^2 + \left(\frac{T_H - T_a}{T_H - T_C}\right)^2 (T_{op})_C^2}\Bigg/\sqrt{\tau B} \qquad (22\text{-}5)$$

and for system noise temperature calibration (Fig. 12-1) (Stelzried, 71, 41), the measurement resolution of T_{op} is given by

---

[20] Obtained from the total power radiometer resolution equations (Sec. 17)

$$(\delta T_{op}/R) = \frac{(T_{op})_H}{(T_{op})_a} \sqrt{2\left[(1/\tau B) + (\delta G/G)^2\right]} \qquad (22\text{-}6)$$

$$\approx 0.030 \text{ K}$$

where

$(T_{op})_H$ = system noise temperature when switched to T_H, K
≈ 300 K

$(T_{op})_a$ = system noise temperature when switched to T_a, K
≈ 30 K

τ = integration time, sec
≈ 10 sec

B = receiving system bandwidth, Hz
≈ 10^7 Hz

$(\delta G/G)$ = gain instability, ratio
(during measurement period)
≈ 0.23 δ G(dB)
≈ 0.23 (0.01)
≈ 0.0023

22. References

1971 Stelzried, C.T., "Operating Noise-Temperature Calibrations of Low-Noise Receiving Systems", Microwave Journal, Vol 14, No. 6, (June 1971), pg. 41.

1981 Franco, M.M., Slobin, S.D., and Stelzried, C.T., "X-Band Narrow Beam Radiometer for DSS 13, TDA Progress Report 42-66, Jet Propulsion Laboratory, Pasadena, CA, (Dec. 15, 1981), pg. 80.

23. Mismatch Error

The previous sections assume that the source impedance, transmission line and receiver are "matched" with no signal reflections. Mismatched components cause multiple reflections with resultant noise calibration errors. Careful analysis of these reflections can be used to correct the calibrations (Otoshi, 68, 675, Wait, 68, 670, Nemoto, 68, 866). In many applications, it is easier (and customary) to reduce the reflections to a suitable level and then ignore the effect.

Consider[21] a transmission line with characteristic impedance Z_o and termination impedance Z_L as shown in Fig. 23-1. From standard transmission line theory (Ramo, 53, 27; Stelzried, 61, 812), the reflection coefficient is given by

$$\rho = V'/V = (Z_L - Z_o)/(Z_L + Z_o) \tag{23-1}$$

where

V = forward traveling voltage wave, V

V' = reflected traveling voltage wave, V

The voltage standing wave ratio (VSWR or S) is given by

$$S = V_{max}/V_{min} = \frac{1 + |\rho|}{1 - |\rho|} \tag{23-2}$$

where

V_{max} = maximum voltage amplitude, V

$= |V| + |V'|$

---

[21]The following analysis is restricted to VSWR theory. Scattering parameters are also frequently used (Otoshi, 68, 675; Hecken, 81, 997).

so that

V_{min} = minimum voltage amplitude, V

$$= |V| - |V'|$$

$$|\rho| = \frac{S-1}{S+1} \tag{23-3}$$

The error in noise temperature calibrations is proportional to power or $|\rho|^2$. As shown in Fig. 23-2, a termination with a VSWR of 1.1 results in $|\rho|^2 \approx 0.0023$. This $\approx 0.23\%$ power reflection could result in ≈ 0.7 K error for an ambient (290 K) thermal standard termination. Precision calibrations usually require transmission components and terminations with VSWR's less than ≈ 1.1.

It is usually necessary to analyze each microwave noise calibration configuration to verify satisfactory performance. Multiple reflections without knowledge of the voltage phase relationships (i.e., using VSWR magnitude information only) require worst case analysis. Consider the configuration for measuring T_{op} using a single thermal termination standard (Fig. 12-3). For this configuration, the maximum error fc a measurement of T_{op} due to mismatches S_a (antenna VSWR), S_p (source termination mismatch) and S_e (receiver mismatch) is (Stelzried, 71, 41; Otoshi, 68, 675),

$$\Delta T_{op}/mm = \frac{T_{op}}{T_p + T_o} \left\{ \text{Max:} \left[1 - \frac{S_p}{S_a} \left(\frac{S_a S_e + 1}{S_p S_c + 1} \right)^2 \right] T_p + \left[1 - \frac{1}{S_a} \left(\frac{S_a S_e + 1}{S_e + 1} \right)^2 \right] T_e \right.$$

$$\text{or:} \left[1 - \frac{S_p}{S_a} \left(\frac{S_a + S_e}{S_p S_e + 1} \right)^2 \right] T_p + \left[1 - \frac{1}{S_a} \left(\frac{S_a + S_e}{S_e + 1} \right)^2 \right] T_e$$

$$\text{or:} \left[1 - \frac{S_p}{S_a} \left(\frac{S_a S_e + 1}{S_p + S_e} \right)^2 \right] T_p + \left[1 - \frac{1}{S_a} \left(\frac{S_a S_e + 1}{S_e + 1} \right)^2 \right] T_e$$

$$\text{or:} \quad \left[1 - \frac{S_P}{S_a}\left(\frac{S_a + S_e}{S_P + S_e}\right)^2\right] T_P + \left[1 - \frac{1}{S_a}\left(\frac{S_a + S_e}{S_e + 1}\right)^2\right] T_e \tag{23-4}$$

For example, if $T_p = 295$ K, $T_e = 5$ K, $T_{op} = 30$ K, $S_p = 1.02$, $S_e = 1.15$ and $S_a = 1.15$, the maximum error in T_{op} due to mismatch is

$$\Delta T_{op}/\text{mm} \approx \frac{30}{295 + 5}\left\{\left[1 - \frac{1.02}{1.15}\left(\frac{1.15 \times 1.15 + 1}{1.02 \times 1.15 + 1}\right)^2\right] 295\right.$$

$$\left. + \left[1 - \frac{1}{1.15}\left(\frac{1.15 \times 1.15 + 1}{1.15 + 1}\right)^2\right] 5\right\} \tag{23-5}$$

$$\approx 0.50 \text{ K peak}$$

The above analysis determines the peak or worst case error due to mismatch. In a statistical sense this is an $\approx 3\sigma$ error. Assume

$$\delta T_{op}/\text{mm} \approx (\Delta T_{op}/\text{mm})/3 \tag{23-6}$$

$$\approx 0.17 \text{ K}$$

It is sometimes advisable to monitor the source termination VSWR in an operational system (Stelzried, 67).

23. Reference

1953 Ramo, S. and Whinnery, J.R., Fields and Waves in Modern Radio, John Wiley, N.Y. 2nd ed. (1953).

1961 Stelzried, C.T., "Interpretation of the Transmission Line Parameters with a Negative Conductance Load and Application to a Negative Conductance Amplifier", IRE Proceedings, Vol. 49, No. 4, (April 1961), pg. 812.

1967 Stelzried, C.T., "Reflectometer for Receiver Input System," NASA Tech Brief B67-10657, Clearinghouse for Federal Scientific and Technical information, Springfield, Va. 22151, (Dec. 1967).

1968 Nemoto, T. and Wait, D. F., "Microwave Circuit Analysis Using the Equivalent Generator Concept". IEEE Transactions on Microwave Theory and Techniques, Vol MTT-16, No. 9, (October 1968), pg. 866.

1968 Otoshi, T.Y., "The Effect of Mismatched Components on Microwave Noise Temperature Calibrations", IEEE Transactions on Microwave Theory and Techniques, (Special Noise Issue), Vol. MTT-16, No. 9, (Sept. 1968), pgs. 675-686.

1968 Wait, D. F., and Nemoto T., "Measurement of the Noise Temperature of a Mismatched Noise Source", IEEE Transactions on Microwave Theory and Techniques, Vol MTT-16, No. 9, (Sept. 1968), pg. 670.

1971 Stelzried, C.T., "Operating Noise - Temperature Calibrations of Low-Noise Receiving Systems", Microwave Journal, Vol. 14, No. 6, (June 1971), pgs. 41-48.

1981 Hecken R.P., "Analysis of Linear Noisy Two-Ports Using Scattering Waves", IEEE Transactions Microwave Theory and Technique, Vol. MTT-29, No. 10 (Oct. 1981), pg. 997.

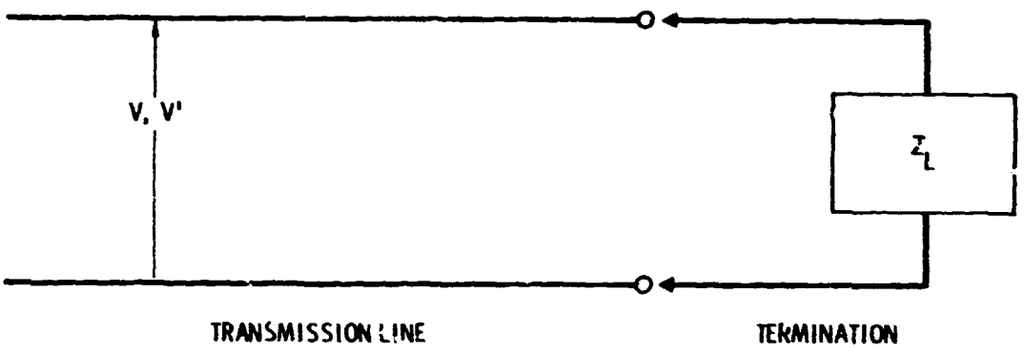

Fig. 23-1. Representation of transmission line with termination

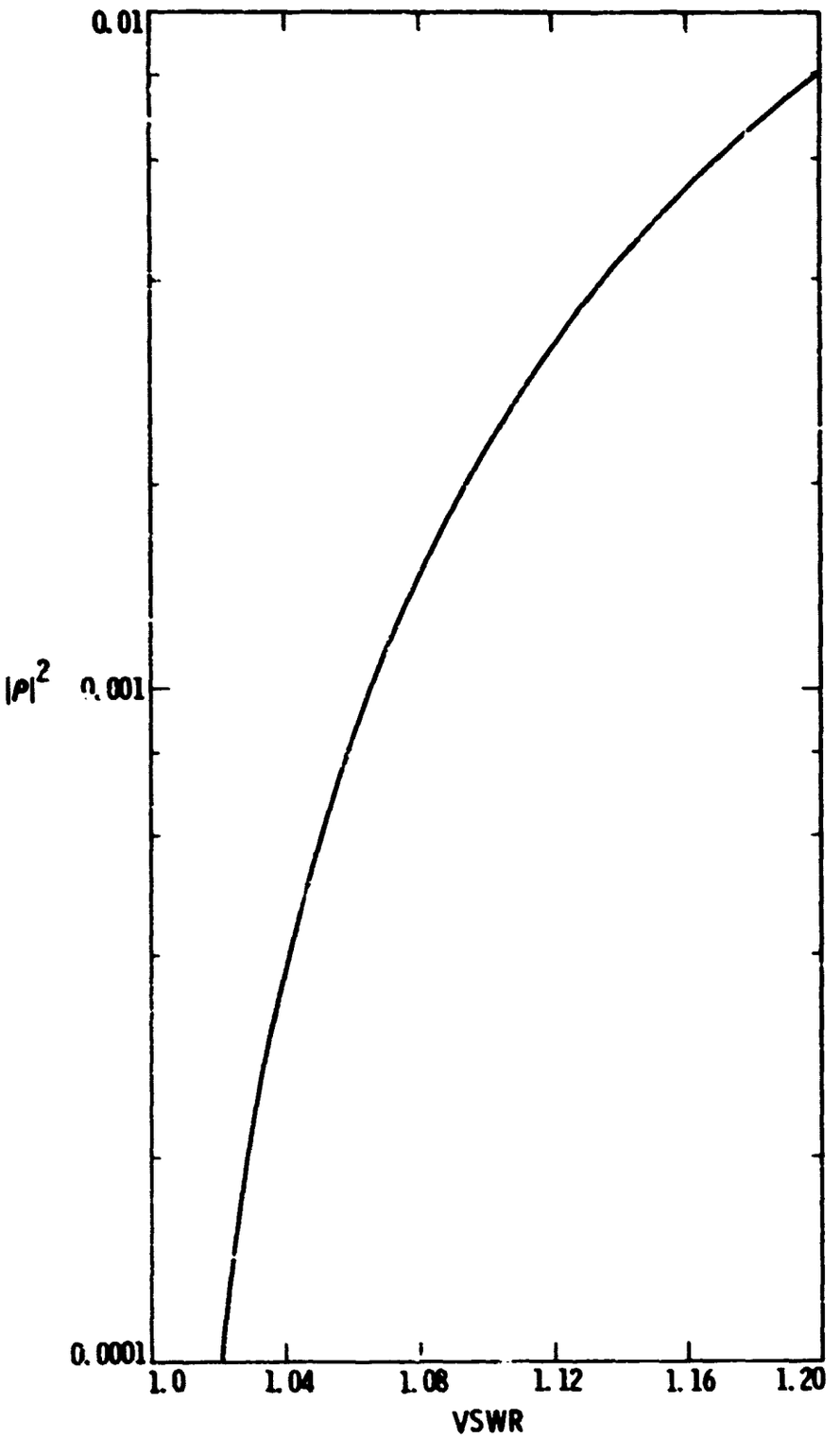

Fig. 23-2. Plot of $|\rho|^2$ vs VSWR from Eq. 23-3

24. Linearity Error

Previous sections assumed perfectly linear receiver amplifiers. It is important that noise calibration instrumentation be operated in the linear region of the receivers. If the receivers are non-linear, either the error contribution of the non-linearity must be known, or a calibration is necessary for a subsequent correction of the measurement results (Stelzried, 80, 98). Fig. 24-1 shows a typical test configuration for an amplifier linearity verification evaluation. The receiver output power (P_{OUT}) is plotted versus input power (P_{IN}) as shown in Fig. 24-2. Receiver saturation is the usual source of non-linearity. Another source of non-linearity error is the precision attenuator used for Y factor measurements (Sec. 10). Typical precision attenuator linearity specifications are 0.02 dB/dB (Stelzried, 71, 41).

As an example of the effect of a receiving system non-linearity consider the measurement of system noise temperature (Sec. 12, Fig. 12-1). For this configuration,

$$T_{op} = (T_H + T_e)/Y \tag{24-1}$$

Differentiating with respect to Y,

$$\left|\partial T_{op}/\partial Y\right| = T_{op}/Y \tag{24-2}$$

The measurement error of T_{op} due to the error in Y is given by

$$\begin{aligned} \delta T_{op}/Y &= (T_{op})\delta Y/Y \\ &\approx 0.23\ (T_{op})\delta Y(dB) \end{aligned} \tag{24-3}$$

or[22]

$$\begin{aligned} \delta T_{op}/Y &\approx 0.23\ (T_{op})\ (\epsilon_L)\ Y(dB) \\ &\approx 0.23\ (30)\ (0.0067)\ (10) \\ &\approx 0.46\ K \end{aligned} \tag{24-4}$$

---

[22]For this example, assume $(T_{op})_H \approx 30$ K, $(T_{op})_H \approx 300$ K, $\epsilon_L \approx 0.0067$ dB/dB.

where

$\delta Y(dB) = (\epsilon_L)\ Y(dB)$

ϵ_L = linearity error, dB/dB

$Y(dB) = 10 \log (T_{op})_H / T_{op}$

T_{op} = system noise temperature when switched to the antenna, K

$(T_{op})_H$ = system noise temperature when switched to T_H, K

24. References

1971 Stelzried, C.T., "Operating Noise-Temperature Calibrations of Low-Noise Receiving Systems", Microwave Journal, Vol. 14, No. 6, (June 1971), pg. 41.

1980 Stelzried, C.T., "Noise Adding Radiometer Performance Analysis", TDA Progress Report 42-59, Jet Propulsion Laboratory, Pasadena, CA, (Oct. 15, 1980). pg. 98.

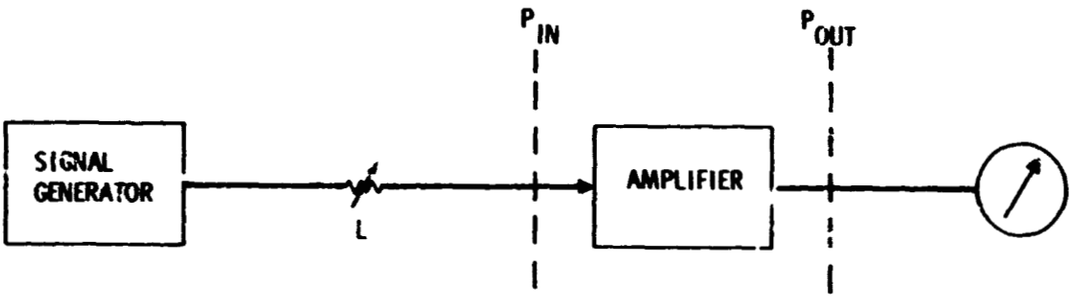

Fig. 24-1. Test configuration for amplifier linearity test

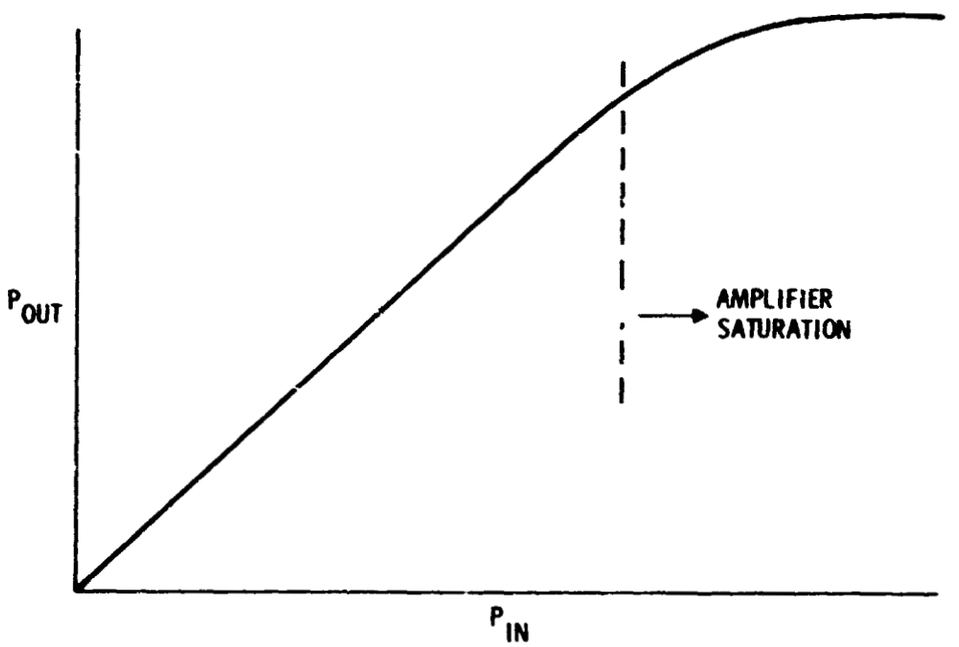

Fig. 24-2. Typical result of amplifier linearity test

25. Cascading of Errors

The previous sections treated the individual error sources separately. In an actual receiving system, multiple errors are present. These separate error sources usually range somewhere between being completely correlated to completely uncorrelated with each other.

Usually, it is not possible to determine the degree of error correlation, nor to even know the type of statistics (Gaussian, Poisson, etc.) applicable to the individual error sources. It is usually satisfactory to indicate error bounds between treating the individual errors as if totally correlated

$$\varepsilon_c = |\varepsilon_1| + |\varepsilon_2| + |\varepsilon_3| + \ldots |\varepsilon_n| \tag{25-1}$$

or totally uncorrelated

$$\varepsilon_u = \sqrt{\varepsilon_1^2 + \varepsilon_2^2 + \varepsilon_3^2 + \ldots \varepsilon_n^2} \tag{25-2}$$

As an example, continue with the analysis of the system operating noise temperature measurement scheme (Fig. 12-3) discussed in Secs. 12, 22, 23, and 24. We had

$$T_{op} = (T_H + T_e)/Y \tag{12-1}$$

where

$$Y = (P_H/P_A)$$

$$T_{op} = T_a + T_e$$

Then[23]

$\delta T_{op}/K$ = 1σ error in σ_{op} due to measurement resolution, K (Sec. 22)

$\simeq$ 0.03 K

---

[23]Assumes (Stelzried, 71, 41) 1σ errors, T_{op} = 30 K, $(T_{op})_H$ = 300 K, $\delta T_H \simeq 0.33$ K, $\delta T_e \simeq 0.1$ K, $\varepsilon_L \simeq 0.0067$ dB/dB.

$\delta T_{op}/T_H$ = error in T_{op} due to an error in T_H, K

$= T_{op}/(T_{op})_H \, \delta T_H$

≈ 0.03 K

$\delta T_{op}/T_e$ = error in T_{op} due to an error in T_e, K

$= T_{op}/(T_{op})_H \, \delta T_e$

≈ 0.01 K

$\delta T_{op}/Y$ = error in T_{op} due to an error in Y, K
(Sec. 24)

≈ 0.46 K

$\delta T_{op}/mm$ = error in T_{op} due to mismatch errors, K
(Sec. 23)

≈ 0.17 K

results in an estimated overall measurement error between $\varepsilon_u \approx 0.5$ K and $\varepsilon_c \approx 0.7$ K.

25. References

1971 Stelzried, C.T., "Operating Noise-Temperature Calibrations of Low-Noise Receiving Systems", Microwave Journal, Vol. 14, No. 6, (June 1971), pg. 41.